Arbeitsbericht NAB 20-08

TBO Bülach-1-1: Data Report

Dossier VII Hydraulic Packer Testing

March 2021

National Cooperative
for the Disposal of
Radioactive Waste

Hardstrasse 73
P.O. Box 280
5430 Wettingen
Switzerland
Tel. +41 56 437 11 11

www.nagra.ch

nagra.

Arbeitsbericht
NAB 20-08

TBO Bülach-1-1:
Data Report

Dossier VII
Hydraulic Packer Testing

March 2021

R. Schwarz[1], L. Schlickenrieder[1] & T. Vogt[2]

[1] CSD Ingenieure AG
[2] Nagra

Keywords:
Bülach-1-1, Bülach-1-1B, Nördlich Lägern, TBO, deep drilling campaign, hydrogeology, hydraulic packer tests, hydraulic conductivity, hydraulic head

National Cooperative
for the Disposal of
Radioactive Waste

Hardstrasse 73
P.O. Box 280
5430 Wettingen
Switzerland
Tel. +41 56 437 11 11

www.nagra.ch

Nagra Arbeitsberichte NAB ("Working Reports") present the results of work in progress that have not necessarily been subject to a comprehensive review. They are intended to provide rapid dissemination of current information.

This NAB aims at reporting drilling results at an early stage. Additional borehole-specific data will be published elsewhere.

In the event of inconsistencies between dossiers of this NAB, the dossier addressing the specific topic takes priority. In the event of discrepancies between Nagra reports, the chronologically later report is generally considered to be correct. Data sets and interpretations laid out in this NAB may be revised in subsequent reports. The reasoning leading to these revisions will be detailed there.

This Dossier was prepared by a project team consisting of:
R. Schwarz (QC of test analysis, QC of test reports, writing)
L. Schlickenrieder (writing)
T. Vogt (project management, conceptualisation, writing)

The present report is based on the detailed reports about the performance and analysis of the hydraulic packer tests. The detailed reports were written by the companies AFRY Schweiz AG (S. Reinhardt, H. Fisch, R. Brauchler) and Solexperts AG (U. Rösli). The hydraulic packer tests were performed by Solexperts AG.

Editorial work: M. Unger

B. Frieg is acknowledged for reviewing a draft of the report. The Dossier has greatly benefitted from technical discussions with, and reviews by, external and internal experts. Their input and work are very much appreciated!

Table of Contents

Table of Contents I

List of Tables II

List of Figures V

1 Introduction 1
1.1 Context 1
1.2 Location and specifications of the borehole 2
1.3 Documentation structure for the BUL1-1 borehole 5
1.4 Structure of Dossier VII 6

2 Strategy for the hydrogeological investigations 7
2.1 Hydrogeological objectives of the TBO boreholes 7
2.2 Hydrogeological investigation concept for BUL1-1 7

3 Drilling fluid monitoring 9
3.1 Flow checks 9
3.2 Mud logging 9

4 Hydraulic packer tests 11
4.1 Test strategy 11
4.2 Test equipment 13
4.2.1 Downhole equipment 13
4.2.1.1 Heavy-duty double packer system 16
4.2.1.2 Packers 18
4.2.1.3 Downhole sensors in the quadruple sub-surface probe 19
4.2.1.4 Autonomous data logger in test interval 20
4.2.1.5 Zero-displacement shut-in tool 21
4.2.1.6 Test tubing 22
4.2.1.7 Slim tubing 23
4.2.1.8 Submersible pumps 24
4.2.1.9 Progressive cavity pump 25
4.2.2 Surface equipment 25
4.2.2.1 Flow board 26
4.2.2.2 Packer pressure control unit 28
4.2.2.3 Additional recorded measurements at surface 28
4.2.2.4 Data acquisition system (DAS) 29
4.3 Test analyses 30
4.3.1 Special effects 32
4.3.1.1 Borehole history 33

4.3.1.2 Interval temperature changes during testing ... 34
4.3.1.3 Mechanical effects ... 34
4.4 Test activities ... 35
4.5 Details of selected tests ... 42
4.5.1 Hydraulic packer test BUL1-1-BDO1 ... 42
4.5.1.1 Interval characterisation ... 42
4.5.1.2 Test execution ... 42
4.5.1.3 Analysis ... 44
4.5.2 Hydraulic packer test BUL1-1-MUK1 ... 48
4.5.2.1 Interval characterisation ... 48
4.5.2.2 Test execution ... 49
4.5.2.3 Analysis ... 51

5 Summary and discussion ... 55
5.1 Drilling fluid monitoring ... 55
5.2 Hydraulic packer test data and results ... 55
5.2.1 Description of tests ... 55
5.2.2 Overview tables and plots ... 55
5.2.3 Discussion of data and results ... 64
5.3 Summary ... 65

6 References ... 66

App. A: Abbreviations, nomenclature and definitions ... A-1

App. B: Analysis plots of the hydraulic packer tests BUL1-1-BDO1 and BUL1-1-MUK1 ... B-1

List of Tables

Tab. 1-1: General information about the BUL1-1 borehole ... 2
Tab. 1-2: List of dossiers included in NAB 20-08 ... 5
Tab. 4-1: Preferred test sequence for formations with medium to high transmissivity ... 12
Tab. 4-2: Preferred test sequence for formations with low to very low transmissivity ... 12
Tab. 4-3: Specifications for the HDDP ... 16
Tab. 4-4: Specifications for the HDDP components ... 17
Tab. 4-5: Specifications for the HDDP packers ... 18
Tab. 4-6: Specifications for the pressure transmitters mounted in the QSSP ... 19
Tab. 4-7: Specifications for the data logger ... 20
Tab. 4-8: Specifications for the zero-displacement shut-in tool ... 21
Tab. 4-9: Specifications for the test tubing ... 22
Tab. 4-10: Specifications for the slim tubing ... 23
Tab. 4-11: Specifications for the submersible pumps ... 24
Tab. 4-12: Specifications for the PC pump ... 25
Tab. 4-13: Specifications for the flow meters ... 26
Tab. 4-14: Specifications for the atmospheric pressure sensor ... 28
Tab. 4-15: Specifications for the physico-chemical sensors ... 29
Tab. 4-16: Summary of analytical analysis methods ... 30
Tab. 4-17: Specific periods of the pre-test[1)] borehole pressure history ... 33
Tab. 4-18: Hydraulic packer testing in borehole BUL1-1: test interval and test specifications ... 37
Tab. 4-19: Hydraulic test BUL1-1-BDO1: information on the test interval ... 42
Tab. 4-20: Hydraulic test BUL1-1-BDO1: borehole pressure history ... 44
Tab. 4-21: Hydraulic test BUL1-1-BDO1: perturbation results applied for the reference case ... 46
Tab. 4-22: Hydraulic test BUL1-1-BDO1: results of pre-test borehole pressure variations ... 46
Tab. 4-23: Hydraulic test BUL1-1-BDO1: results of packer pressure variations ... 47
Tab. 4-24: Hydraulic test BUL1-1-BDO1: results of single-phase evaluations ... 47
Tab. 4-25: Hydraulic test BUL1-1-BDO1: results of overall phases performed parameter optimisation ... 48
Tab. 4-26: Hydraulic test BUL1-1-MUK1: information on test interval ... 48
Tab. 4-27: Hydraulic test BUL1-1-MUK1: borehole pressure history ... 51
Tab. 4-28: Hydraulic test BUL1-1-MUK1: reference fit parameter set ... 52
Tab. 4-29: Hydraulic test BUL1-1-MUK1: perturbation results ... 53

Tab. 4-30: Hydraulic test BUL1-1-MUK1: non-fitting parameter analysis of flow dimension ... 54

Tab. 4-31: Hydraulic test BUL1-1-MUK1: overall simulation parameter set ... 54

Tab. 5-1: Summary of hydraulic packer testing in borehole BUL1-1: transmissivity and hydraulic conductivity ... 56

Tab. 5-2: Summary of hydraulic packer testing in borehole BUL1-1: hydraulic head estimates ... 57

Tab. 5-3: Summary of hydraulic packer testing in borehole BUL1-1: permeability ... 58

Tab. A-1: Geological formation abbreviations for test names in BUL1-1 ... A-1

Tab. A-2: Test name definitions for hydraulic packer testing ... A-1

Tab. A-3: Test event abbreviations for hydraulic packer testing ... A-1

Tab. A-4: Parameter definitions ... A-2

List of Figures

Fig. 1-1: Tectonic overview map with the three siting regions under investigation 1
Fig. 1-2: Overview map of the investigation area in the Nördlich Lägern siting region with the location of the BUL1-1 borehole and the existing Weiach-1 borehole 3
Fig. 1-3: Lithostratigraphic profile and casing scheme for the BUL1-1 borehole 4
Fig. 4-1: General configuration and specifications of the HDDP in double packer configuration.. 14
Fig. 4-2: General configuration and specifications of the HDDP in single packer configuration.. 15
Fig. 4-3: Schematic layout of the flow control unit.. 27
Fig. 4-4: Schematic layout of the packer control unit 28
Fig. 4-5: Flowcharts for the on-site hydraulic packer test analysis (left) and QLA (right)... 31
Fig. 4-6: Flowchart for the off-site DA of a hydraulic packer test....................................... 32
Fig. 4-7: Hydraulic packer test BUL1-1-MAL1: overview plot of pressure vs. time 38
Fig. 4-8: Hydraulic packer test BUL1-1-MAL2: overview plot of pressure vs. time 38
Fig. 4-9: Hydraulic packer test BUL1-1-MAL3: overview plot of pressure vs. time 39
Fig. 4-10: Hydraulic packer test BUL1-1-BDO1: overview plot of pressure vs. time............ 39
Fig. 4-11: Hydraulic packer test BUL1-1-BDO2: overview plot of pressure vs. time............ 40
Fig. 4-12: Hydraulic packer test BUL1-1-KEU1: overview plot of pressure vs. time............ 40
Fig. 4-13: Hydraulic packer test BUL1-1-MUK1: overview plot of pressure vs. time........... 41
Fig. 4-14: Hydraulic test BUL1-1-BDO1: downhole equipment installation record with system layout as used in the field tests 43
Fig. 4-15: Hydraulic test BUL1-1-MUK1: downhole equipment installation record with system layout as used in the field tests 50
Fig. 5-1: Summary of hydraulic testing in borehole BUL1-1: transmissivity profile 59
Fig. 5-2: Summary of hydraulic testing in borehole BUL1-1: hydraulic conductivity profile.. 60
Fig. 5-3: Summary of hydraulic testing in borehole BUL1-1: static formation pressure profile.. 61
Fig. 5-4: Summary of hydraulic testing in borehole BUL1-1: hydraulic head profile (m bgl) 62
Fig. 5-5: Summary of hydraulic testing in borehole BUL1-1: hydraulic head profile (m asl) 63
Fig. B-1: Hydraulic test BUL1-1-BDO1, borehole history.. B-1
Fig. B-2: Hydraulic test BUL1-1-BDO1, log-log diagnostic plots of PSR phase (top), SW-deconvolved (middle) and SWS phase (bottom).. B-2

Fig. B-3: Hydraulic test BUL1-1-BDO1, SW-SWS sequence: Cartesian pressure plot and numerical fits based on the best fit of 577 perturbations using a homogeneous model (green) and a composite model (red) B-3

Fig. B-4: Hydraulic test BUL1-1-BDO1, SW-SWS sequence: cumulative distribution function plots based on a homogeneous model (left) and a composite model (right) B-3

Fig. B-5: Hydraulic test BUL1-1-BDO1, SW-SWS sequence: varied parameter scaled sensitivities for the radial-homogeneous model (top) and the radial-composite (skin) model (bottom) B-4

Fig. B-6: Hydraulic test BUL1-1-BDO1, SW-SWS sequence: histograms of optimized parameters (K, S_S and P_f) and SSE values from the perturbation analysis using a homogeneous model B-5

Fig. B-7: Hydraulic test BUL1-1-BDO1, SW-SWS sequence, radial homogeneous flow model: scatter plots and associated SSE values of the optimised parameters K, S_S and P_f from perturbation analysis B-6

Fig. B-8: Hydraulic test BUL1-1-BDO1, SW-SWS sequence, radial homogeneous flow model: 3D plots and associated SSE values of the optimised parameters K, S_S and P_f from perturbation analysis B-7

Fig. B-9: Hydraulic test BUL1-1-BDO1, SW-SWS sequence: Cartesian pressure plot and best fit based on 577 perturbations and forward simulation without temperature-induced volume change using the best-fit parameters...................... B-8

Fig. B-10: Hydraulic test BUL1-1-BDO1, PW test phase: Cartesian pressure plot of the PW test phase and numerical fit based on a homogeneous model................. B-8

Fig. B-11: Hydraulic test BUL1-1-BDO1, PI test phase: Cartesian pressure plot of the PI test phase and numerical fits based on a homogeneous model B-9

Fig. B-12: Hydraulic test BUL1-1-BDO1, PI test phase, PSR to PI entire sequence fit: Cartesian pressure plot of the entire sequence and the numerical fit based on a homogeneous model B-9

Fig. B-13: Hydraulic test BUL1-1-MUK1, chemical parameters measured during the step rate test B-10

Fig. B-14: Hydraulic test BUL1-1-MUK1, borehole pressure history and measured interval test data.. B-10

Fig. B-15: Hydraulic test BUL1-1e-MUK1, diagnostic plots of PSR phase (no superposition plot, top), slug shut-in phase (SWS, log-log plot using Agarwal time, middle) and the recovery phase after the step rate test (MRS, Agarwal time, bottom) B-11

Fig. B-16: Hydraulic test BUL1-1-MUK1, MR-MRS sequence, GRF model, reference fit: normalised (top) and cumulative distribution function plot (bottom)........... B-12

Fig. B-17: Hydraulic test BUL1-1-MUK1, MR-MRS sequence, best fit: Cartesian pressure and flow data and numerical Cartesian fit on the pressure data of the MR1-MR2-MR3-MR4-MRS sequence using the GRF model B-13

Fig. B-18: Hydraulic test BUL1-1-MUK1, MR-MRS sequence, GRF model, reference fit: scaled sensitivities of the fitting parameters B-14

Fig. B-19: Hydraulic test BUL1-1-MUK1, MR-MRS sequence, GRF model, perturbation analysis: scatter plots and associated SSE values of the optimised parameters from perturbation analysis showing K versus S_S (top), K versus n (middle) and K versus P_f (bottom) B-15

Fig. B-20: Hydraulic test BUL1-1-MUK1, MR-MRS sequence, GRF model, perturbation analysis: scatter plots and associated SSE values of the optimised parameters from perturbation analysis showing S_S versus P_f and n (top and middle) and n versus P_f (bottom) B-16

Fig. B-21: Hydraulic test BUL1-1-MUK1, MR-MRS sequence, GRF model, perturbation analysis: histograms of optimized parameters K, S_S, P_f B-17

Fig. B-22: Hydraulic test BUL1-1-MUK1, MR-MRS sequence, GRF model: parameter ranges of the parameters K, S_S and P_f together with respective SSE values against the flow dimension n using the sampling technics B-18

Fig. B-23: Hydraulic test BUL1-1-MUK1, PW-MRS entire sequence fit: pressure data and numerical pressure fit of the entire test sequence in a Cartesian plot using the GRF mode B-19

1 Introduction

1.1 Context

To provide input for site selection and the safety case for deep geological repositories for radioactive waste, Nagra has drilled a series of deep boreholes in Northern Switzerland. The aim of the drilling campaign is to characterise the deep underground of the three remaining siting regions located at the edge of the Northern Alpine Molasse Basin (Fig. 1-1).

In this report, we present the results from the Bülach-1-1 borehole.

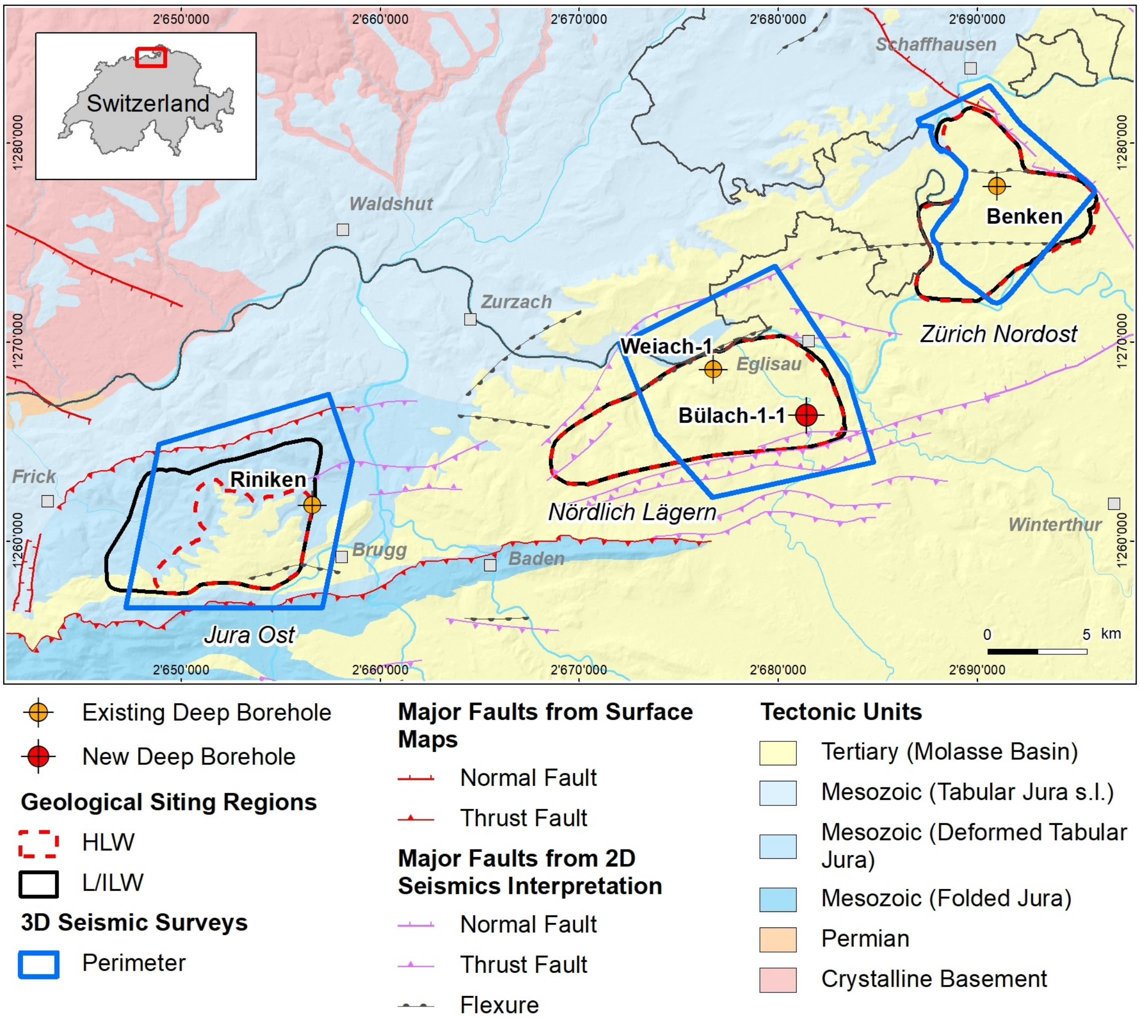

Fig. 1-1: Tectonic overview map with the three siting regions under investigation

1.2 Location and specifications of the borehole

The Bülach-1-1 (BUL1-1) exploratory borehole is the first deep borehole drilled within the framework of the TBO project. BUL1-1 is a vertical borehole. The drill site is located in the south-eastern part of the Nördlich Lägern siting region (Fig. 1-2). The borehole specifications are provided in Tab. 1-1. The lithostratigraphic profile and the casing scheme are shown in Fig. 1-3. Due to instabilities, the borehole was plugged back from 1'043.00 m to 918.70 m (*cf.* Dossier I). Resuming coring operations, a sidetrack was initiated with a kickoff point at 995.85 m. This sidetrack was labelled Bülach-1-1B (BUL1-1B). BUL1-1B reached the final depth of 1'370.19 m (measured depth MD core depth)[1]. For easier communication and labelling, the name BUL1-1 is generally used for the complete vertical borehole unless stated otherwise. Fig. 1-3 shows the combined lithostratigraphic profile of BUL1-1.

Tab. 1-1: General information about the BUL1-1 borehole

Location	Bülach (Canton Zurich / ZH), Switzerland
Siting region	Nördlich Lägern
Coordinates	2'681'446.028 / 1'266'298.472
Elevation	389.62 m asl (top of rig cellar)
Borehole depth	1'370.19 m MD core depth
Drilling period	15 April 2019 – 27 November 2019 (spud – rig release)
Drilling company	Daldrup & Söhne AG
Drilling rig	Wirth B 152t
Drilling fluid	Water-based mud with varying amounts of Pure-Bore®, Pure-Bore® ULV, soda ash, sodium bicarbonate, xanthan gum

[1] *Measured depth (MD)* below top rig cellar along borehole trajectory. In all dossiers, depth refers to MD unless stated otherwise.

MD core depth refers to the depth marked on the cores. Note that petrophysical logs have not been shifted to core depth, hence MD log depth differs from MD core depth. The depth shift between core depth and log depth is documented in Dossier V, Appendix E-1.

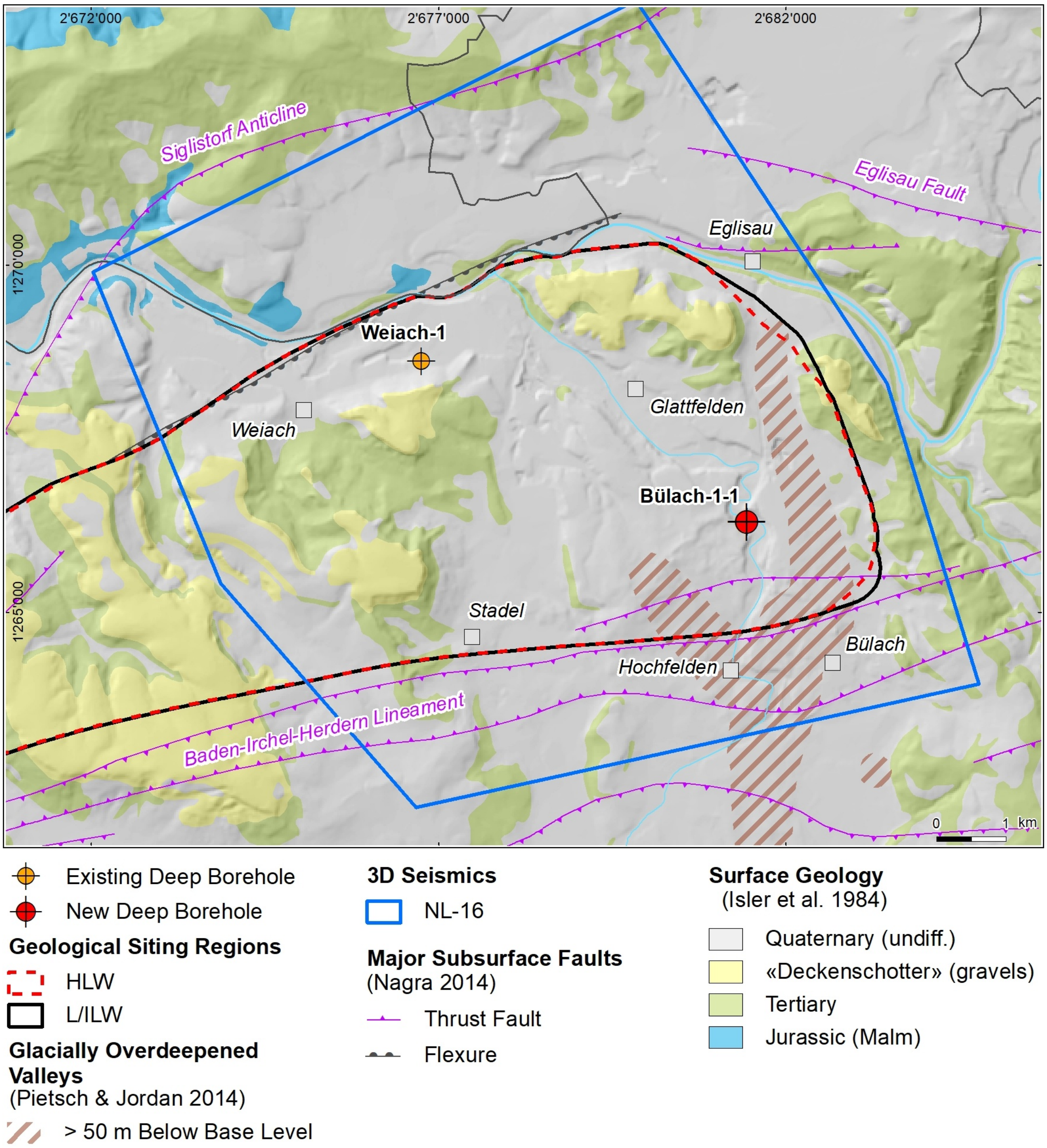

Fig. 1-2: Overview map of the investigation area in the Nördlich Lägern siting region with the location of the BUL1-1 borehole and the existing Weiach-1 borehole

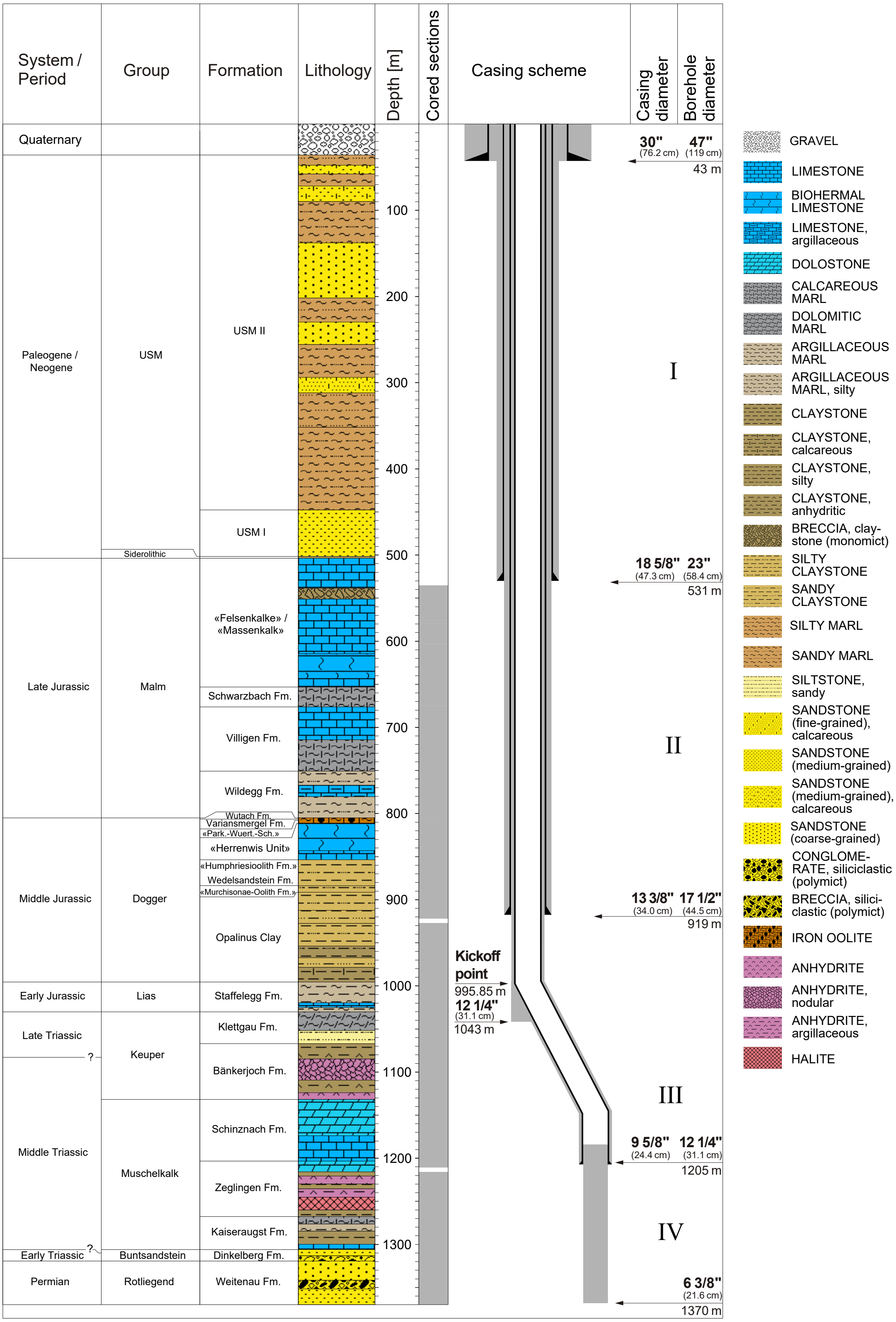

Fig. 1-3: Lithostratigraphic profile and casing scheme for the BUL1-1 borehole

1.3 Documentation structure for the BUL1-1 borehole

NAB 20-08 documents the majority of the investigations carried out in the BUL1-1 borehole, including laboratory investigations on core material. The NAB comprises a series of stand-alone dossiers addressing individual topics and a final dossier with a summary composite plot (Tab. 1-2).

This borehole documentation aims at early publication of the data collected in the BUL1-1 borehole. It includes the majority of the data available approximately one year after completion of the borehole. Some analyses are still ongoing (e.g. diffusion experiments, analysis of veins, hydrochemical interpretation of water samples) and will be published in separate reports.

The current borehole report will provide an important basis for the integration of datasets from different boreholes. The integration and interpretation of the results in the wider geological context will be documented later in separate geoscientific reports.

Tab. 1-2: List of dossiers included in NAB 20-08

Black marks the dossier at hand.

Dossier	Title	Authors
I	TBO Bülach-1-1: Drilling	M. Ammen & P.-J. Palten
II	TBO Bülach-1-1: Core Photography	D. Kaehr & M. Gysi
III	TBO Bülach-1-1: Lithostratigraphy	P. Jordan, H. Naef, P. Schürch, M. Schwarz, T. Ibele, R. Felber & M. Gysi
IV	TBO Bülach-1-1: Microfacies, Bio- and Chemostratigraphic Analysis	S. Wohlwend, H.R. Bläsi, S. Feist-Burkhardt, B. Hostettler, U. Menkveld-Gfeller, V. Dietze & G. Deplazes
V	TBO Bülach-1-1: Structural Geology	A. Ebert, L. Gregorczyk, E. Hägerstedt & M. Gysi
VI	TBO Bülach-1-1: Wireline Logging and Microhydraulic Fracturing	R. Garrard, J. Gonus, J. Desroches & E. Bailey
VII	TBO Bülach-1-1: Hydraulic Packer Testing	R. Schwarz, L. Schlickenrieder & T. Vogt
VIII	TBO Bülach-1-1: Rock Properties, Porewater Characterisation and Natural Tracer Profiles	M. Mazurek, L. Aschwanden, L. Camesi, T. Gimmi, A. Jenni, M. Kiczka, U. Mäder, D. Rufer, H.N. Waber, P. Wanner, P. Wersin & D. Traber
IX	TBO Bülach-1-1: Rock-mechanical and Geomechanical Laboratory Testing	E. Crisci, L. Laloui & S. Giger
X	TBO Bülach-1-1: Petrophysical Log Analysis	S. Marnat & J.K. Becker
	TBO Bülach-1-1: Summary Plot	Nagra

1.4 Structure of Dossier VII

The objective of this report is to provide a summary of the conducted hydrogeological investigations and acquired hydrogeological data, including assessments of tests and results, but without interpretation.

The report focuses on hydraulic packer testing and is organised as follows:

- Chapter 2 presents the strategy for the hydrogeological investigations in the BUL1-1 borehole.
- Chapter 3 is dedicated to drilling fluid monitoring and identifies any drilling fluid losses and groundwater inflow based on flow checks and mud logging.
- Chapter 4 discusses all aspects of the hydraulic packer tests including planning of test strategies, test equipment used, and required test analyses. One subchapter provides a summary of given objectives, test types, drilling related information and data plots for each tested formation. In addition, selected tests and analyses are presented in detail.
- Chapter 5 summarises and discusses the data and results mainly for the hydraulic packer tests. The results are summarised in tables and plots and some assessments are made.
- Finally, this report includes a set of appendices, which present relevant general project information and further investigation details.

2 Strategy for the hydrogeological investigations

2.1 Hydrogeological objectives of the TBO boreholes

The overall objectives of the hydrogeological investigations are the detailed determination of the hydraulic conductivity and hydraulic head in the aquifers and aquitards on the one hand, and the chemistry and isotopic composition of the deep groundwaters in the aquifers and the porewaters in the aquitards on the other. The results of the hydrogeological investigations in the TBO boreholes form an important dataset for the safety case and the site selection. These data are mainly needed for characterisation of:

- Hydraulic and hydrochemical barrier properties of the containment-providing rock zone, which consists of the host rock Opalinus Clay and the confining geological units above and below.
- Hydrogeological conditions in the aquifers providing the hydraulic and hydrochemical boundary conditions for the containment-providing rock zone, and providing input for the identification of potential release paths and for the planning of the future access structures.

2.2 Hydrogeological investigation concept for BUL1-1

The hydrogeological investigations for BUL1-1 comprised:

- Monitoring of drilling fluid
- Hydraulic packer testing

The monitoring of drilling fluids involved the registration of all water inflows and losses as well as gas influx during drilling, standstill and test phases in order to determine the mud balance and the borehole history. These, in turn, served as prerequisites for the definition of boundary conditions for hydraulic packer testing.

Hydraulic packer tests were used for the detailed hydraulic characterisation of selected borehole sections to determine transmissivity (T), hydraulic conductivity (K), hydraulic head (h_s), and to identify the appropriate flow model. Hydraulic packer tests were performed in scheduled testing phases between drilling phases but also during drilling phases when potentially highly transmissive features or faults are encountered. Depending on the transmissivity of the test interval, different test methods were applied:

- Pumping tests
- Slug tests
- Pulse tests

These test methods usually are combined, i.e. executed one after the other as a test sequence in test-specific order.

Neither fluid-logging nor a gas threshold pressure test were conducted in the BUL1-1 borehole. Moreover, no hydraulic long-term monitoring system was installed, because of the encountered borehole instabilities (*cf.* Dossier I).

The detailed groundwater sampling, subsequent hydrochemical and isotope analyses (including results) and porewater investigations are the subject of Lorenz (2020) and Dossier VIII. The permeability measurements on drill-core sections are discussed in Dossier IX.

3 Drilling fluid monitoring

Drilling fluid monitoring was performed to identify and quantify any losses of drilling fluid to a formation or any groundwater inflow that occurred during coring. This information provided input for the design of the hydraulic packer tests and also for the borehole pressure history used in the analyses of hydraulic packer tests.

3.1 Flow checks

Flow checks are a standard operation performed during drilling for well control purposes. In TBO boreholes flow checks are performed to identify and quantify any drilling fluid losses into a formation or groundwater inflow to the borehole during coring. Short breaks in drilling occur when a core has just arrived at the surface. These breaks are used routinely to monitor the drilling fluid level in the trip tank (if integrated into drilling fluid circulation) or to visually identify changes in drilling fluid level in the borehole. In the cored section of borehole BUL1-1 the drilling fluid level was monitored with a water level sounder. In BUL1-1 the regular flow checks were performed by the drilling company and based on these, no detectable losses or groundwater inflows were identified.

3.2 Mud logging

The drilling-fluid system is a closed circulation system. Inflows of formation water into the borehole or losses of drilling fluid into the formation therefore result in fluctuations of the mud balance and can be continuously detected and quantified by monitoring levels in the mud tanks (*cf.* Dossier I). This, along with monitoring of pumping pressures, depth-tracking and several other drilling parameters, is referred to as mud logging and provides the database for establishing the borehole pressure history.

Only one significant event was detected by the mud logging system (*cf.* Dossier I) namely dynamic loss of 2 m^3/h to 6 m^3/h occurred at 1'153 m and 0.3 m^3/h to 0.8 m^3/h from 1'156 m to 1'162 m, respectively, making up 5 m^3 in total in the Schinznach Formation (Stamberg Member).

The gas monitoring of the mud logging system indicated no gas inflows (*cf.* Dossier I).

4 Hydraulic packer tests

4.1 Test strategy

The geological formations examined in the TBO boreholes exhibit a wide range of transmissivities. The host rock, Opalinus Clay, and its confining units are expected to have very low transmissivities, whilst the regional aquifers like the Malm and the Muschelkalk formations are expected to have relatively high transmissivities.

Nagra has long established hydraulic testing strategies (e.g. Nagra 1997) to extract the maximum information about the hydraulic characteristics of the various geological formations. Two testing strategies are preferred (Tab. 4-1 and Tab. 4-2). A typical test sequence is divided into different test phases: test preparation, diagnostic and main phase. The test sequence may be concluded with a pulse test (PW/PI) to check if the total test interval compressibility changed during the test. Modifications to the strategies are made according to the encountered specific test conditions and obtained results while testing.

The main difference in the two testing strategies is the selection of appropriate test types and phases as well as the duration of the test phases. In a formation with medium to high transmissivity, pressure disturbances due to drilling or temperature effects dissipate relatively quickly. Accordingly, the test preparation phase is short. The main phase delivers results of sufficient accuracy with respect to the hydraulic properties of the formation in a relatively short period.

In the case of formations with low to very low transmissivity, the test types and their duration is different. For the determination of hydraulic head the borehole pressure history and test duration are an important issue. Depending on the pressure difference between the static formation conditions and the pressure induced in the borehole during the pre-test pressure history, the estimates of hydraulic head can be strongly affected due to non-static pressure conditions in the surrounding borehole area.

A further aspect of the testing strategy is the use of drilling fluid as test fluid. In contrast to previous exploration boreholes drilled by Nagra (e.g. Benken), no exchange of drilling fluid in the test interval was performed in the BUL1-1 borehole. The main reason was borehole stability.

Pure-Bore®, a product of Clear Solutions International Ltd., was used as a drilling fluid additive. It is based on a long-chain biopolymer. According to the manufacturer the polymer forms a membrane coating the borehole wall and preventing swelling of claystones and shales. The model implementation as a skin in the packer-test analysis is assumed to address issues linked with the drilling fluid properties at the borehole wall adequately.

Tab. 4-1: Preferred test sequence for formations with medium to high transmissivity

Test phase	**Phase**[1)]	**Aims**
Test preparation phase	COM	Temperature and pressure equilibration in the test interval
	PSR	Pressure static recovery with closed shut-in tool; create pressure conditions for the initiation of the first test, first estimate of formation pressure; recognition of temperature and pressure trends
Diagnostic phase	PW	First estimates of hydraulic conductivity, which is used to plan the following test sequence
Main phase	SW	First estimates of hydraulic conductivity, which is used to plan the following test sequence as well as the pumping rate and drawdown of the RW phase
	SWS	Estimation of an accurate flow model and hydraulic parameters; hydrostatic pressure for subsequent pumping phase
	RW	Defined signal with a larger radius of influence; allows a representative groundwater sample of the formation to be taken as well as the detection of boundary conditions
	RWS	Estimation of an accurate flow model and hydraulic parameters as well as boundary conditions
Optional	PW/PI	Estimation of the total test interval compressibility at the end of the test

1) For explanation of abbreviations see Tab. A-3.

Tab. 4-2: Preferred test sequence for formations with low to very low transmissivity

Test phase	**Phase**[1)]	**Aims**
Test preparation phase	COM	Temperature and pressure equilibration in the test interval
	PSR	Pressure static recovery with closed shut-in tool; create pressure conditions for the initiation of the first test, first estimate of formation pressure; recognition of temperature and pressure trends
Diagnostic phase	PW	First estimates of hydraulic conductivity, which is used to plan the following test sequence
Main phase Version 1	SW	Estimation of hydraulic formation parameters during a flow phase
	SWS	Estimation of an accurate flow model and hydraulic parameters during shut-in conditions
	PI/PW (optional)	Estimation of the total test interval compressibility at the end of the test
Main phase Version 2	PW/PI	Estimation of hydraulic formation parameters (as an alternative to SW/SWS)

1) For an explanation of the abbreviations see Tab. A-3.

4.2 Test equipment

The most relevant components of the test equipment are presented below.

4.2.1 Downhole equipment

The packer system referred to as the heavy-duty double packer system (HDDP) was used for all hydraulic packer tests in open borehole sections. It consists of a top and bottom inflatable packer (non-inflated outer diameter 114 mm for borehole BUL1-1) in order to confine a test interval section of appropriate length for the intended test (Fig. 4-1). Inflow and outflow occurred through a perforated filter segment covered by a filter screen mounted on a 2⅞" tubing above the bottom packer.

Four pressure transducers, mounted in a probe carrier shell above the top packer and referred to as the quadruple sub-surface probe or quadruple probe (QSSP), measured the pressures below (P1), within (interval pressure P2) and above the test interval (annulus pressure P3) as well as in the test tubing above the downhole shut-in tool (P4). In addition, the pressure in the test interval was recorded with an autonomous memory gauge at the bottom of the filter screen (P2*).

Temperatures were measured at the level of the QSSP by the temperature sensors associated with each pressure transducer (referred to as T1, T2, T3, T4, respectively) and additionally by the sensor associated with the memory gauge mentioned above (named T2*).

A hydraulically controlled non-displacement downhole shut-in tool (SIT) placed above the probe carrier shell was used to isolate the test zone from the test tubing (2 ⅞" EU API CT5 N80). A progressive cavity (PC) pump or Moyno® type pump or a pump housing with a 4" submersible pump integrated in the test tubing can be used for production pumping tests.

For testing in a single packer configuration (Fig. 4-2), the system was set up without the bottom packer but with a prolongation of the interval string with the filter at the bottom. Inflow and outflow occurred through a perforated filter segment covered by a filter screen mounted on a 2⅞" tubing at the bottom of the prolongation.

The quadruple flat-pack consists of three hydraulic steel pipes of ¼" outer diameter (OD) and one electrical conductor coated in a thermoplastic protective cover. Two steel pipes were used for packer inflation and one for the control of the SIT and the pressure release valve (PRV), which was only used when the packers could not be sufficiently deflated by opening the packer lines at the surface.

Certain parts of the downhole equipment are described below in more detail.

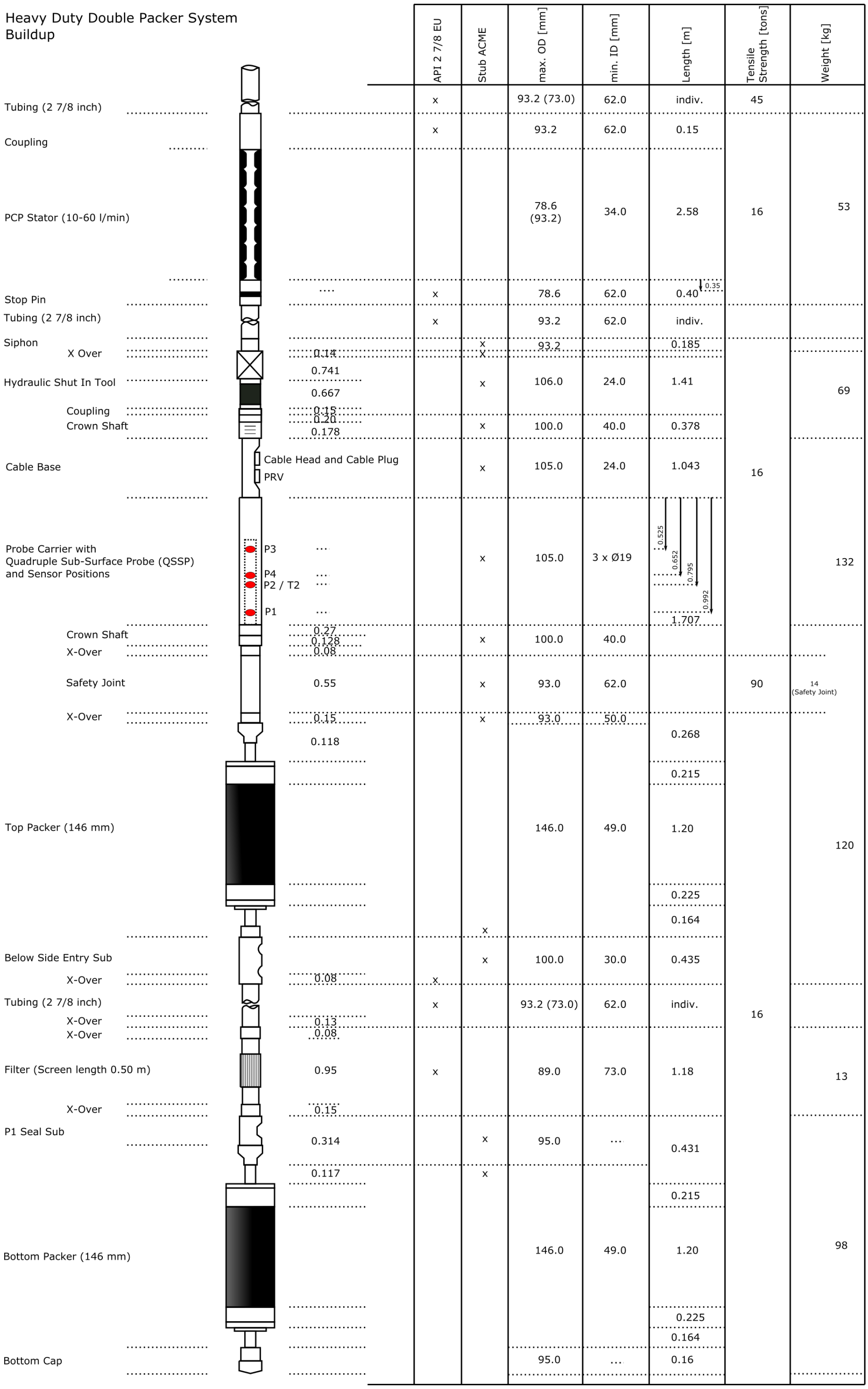

Fig. 4-1: General configuration and specifications of the HDDP in double packer configuration

Heavy Duty Single Packer System Buildup

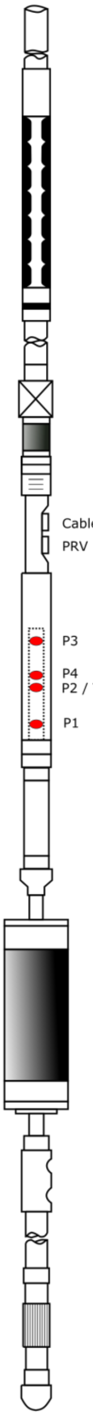

		API 2 7/8 EU	Stub ACME	max. OD [mm]	min. ID [mm]	Length [m]	Tensile Strength [tons]	Weight [kg]
Tubing (2 7/8 inch)		x		93.2 (73.0)	62.0	indiv.	45	
Coupling		x		93.2	62.0	0.15		
PCP Stator (10-60 l/min)				78.6 (93.2)	34.0	2.58	16	53
Stop Pin		x		78.6	62.0	0.40 (0.35)		
Tubing (2 7/8 inch)		x		93.2	62.0	indiv.		
Siphon			x	93.2		0.185		
X Over	0.14		x					
Hydraulic Shut In Tool	0.741 / 0.667		x	106.0	24.0	1.41		69
Coupling	0.15							
Crown Shaft	0.20 / 0.178		x	100.0	40.0	0.378		
Cable Base (Cable Head and Cable Plug; PRV)			x	105.0	24.0	1.043	16	
Probe Carrier with Quadruple Sub-Surface Probe (QSSP) and Sensor Positions (P3, P4, P2 / T2, P1)			x	105.0	3 x Ø19	1.707 (0.525; 0.652; 0.795; 0.992)		132
Crown Shaft	0.27		x	100.0	40.0			
X-Over	0.128 / 0.08							
Safety Joint	0.55		x	93.0	62.0		90	14 (Safety Joint)
X-Over	0.15		x	93.0	50.0			
Top Packer (146 mm)	0.118		x	146.0	49.0	0.268 / 0.215 / 1.20 / 0.225 / 0.164		120
Below Side Entry Sub			x	100.0	30.0	0.435		
X-Over	0.08	x						
Tubing (2 7/8 inch)		x		93.2 (73.0)	62.0	indiv.	16	
X-Over	0.13							
X-Over	0.08							
Filter (Screen length 0.50 m)	0.95	x		89.0	73.0	1.18		13
X-Over	0.15							
Bottom Cap	0.314							6

Fig. 4-2: General configuration and specifications of the HDDP in single packer configuration

4.2.1.1 Heavy-duty double packer system

The technical data of the HDDP are provided in Tab. 4-3. A summary of the downhole equipment with the most important specifications is given in Tab. 4-4.

Tab. 4-3: Specifications for the HDDP

Tool Description	**HDDP**
Packer configuration	Double packer or single packer
Maximum installation depth	1'400 m (vertical); 1'500 m (inclined) along borehole axis
Maximum fluid pressure	20'000 kPa
Maximum differential pressure	114 mm packer system for 162 mm borehole: ~ 12'200 kPa 146 mm packer system for 216 mm borehole: ~ 8'000 kPa
Maximum downhole temperature	80 °C
Range of interval length	3 – 100 m
Probe	QSSP
Shut-in tool (SIT)	Zero-displacement valve
Control lines	4 core encapsulated flat-pack • Hydraulic line – bottom packer (PA1) • Hydraulic line – top packer (PA2) • Hydraulic Line – shut-in tool (SIT) and packer pressure release valve (PRV) • ⅛" (3.175 mm) OD tubing encased single conductor cable

Tab. 4-4: Specifications for the HDDP components

Component	**Specifications**	**Min. ID** [mm]	**Weight**	**Max. tensile force** [t]
Quadruple flat-pack	3 each ¼" OD x 0.035" WT 316L stainless steel welded and cold drawn annealed tubes. 153'339 kPa nominal burst pressure. 49'139 kPa maximum test pressure. Incorporating 1 each ⅛" OD x 0.022" WT316L stainless steel 16 AWG solid CU conductor /P/N 024440) encapsulated to ¼" OD in TT200 thermoplastic. Encapsulated as 33 mm × 11 mm in TT210 thermoplastic, suitable for maximum 98.9 °C brine service.		0.637 kg/m	n/a
Tubing	2⅞" EU API CT5 N80	62	9.68 kg/m	45.3
Pup joints	2⅞" EU API CT5 L80/N80	62	9.68 kg/m	45.3
Shut-in tool (SIT)	Duplex 1.4462	24	69 kg	16
Pressure release valve (PRV)	Duplex 1.4462	24	132 kg	16
Cable base	Duplex 1.4462			16
Quadruple sub-surface probe (QSSP)	Duplex 1.4462 4 pressure sensors P1, P2, P3 and P4	3 × Ø19		16
Coarse thread safety joint	3 21/32" OD, with 2 7/16" bore with 2⅞" EUE box x pin connections	62	26 kg	90
Packers for large borehole diameter	IPI 5¾" (146 mm), steel wire reinforced, duplex, natural rubber Packer 1 Packer 2	 49 49	 98 kg 106 kg	16
Packers for normal borehole diameter	IPI 4½" (114 mm), steel wire reinforced, duplex, natural rubber Packer 1s Packer 2	 49 49	 78 kg 67 kg	16
Filter	HP well screen: sand free filter screen mounted on 2⅞" tubing L 80 Length: 0.50 m Length: 1.00 m	 73 73	 13 kg 19 kg	16
Total system weight	At 1'400 m depth including PC Pump, quadruple flat-pack cable and centralisers		Ca. 15.2 t	
Maximum applicable tensile force for entire system:	Actual system weight at the corresponding depth, plus 16 t (weakest point)			

4.2.1.2 Packers

Two types of packers were available for use, a 114 mm packer for 162 mm diameter boreholes and a 146 mm packer for 216 mm diameter boreholes (Tab. 4-5). The packers were individually inflated with water through the packer inflation line. The inflation line was integrated in the quadruple flat-pack using a booster pump. Depending on the environmental temperatures, an anti-freeze was added to the water. Both packer pressure lines were connected to the packer control board at the winch and equipped with pressure sensors (pressure range 0 – 60'000 kPa) for packer pressure monitoring. The packer pressure sensors were connected to the data acquisition system (DAS) for continuous recording. To keep packer pressures constant, the packers were connected to a pressure vessel via the packer control board for the entire test time. The pressure vessel was placed in a water bath to keep its temperature as constant as possible.

Tab. 4-5: Specifications for the HDDP packers

Manufacturer	Inflatable Packers International, Perth, Australia	
Packer types	IPI 4½" (114 mm)	IPI 5¾" (146 mm)
Material and type	Duplex, natural rubber, sliding end	Duplex, natural rubber, sliding end
Reinforcement type	Steel wire reinforced	Steel wire reinforced
Borehole diameter	162 mm	216 mm
Packer diameters	125 – 230 mm (pressure dependent)	162 – 280 mm (pressure dependent)
Outer diameter, not inflated	114 mm max.	146 mm max.
Inner diameter	49 mm min.	49 mm min.
Overall length: Bottom packer Top packer	 1.93 m 2.08 m	 1.92 m 1.92 m
Rubber sleeve length	1.20 m	1.20 m
Thread connections	2⅞" EU pin x 2⅞" EU box	2⅞" EU pin x 2⅞" EU box
Max. working temperature for a period > 100 h	+ 80 °C	+ 80 °C
Packer inflation lines	Quadruple flat-pack, see Tab. 4-4	Quadruple flat-pack, see Tab. 4-4
Inflation method	Surface controlled	Surface controlled
Inflation fluid	Water and anti-freeze (if necessary)	Water and anti-freeze (if necessary)

4.2.1.3 Downhole sensors in the quadruple sub-surface probe

Four Keller PA-27XW transducers (for transducer types and specifications see Tab. 4-6) were used to monitor fluid pressures in the interval below the bottom packer (P1), within the testing interval (P2), in the annulus between the tubing and borehole wall above the top packer (P3) and in the test string (P4) above the downhole SIT. These four transducers were mounted in the QSSP probe, which was integrated in the probe carrier (see Fig. 4-1). The pressure sensors measured absolute pressure and corrected it to atmospheric pressure; the sensor showed ±0 kPa at atmospheric pressure conditions.

Each pressure transducer had an associated temperature sensor (referred to as T1, T2, T3 and T4) for full thermal compensation of the pressure measurement (Tab. 4-6). The temperature sensor was mounted inside the pressure transducer housing. Because the temperature measurements were taken at the positions of the pressure transducers, they may not represent the effective temperature of the test interval fluid.

Tab. 4-6: Specifications for the pressure transmitters mounted in the QSSP

Pressure transducer type	Keller PA-27XW, custom-made
Manufacturer	Keller, Winterthur, Switzerland
Year of commissioning	2018
Pressure range (full scale)	0 – 20'000 kPa (absolute)
Accuracy	-0.004…0.005 % FS[1)]
Resolution	< 0.0007 % FS
Minimum recording rate	1 Hz
Temperature range (FS)	-10 °C to 80 °C
Accuracy (temperature)	1 °C
Resolution (temperature)	0.01 °C
Output signal	RS485 (digital)

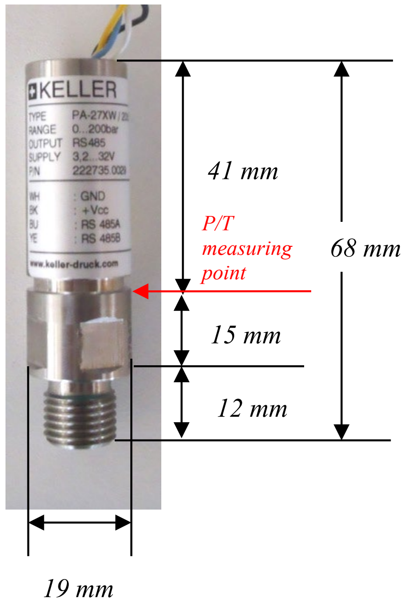

Pressure sensor

1) FS = full scale

4.2.1.4 Autonomous data logger in test interval

Pressures and temperatures were recorded as redundant measurements in the interval at the lower end of the filter screen (referred to as P2* and T2*, respectively) with an autonomous data logger of the type DataCan Memory Pressure Gauges. The specifications are given in Tab. 4-7. The recorded pressure measurement is an absolute measurement.

Tab. 4-7: Specifications for the data logger

Data logger type	DataCan Memory Pressure Gauge 1.25" Welded Piezo III
Manufacturer	Data Can, Red Deer, Canada
Serial number	DC4170
Pressure range (FS)	0 – 20'684 kPa (absolute)
Pressure accuracy	0.03% FS
Resolution	0.0003% FS
Temperature range	0 – 150 °C
Temperature accuracy	0.5 °C
Resolution	0.005 °C
Memory capacity	1'000'000 data sets
Minimum recording rate	10 Hz
Year of commissioning	2018

4.2.1.5 Zero-displacement shut-in tool

The downhole SIT controls the fluid connection between the interior of the test tubing and the test interval. The SIT is a zero-displacement valve that is hydraulically operated via a hydraulic line integrated in the quadruple flat-pack using a hand pump. An axially moveable valve piston opens and closes the valve. The valve piston is moved via the hydraulic (closure) line by applying pressure to close the valve. Releasing the pressure with a pre-stressed spring resets the valve piston and opens the valve (pressure-free opening).

With a pressure compensation element, the pressure at interval depth (annulus pressure) is used to support the spring and to keep the opening/closing pressure constant for the entire borehole depth. The spring force is high enough to ensure a proper functioning of the valve also at low groundwater levels. The specifications are given in Tab. 4-8.

Tab. 4-8: Specifications for the zero-displacement shut-in tool

Zero displacement shut-in tool (SIT)	Manufactured by Solexperts
Maximum water flow rate	Below 40 l/min without friction loss, max. 350 l/min
Pressure loss caused by SIT at a flow rate of 1 l/min and 10 l/min	± 0 kPa
Closing pressure	9'000 – 10'500 kPa
Maximum applicable tensile force	16 t

4.2.1.6 Test tubing

API Spec. 5 CT-05 2⅞" tubing was used as test rods. The detailed specifications of the test tubing are summarised in Tab. 4-9.

Tab. 4-9: Specifications for the test tubing

Test tubing type	Seamless steel tubing pipes: API 5CT-05 (PSL1), 8th edition End of pipes: EUE, tubing & coupling API 5CT-05 (PSL1), 8th edition
Manufacturer	Interpipe Nikopolsky Normec, Celle, Germany
Steel grade	N80 (Tubing), N80/L80 (Pup Joints)
Inner diameter	62.00 mm
Outer diameter	73.02 mm
Coupling outer diameter	93.20 mm
Thread	API 2⅞" EUE
Weight per meter	9.68 kg
Volume per meter	3.02 l
Individual tubing length	Range 2, ~ 9.5 m
Number of individual tubings	174
Total length of test tubing	Ca. 1'500 m
Lengths of pup joints	Length, quantity 1.00 m, 2 1.03 m, 1 1.50 m, 2 1.55 m, 1 1.75 m, 1 1.83 m, 1 3.00 m, 3
Maximum applicable tensile force	45.3 t

4.2.1.7 Slim tubing

The rate of pressure increase during the flow phase of a slug test depends on the formation transmissivity and the diameter of the test tubing, which defines the wellbore storage of the test system during the slug. To improve the resolution of the pressure change, a slim tubing was used to reduce the diameter of the test tubing for slug tests in formations with low transmissivity.

The slim tubing consists of a stiff tube, which is installed into the test tubing. A packer at the bottom of the slim tubing with an outer diameter of 56 mm sealed the annulus between the 2⅞" tubing and the slim tubing. The water level in the slim tubing was measured with the P4 sensor from the QSSP and additionally with a backup pressure sensor installed at the bottom of the slim tubing packer, referred to as P4-slim. P4-slim has a smaller pressure range and thus a higher precision compared to P4. The technical specifications of the slim tubing are summarised in Tab. 4-10.

After lowering the water level in the 2⅞" test tubing for a slug withdrawal test to the specified depth, the slim tubing was installed in the tubing below the water level. Afterwards, the slim tubing packer was inflated and the test was started by opening the SIT valve. The water only increased in the pipe. The use of a stiff tube ensured a constant inner diameter independent of the pressure (fluid level).

Tab. 4-10: Specifications for the slim tubing

Slim tubing type	Polyethylene tube	Polyamide tube
Inner diameter	12 mm	6 mm
Outer diameter	16 mm	8 mm
Length	300 m	300 m
Packer specifications	Diameter 56 mm, sealing length 1000 mm, working pressure 1 – 13.5 MPa	
Packer pressure line	Polyamide OD: 6 mm; ID: 3 mm	
Packer pressure sensor	Keller PAA-33X, 0-5000 kPa, accuracy 0.1 % FS, SN 148177	
Pressure sensor (P-slim)	Memory gauge Keller DCX-22 0 – 5'000 kPa, accuracy 0.05% FS, resolution 0.0025% FS, SN 151129	
Installation procedure	Wireline system of the drill rig	

4.2.1.8 Submersible pumps

Frequency driven 3" and 4" Grundfos submersible pumps can be used for pumping tests. The specifications are included in Tab. 4-11. The flow rate can be arbitrarily adjusted because of the frequency control of the pump.

Tab. 4-11: Specifications for the submersible pumps

Submersible pump types:	4" down-hole pump	3" down-hole pump
Manufacturer	Grundfos, Fällanden, Schweiz	
Type	SP14-27E	SQE1-110
Serial number	100000002	1842
Regulation	Frequency-controlled	Frequency-controlled
Dimensions	101 x 3040 mm	74 x 852 mm
Pumping rate at 150 m	100 l/min	10 l/min
Range of pumping rates	Max. 300 l/min	Max. 28 l/min
Maximum installation depth	160 m	160 m
Maximum temperature	40 °C	35 °C
Weight	57 kg (pump) 31 kg (motor)	6 kg
Pump housing	Yes	No
Specifications of pump housing	Length: 4.22 m OD max: 180 mm Weight: 130.3 kg	
Purpose	Pumping tests	Injection tests, fluid logging

4.2.1.9 Progressive cavity pump

For constant rate or constant head withdrawal tests (pumping tests) a progressive cavity (PC) pump, a so-called Moyno® type pump, was used. The PC pump consists of a helical rotor and a twin helix in a rubber stator. The stator is integrated into the test tubing string and allows for pumping, if necessary, but does not preclude any other test methods. For pumping, a suitable rotor had to be installed by means of the so-called sucker rods until the rotor had fully penetrated the stator. The specifications are listed in Tab. 4-12.

Tab. 4-12: Specifications for the PC pump

PC pump type	Progressive cavity pump
Manufacturer	Netzsch
Dimensions	Drive head: L × W × H: 1'375 × 767 × 1'263 mm
Pumping rates	1.7 – 60 l/min. Pumping rates of < 1.7 l/min can be reached by closing the valve installed in-line at the wellhead.
Maximum installation depth	300 m
Temperature	10 °C to 70 °C
Sucker rods, type	¾" × 7.62 m
Sucker rods, quantity	45
Total length	Approx. 300 m
Available stators	1 for pump rates 10.4 – 60 l/min, Temp. 10 °C to 70 °C 1 for pump rates 1.7 – 5.5 l/min, Temp. 10 °C to 70 °C
Available rotors	3 for pump rate 10.4 – 60 l/min, Temp. 10 °C to 30 °C, 30 °C to 50 °C, 50 °C to 70 °C 3 for pump rate 1.7 – 5.5 l/min, Temp. 10 °C to 30 °C, 30 °C to 50 °C, 50 °C to 70 °C

4.2.2 Surface equipment

The surface equipment consisted of the following equipment:

- Winch for quadruple flat-pack cable
- Flow control system
- Pressure vessel for packer pressure stabilisation
- Injection and pumping head
- PC pump drive head and control unit
- Data acquisition system

The surface equipment was installed in a mobile measuring container.

4.2.2.1 Flow board

For the control and measuring of pump (and injection) rates, a flow board with three flow meters of type Yokogawa AXF/ADMAG were available. The flow meters covered a flow range between 0.03 and 100 l/min (Tab. 4-13). The schematic layout of the flow control unit is displayed in Fig. 4-3.

Tab. 4-13: Specifications for the flow meters

	Serial number	**Measuring range**		**Accuracy**
		Lower limit	**Upper limit**	
	SN	[l/min]	[l/min]	[%]
AXF 002	S5E902498 535	0.030	2.945	0.35
AXF 005	S5E902499 535	0.1	11.78	0.35
ADMAG SE202	0182 123 219	1.0	100	0.35

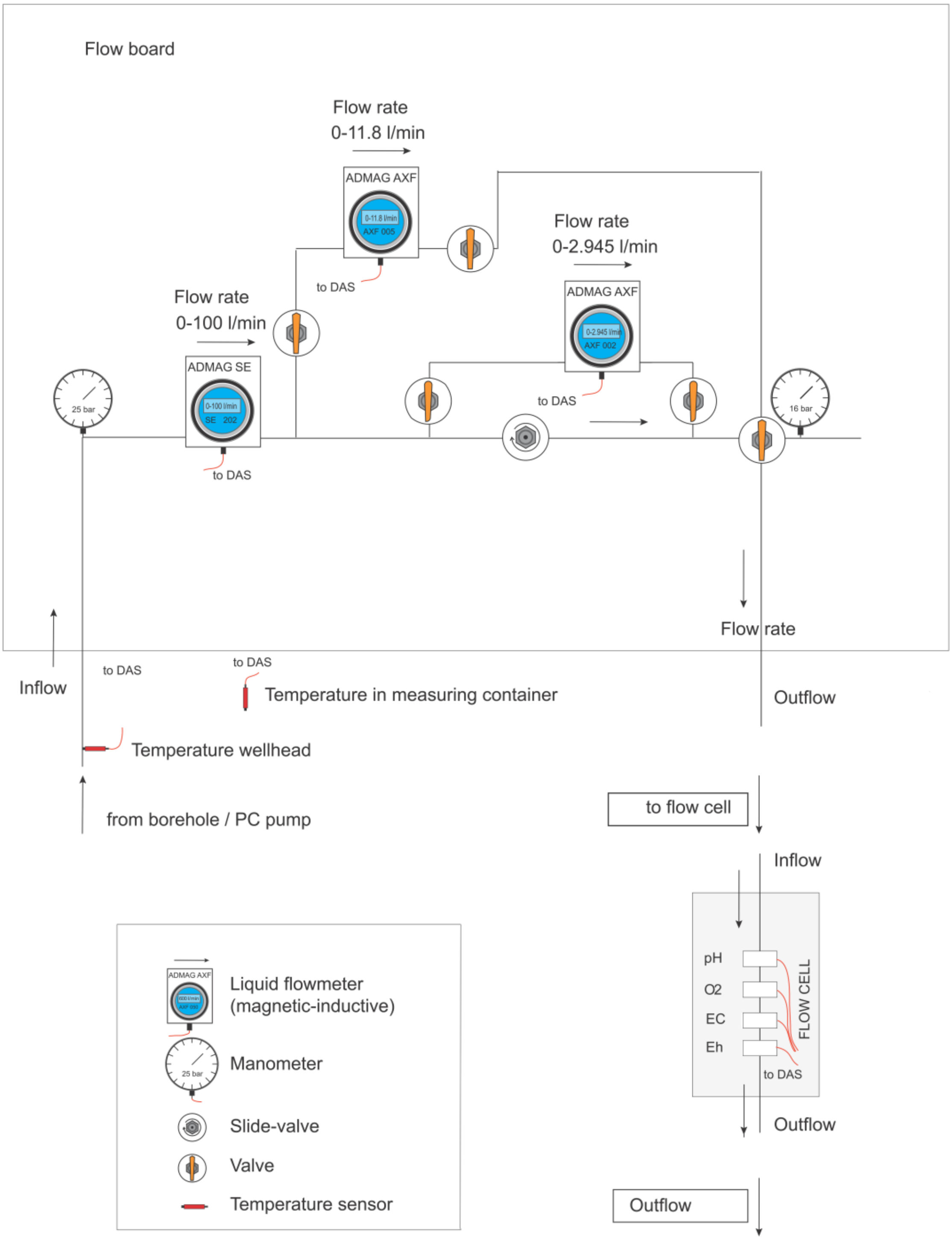

Fig. 4-3: Schematic layout of the flow control unit

4.2.2.2 Packer pressure control unit

Two transducers (type Keller PA-23SY, 60'000 kPa) mounted on the surface inflation control panel were used to monitor the packer inflation pressures (Fig. 4-4).

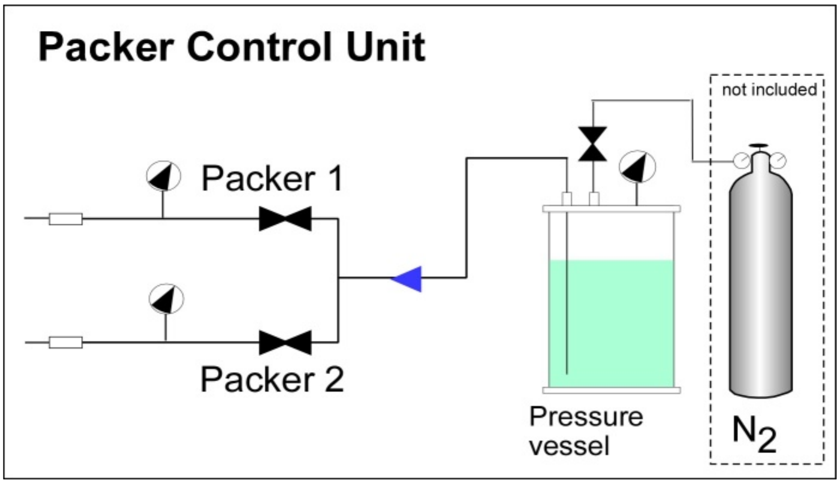

Fig. 4-4: Schematic layout of the packer control unit

4.2.2.3 Additional recorded measurements at surface

A single pressure transducer (type Keller PAA-33X, 80 – 120 kPa absolute) was mounted in the monitoring trailer and used to monitor barometric pressure (Tab. 4-14).

During pumping tests, the physico-chemical parameters (e.g. pH, EC, Eh, temperature and oxygen concentration) and the temperature of the extracted fluid were recorded. The specifications of the physico-chemical sensors are given in Tab. 4-15. The specifications of the temperature sensor are also given in Tab. 4-15. The sensors were calibrated on-site before each use.

Tab. 4-14: Specifications for the atmospheric pressure sensor

Temperature sensor type	Keller PAA-33X
Manufacturer	Keller, Winterthur, Switzerland
Pressure range	80 – 120 kPa
Accuracy	0.02% FS
Resolution	0.002% FS

Tab. 4-15: Specifications for the physico-chemical sensors

Sensor type	EC	pH	Eh	O2	Temp
Manufacturer	Xylem analytics, Weilheim, Germany				IST AG
Model	WTW TetraCon 325	WTW SensoLyt DW	WTW SensoLyt PtA/Pt	WTW FDO 700 IQ	Pt 1000
Serial number	16490290	A165105004	C163112009	16510968	n/a
Range	1 µS/cm – 2 S/cm	0 – 14	± 2'000 mV	0 – 20 mg/l	-50 – 650 °C
Accuracy	n/a	n/a	n/a	n/a	± 0.15 °C at 0 °C ± 0.35 °C at 100 °C
Resolution	n/a	n/a	n/a	0.01 mg/l (0.01 ppm)	$1.5 \cdot 10^{-3}$ °C
Temperature range	0 °C to 100 °C	0 °C to 60 °C	0 °C to 60 °C	-5 °C to 50 °C	-50 °C to 650 °C

4.2.2.4 Data acquisition system (DAS)

The DAS consisted of industrial PCs, screens and keyboard. Data acquisition was performed through the Solexperts GeoMonitor II (GMII) software. The downhole pressures (P1, P2, P3, P4) and temperature measurements (T1, T2, T3, T4) were recorded in real time through the quadruple flat-pack cable assembly. Surface measurements like flow meter rates, packer pressures, atmospheric pressure and temperature, slim tubing packer pressure and the physico-chemical parameters were recorded either permanently or, if required, with an interface with the same scan rate as the downhole pressures from the QSSP.

The scan rates could be adjusted as required between 0.5 s (using a reduced number of sensors) and > 30 s.

The measurements were written to a data file on the PC hard drive in real-time with a continuous data collection and database model. From the PC hard drive, the data were transferred to another network PC every 20 s for 'online' analysis and data back-up. An uninterruptible power supply was utilised to protect the system from short power interruptions.

4.3 Test analyses

For BUL1-1 the general on-site analysis approach involved both analytical and numerical techniques. This ensured a comprehensive evaluation of the recorded data and an additional internal consistency check. Prior to commencement of the hydraulic tests, particularly the representation of the borehole history period and the starting input parameters were defined.

The analytical analysis was performed first. The best estimates and the flow model from the analytical analysis are then used as an input to the numerical simulations for the so-called Quick Look Analysis (QLA). The on-site analysis results were used to continuously optimise the test design during testing to achieve the test objectives within the dedicated time of testing. A general flowchart of the on-site analysis work is provided in Fig. 4-5.

The programme Hugo TM (Solexperts) was used for the analytical analysis and for the numerical and statistical analysis the numerical borehole simulator Multisim (AFRY Schweiz AG) was used. A summary of the applied analytical test analysis methods is presented in Tab. 4-16.

Tab. 4-16: Summary of analytical analysis methods

Test phase	**Analysis method**	**Reference**
Pulse test	Type-curve matching	Bredehoeft & Papadopulos (1980)
Slug test (flow phase SW)	Type-curve matching	Cooper et al. (1967)
Slug test (pressure recovery after slug flow phase, SWS)	Diagnostics: log-log plot showing ΔP and derivative versus 'equivalent time' (Agarwal time)	Agarwal (1980) Bourdet et al. (1989)
	Straight-line analysis on transient pressure data	Agarwal (1980)
Constant rate test	Diagnostics: log-log plot showing ΔP and derivative versus time	Bourdet et al. (1989)
	Straight-line analysis on transient pressure data	Cooper & Jacob (1946)
Pressure recovery after constant rate tests	Diagnostics: log-log plot showing ΔP and derivative versus 'equivalent time' (Agarwal time)	Agarwal (1980) Bourdet et al. (1989)
	Straight-line analysis on transient pressure data	Agarwal (1980)

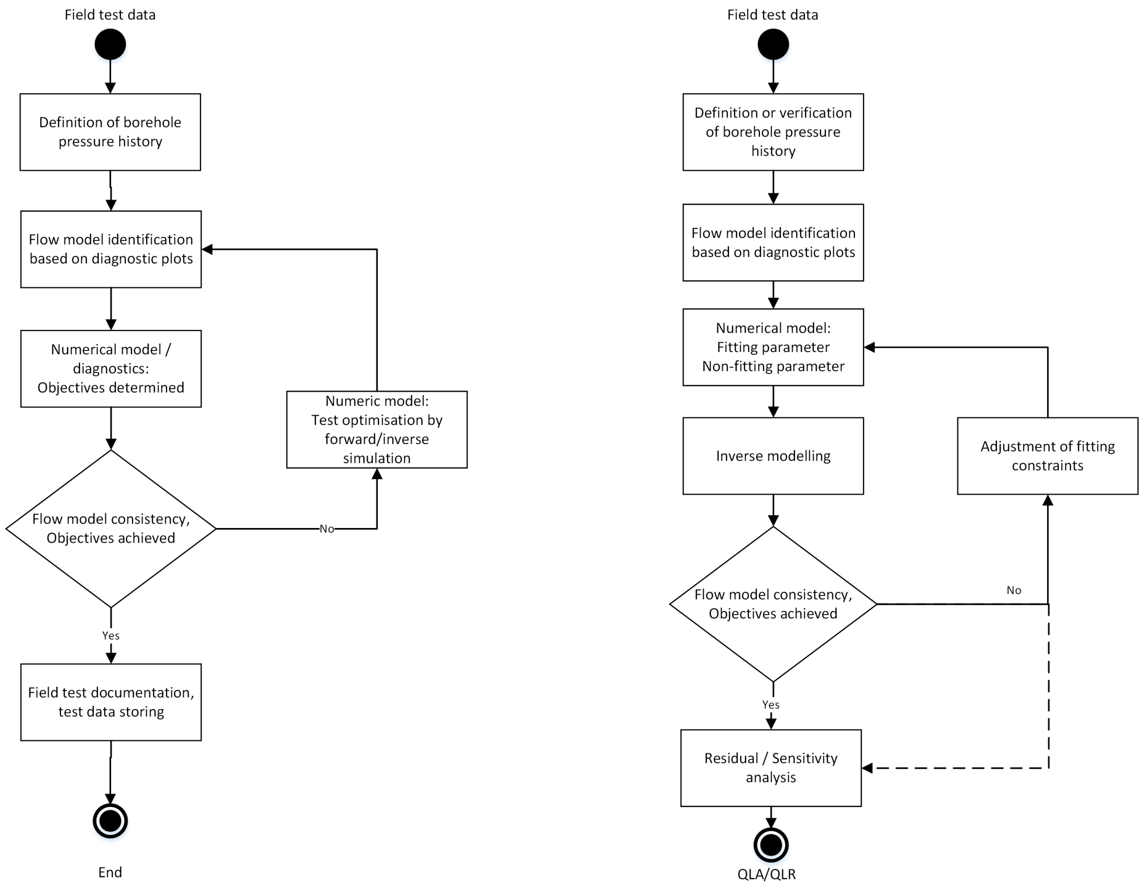

Fig. 4-5: Flowcharts for the on-site hydraulic packer test analysis (left) and QLA (right)

The Detailed Analysis (DA) was performed off-site after the test was completed and is based on the QLA. The QLA was reviewed as part of the Quality Control (QC) programmes. Based on the outcome of the QC review, further specifications and further analyses (mainly numerical analyses) were implemented in the DA. Fig. 4-6 provides the general flowchart of the DA, which includes perturbation and non-fitting parameter analysis, to obtain the most reasonable parameter results and ranges of uncertainty.

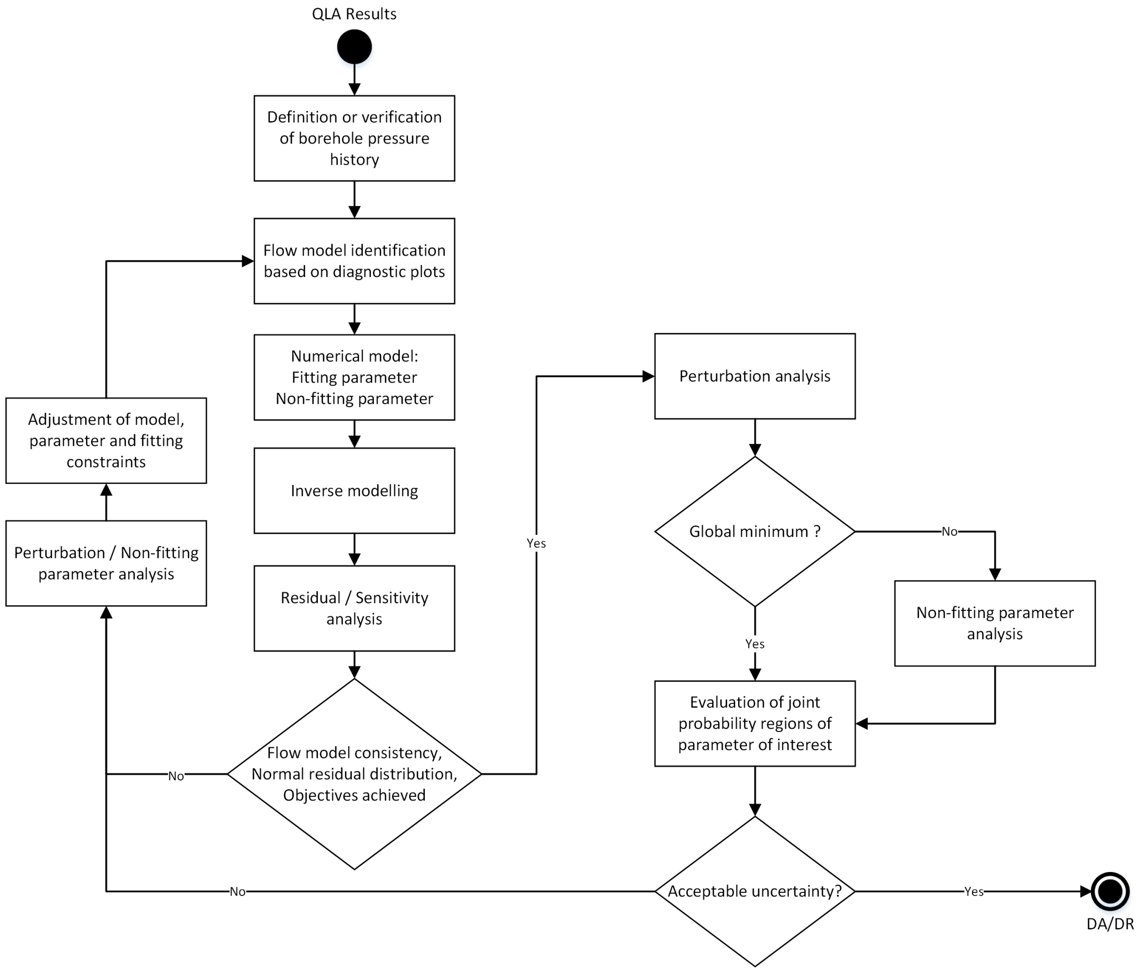

Fig. 4-6: Flowchart for the off-site DA of a hydraulic packer test

4.3.1 Special effects

The time series measured during hydraulic packer tests are the pressure and temperature inside the test interval. Their development over time was analysed to estimate the hydraulic properties of the formation surrounding the test interval. Various factors can affect the recorded time series. Many hydraulic tests are affected by factors beyond the test execution and the model used for their analysis (analytical solutions based on assumptions to derive them, numerical models based on the physical processes included in their base equation system). They are referred to as disturbances because they are not considered in the analysis. However, it is possible to describe the development of temperature and pressure signals by the diffusion equation. Disturbances are of short duration in formations with medium to high transmissivity. In formations with low transmissivity, disturbances of the pressure or temperature field can have a significant influence on the pressure signal measured during the test in the test interval (e.g. Grauls 1999, Nagra 2001).

Any disturbances of the pressure field during the time before the hydraulic test is started, are summarised under the name 'borehole pressure history'. Disturbances in the pressure and temperature fields can be caused by drilling and other activities before testing. In addition, disturbances can occur even during testing, e.g. mechanical effects due to changes in the stress field surrounding the interval, or osmosis due to the chemical interaction of the formation and drilling fluid. However, results from the experiment 'Deep Borehole Hydraulic Testing Experiment' in the Mont Terri Rock Laboratory show that osmotic effects have no significant impact on the determination of transmissivity and hydraulic head (Marschall et al. 2003).

As the TBO boreholes are multi-purpose boreholes with many other objectives besides hydraulic packer testing, there is always a trade-off between disciplines in regard to optimal test conditions. The hydraulic packer tests were performed without exchange of drilling fluid with testing fluid with the aim to reduce potential pressure and temperature disturbances. In addition to this preventive measure, the numerical analysis tool can estimate the effect of these influences, so that plausibility ranges for the parameter estimations can be defined. In the following, possible individual special effects that had already been identified, e.g. for borehole Benken (Nagra 2001), are discussed in more detail.

4.3.1.1 Borehole history

All numerical analyses took into account the borehole pressure history. The borehole pressure history was constructed based on activities that took place prior to hydraulic testing. Drilling through the midpoint of the test interval was used as the starting point of the pressure history. The borehole pressure history data were incorporated into the numerical analyses. The following information was used:

- Date and time of drilling through the interval midpoint, from drilling logs
- Drilling fluid density
- Pressure records of preceding hydraulic testing

Tab. 4-17: Specific periods of the pre-test[1)] borehole pressure history

Test name	**Drilling through midpoint: date and time**	**Start hydraulic testing: date and time**	**Borehole history duration** [h]
BUL1-1-MAL1	17.05.2019 18:20	19.05.2019 09:38	39.31
BUL1-1-MAL2	29.05.2019 13:19	15.06.2019 02:22	397.06
BUL1-1-MAL3	29.05.2019 13:19	16.06.2019 01:10	419.87
BUL1-1-BDO1	08.06.2019 07:58	12.06.2019 15:22	103.40
BUL1-1-BDO2	09.06.2019 14:48	22.06.2019 19:44	316.93
BUL1-1-KEU1	30.09.2019 20:08	03.10.2019 00:00	51.87
BUL1-1-MUK1	14.10.2019 06:32	20.10.2019 14:00	151.48

1) Borehole pressure history before start of data acquisition system.

Most affected by the borehole pressure history is the determination of the static formation pressure (hydraulic head), which in turn depends on the transmissivity of the formation. In formations with low transmissivity, like Opalinus Clay, the determination of the static formation pressure can be impossible in a reasonable time due to the long duration of the pressure history. This was proven by the measurements of the Benken long-term monitoring system, which demonstrated that the static formation pressures of Opalinus Clay determined by hydraulic tests were much higher than those subsequently determined by long-term measurements (e.g. Jäggi & Vogt 2020).

The specific periods of the borehole pressure history taken into account for the analysis of the hydraulic packer tests in borehole BUL1-1 are provided in Tab. 4-17.

4.3.1.2 Interval temperature changes during testing

All activities inside the open borehole also affect the temperature field in and around the borehole. In formations with low transmissivity this temperature disturbance affects the pressure field surrounding the borehole due to coupled thermo-hydraulic processes. The analysis of hydraulic tests using the applied numerical software (Multisim) can incorporate temperature changes during the hydraulic test that lead to a change in fluid volume and thus pressure within a confined test interval volume. The fluid volume change in the test interval was calculated using the volumetric thermal expansion coefficient of the fluid (water), which itself is temperature-dependent. The pressure change is linearly dependent on the interval fluid volume change using a proportionality factor, the compressibility of the interval.

The temperature exchange between the surrounding rock and the borehole fluid is neglected in the above-mentioned numerical analysis tools. The rock surrounding the test interval is heated up during hydraulic testing while it is cooled down by the drilling fluid circulation during drilling. In formations with low transmissivity the temperature field surrounding the borehole affects the pressure field around the borehole as well as the measured pressure signals in the test interval. The coupled thermo-hydraulic processes in Opalinus Clay have been investigated by Nagra in previous studies (e.g. in experiments in the Mont Terri Rock Laboratory, Nagra 2019).

4.3.1.3 Mechanical effects

The mechanical deformations caused by drilling- and testing-related stress redistribution in the formation can also influence the pressure response during a hydraulic test. Normally, the conceptual model for the description of the storage coefficient used in the underlying hydraulic models assumes a compressible pore volume and an incompressible grain structure. In this model, changes in pore pressure are considered as movement of the fluid into and out of the pore volume. Time-dependent deformations generally are neglected in this hydraulic model. In formations with low transmissivity, they can have an influence on the pressure signal observed in the test interval. However, there are no data on mechanical deformations available for the tests in borehole BUL1-1 that would allow the characterisation of mechanical effects on the tests in formations with low transmissivity. Deformations of the borehole wall caused by creeping can be included in the analysis of the numerical software package by means of an appropriate parameterisation during the analysis in the same way as for temperature changes inside the interval. The resulting pressure change is caused by volume changes, which can be either linear or quadratic. The proportionality factor between the volume change and the pressure change is the interval compressibility.

4.4 Test activities

A total of six test intervals were investigated in borehole BUL1-1 using the HDDP in single and double packer configuration. The most important test specifications are summarized in Tab. 4-18. In Lias and Opalinus Clay additional hydraulic tests were planned for borehole BUL1-1, but could not be executed due to borehole wall stability problems. The hydraulic packer tests were performed in the following geological formations:

- Malm ('Felsenkalke'/'Massenkalk') with a focus on fault zones (BUL1-1-MAL1) and on cm-sized open karst cavities (BUL1-1-MAL2 and BUL1-1-MAL3)
- Dogger, with a focus on the coralligenous limestones of the 'Herrenwis Unit' (BUL1-1-BDO1) and the claystones, siltstones, marls, limestones and iron oolites of the 'Humphriesioolith Formation', Wedelsandstein Formation (BUL1-1-BDO2)
- Keuper (Klettgau Formation and Benkerjoch Formation) with a focus on a heterogeneous sequence of marls, sandstones, and anhydrites (BUL1-1-KEU1)
- Muschelkalk (Schinznach Formation) with a focus on a sub-vertical fracture (BUL1-1-MUK1).

All tests were performed in the cored borehole section with a borehole diameter of 6⅜", with 114 mm (deflated diameter) packers, and without any prior fluid exchange, i.e. with the drilling fluid being used as the interval test fluid. The density and viscosity of the drilling fluid were reported by the mud engineer in daily mud reports. The tubing was filled with tap water spiked with Na-Naphthionate (at a concentration of approximately 10 ppm) during all packer installations. The SIT was closed during the whole time of lowering and installing the HDDP at the test interval. Therefore, in test intervals with low transmissivity, the interval fluid density was not affected by traced water in the test tubing due to any testing activities that involved mostly withdrawal tests, and no or only very little fluid flow occurred. If a pressure increase of more than 100 kPa was observed in the test interval during inflation of the top packer, the SIT was opened and the COM phase started. Due to the higher density of the mud in the test interval, no flow from the tubing into the test interval can be assumed during the COM phase in formations with low transmissivity. It was possible to create flow from the formation into the borehole by means of slug and pumping tests only during tests BUL1-1-MAL2, BUL1-1-MAL3 and BUL1-1-MUK1.

A swabbing tool was used to create the pressure difference between the test tubing and the test interval.

For each of the pumping tests the PC pump was used, and the position of the stator of the PC pump in the test string was optimised. If two tests were performed sequentially without pulling the HDDP out of the borehole between tests, a stator was already installed for the first test (usually the deeper test). In the case of BUL1-1-BDO1 for example, the equipment was moved post-test to the position of test BUL1-1-MAL2 (above). After indication of a possible production phase, test BUL1-1-MAL2 was terminated in order to reposition the PC pump stator in order to achieve maximum drawdown during the following production phase. Thereafter, the HDDP was pulled out of and lowered back into the borehole before commencement of test BUL1-1-MAL3. Consequently, BUL1-1-MAL2 and BUL1-1-MAL3 share the same interval (Tab. 4-18).

For the tests BUL1-1-MAL1 and BUL1-1-KEU1 drilling was stopped for hydraulic testing. For the other tests, a longer section was drilled and then the hydraulic tests were performed. The curves of measured pressures (measured by the downhole sensors in the QSSP and the autonomous data logger in the interval) and pumping rates (measured by the flow board at the surface) for all tests conducted in borehole BUL1-1 are provided in Fig. 4-7 to 4-13.

The temperature increase was included in the analysis only for formations with low transmissivity. The temperature increase in the test interval from the start of the initial pressure recovery after closing the shut-in valve (PSR) until the end of the test ranged from 1.0 °C and 1.5 °C for tests BUL1-1-MAL1, BUL1-1-BDO1 and BUL1-1-BDO2.

Tab. 4-18: Hydraulic packer testing in borehole BUL1-1: test interval and test specifications

Test name[1)]	**Interval depth**[2)] [m bgl]	**Interval midpoint**[2)] **[m bgl]**	**Packer configuration**	**Test phases**[1)]	**Testing period** (duration)	**Lithology and structural geology features** (formation)	**Objectives**[3)]
BUL1-1-MAL1	537.20 – 545.00	541.10	Single	INF, COM, PSR, PW	19.05. – 20.05.2019 (30.2 h)	Limestone, calcareous breccia with claystone matrix; potential karstic dissolution, tectonically overprinted, fault zone, joints and fractures (Malm, 'Felsenkalke'/'Massenkalk')	T, h_s
BUL1-1-MAL2/3	608.80 – 641.51	625.16	Double	MAL2: INF1, INF2, COM, PSR, PW, SW, SWS MAL3: INF1, INF2, COM, PSR, RW, RWS, MR1, MR2, MR3, MRS, SW, SWS	15.06. – 19.06.2019 (MAL2 13.6 h) (MAL3 89.6 h)	Limestone; cm-sized open karst cavities (MAL2 and MAL3: Malm, 'Felsenkalke'/'Massenkalk')	T, h_s, FM, WS
BUL1-1-BDO1	814.00 – 846.71	830.36	Double	INF, COM, PSR, PW, SW, SWS, PI	12.06. – 14.06.2019 (50.7 h)	Coralligenous limestone and calcareous marl (Dogger, 'Herrenwis Unit')	T, h_s
BUL1-1-BDO2	848.20 – 869.00	858.60	Single	INF, PW, PI, PW2	22.06. – 25.06.2019 (65.6 h)	Silty claystone, calcareous siltstone, silty marl, sandy or bioclastic limestone, iron oolite (Dogger, 'Herrenwis Unit', 'Humphriesioolith Fm', Wedelsandstein Fm)	T, h_s
BUL1-1-KEU1	1'052.23 – 1'074.00	1'063.12	Single	INF, COM, PSR, PW, SW, SWS, PI	03.10. – 04.10.2019 (39.0 h)	Siltstone, marl, sandstone, claystone, anhydrite (Klettgau Fm [Ergolz Mb., Asp Mb.] with boundary to Benkerjoch Fm)	T, h_s
BUL1-1-MUK1	1'137.70 – 1'173.73	1'155.72	Double	INF1, INF2, PSR, PW, SW, SWS, RW[4)], RWS[4)], MR1, MR2, MR3, MR4, MRS	20.10. – 22.10.2019 (52.8 h)	Dolostone with sub-vertical fracture (Muschelkalk, Schinznach Fm)	T, h_s, FM, WS

1) For an explanation of the test names and test phases see Tab. A-3 and Tab. A-4, respectively.
2) The depth relates to the measured depth of the packer-test equipment.
3) FM = flow model, T= transmissivity, K = hydraulic conductivity, h_s = static hydraulic head (freshwater head), WS = water sample
4) Phase of poorly defined test conditions and without the possibility for evaluation

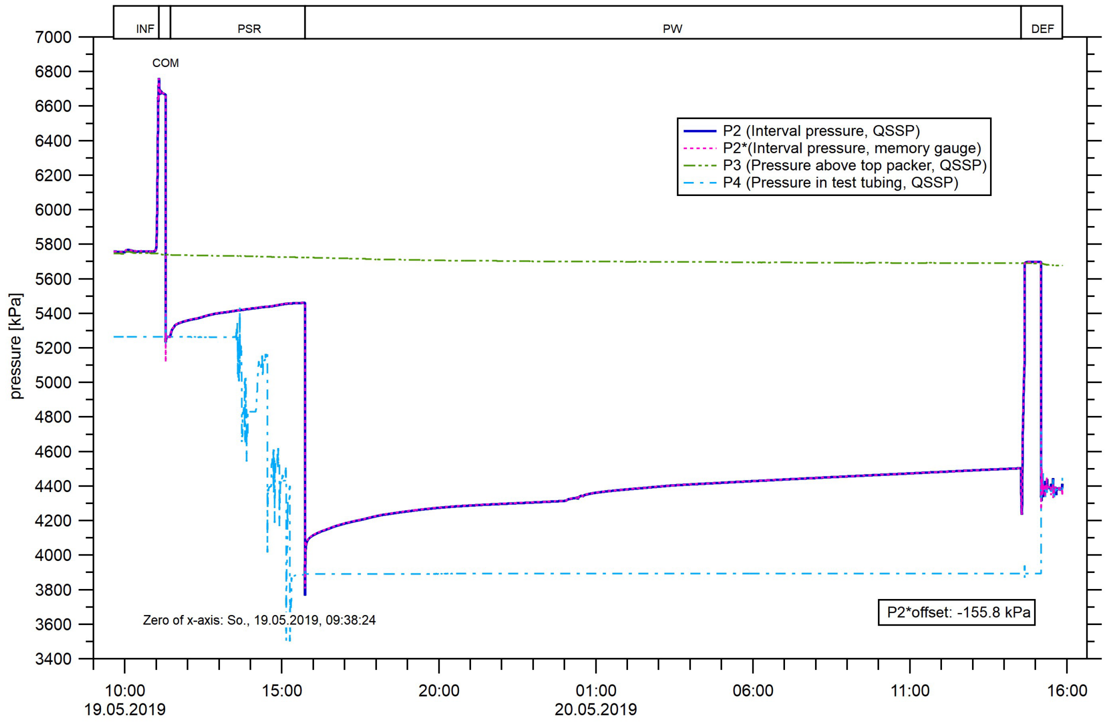

Fig. 4-7: Hydraulic packer test BUL1-1-MAL1: overview plot of pressure vs. time

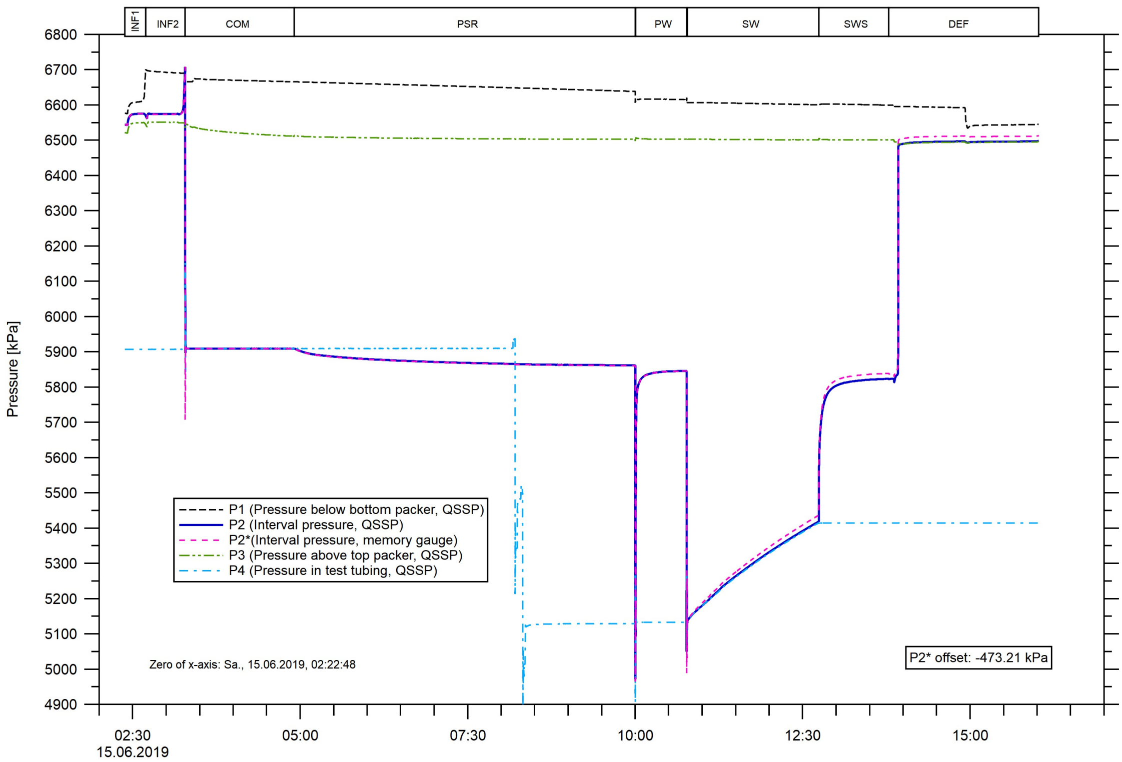

Fig. 4-8: Hydraulic packer test BUL1-1-MAL2: overview plot of pressure vs. time

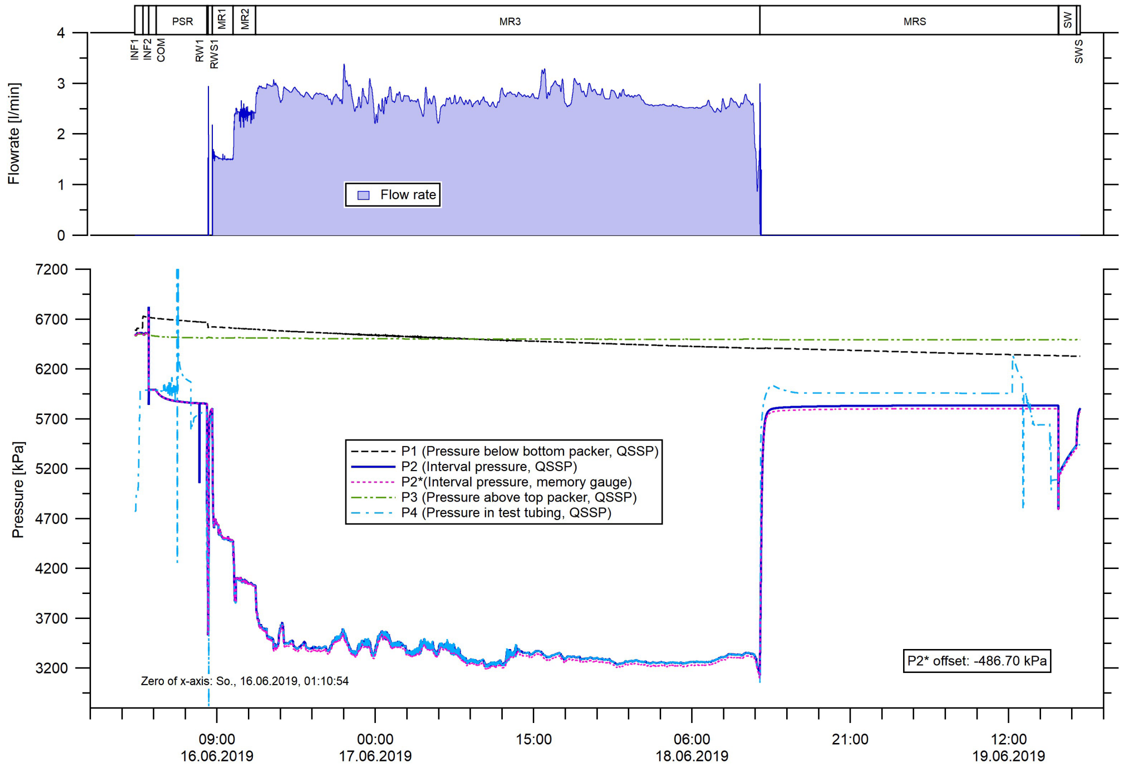

Fig. 4-9: Hydraulic packer test BUL1-1-MAL3: overview plot of pressure vs. time

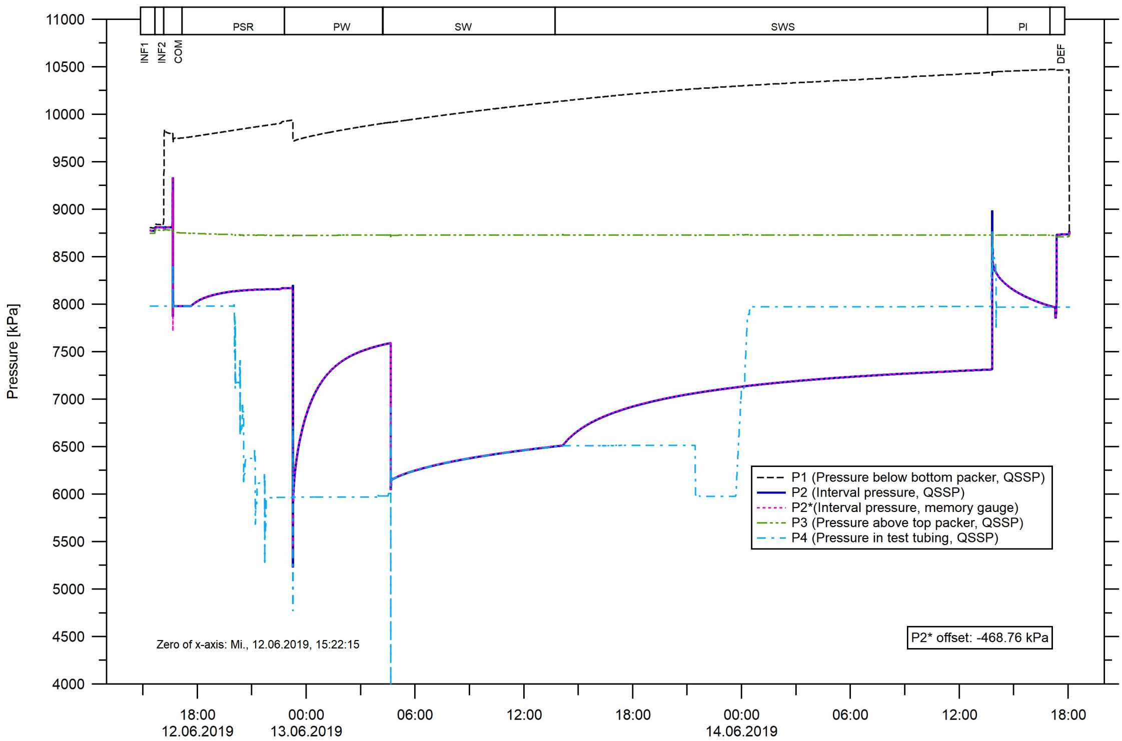

Fig. 4-10: Hydraulic packer test BUL1-1-BDO1: overview plot of pressure vs. time

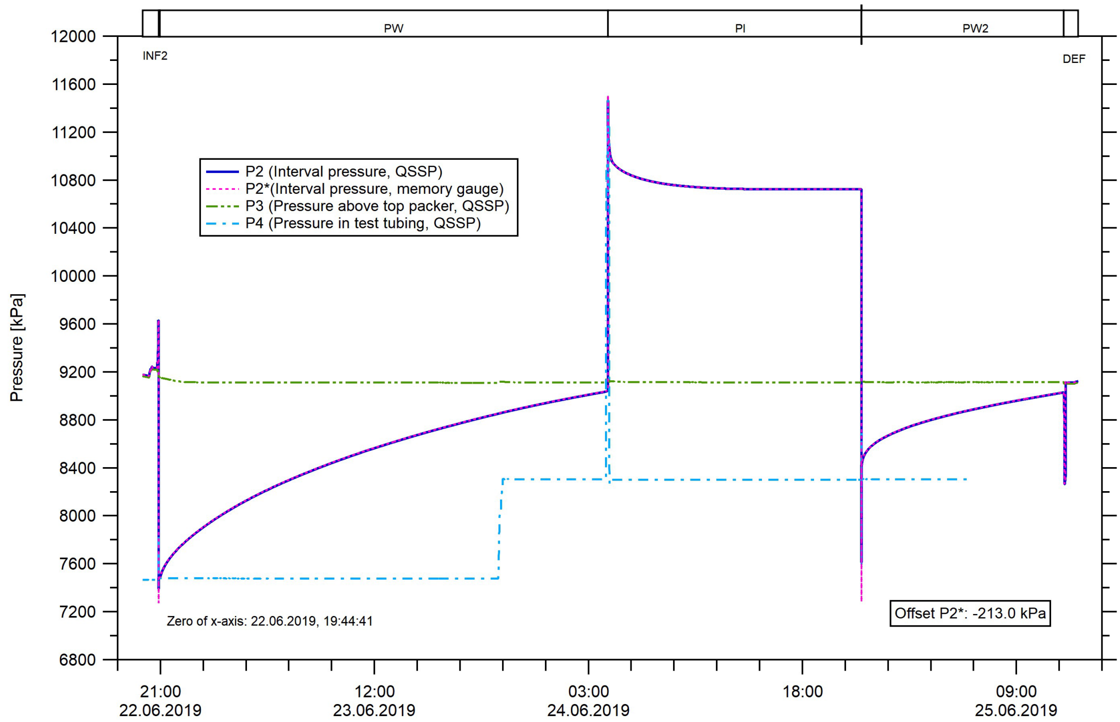

Fig. 4-11: Hydraulic packer test BUL1-1-BDO2: overview plot of pressure vs. time

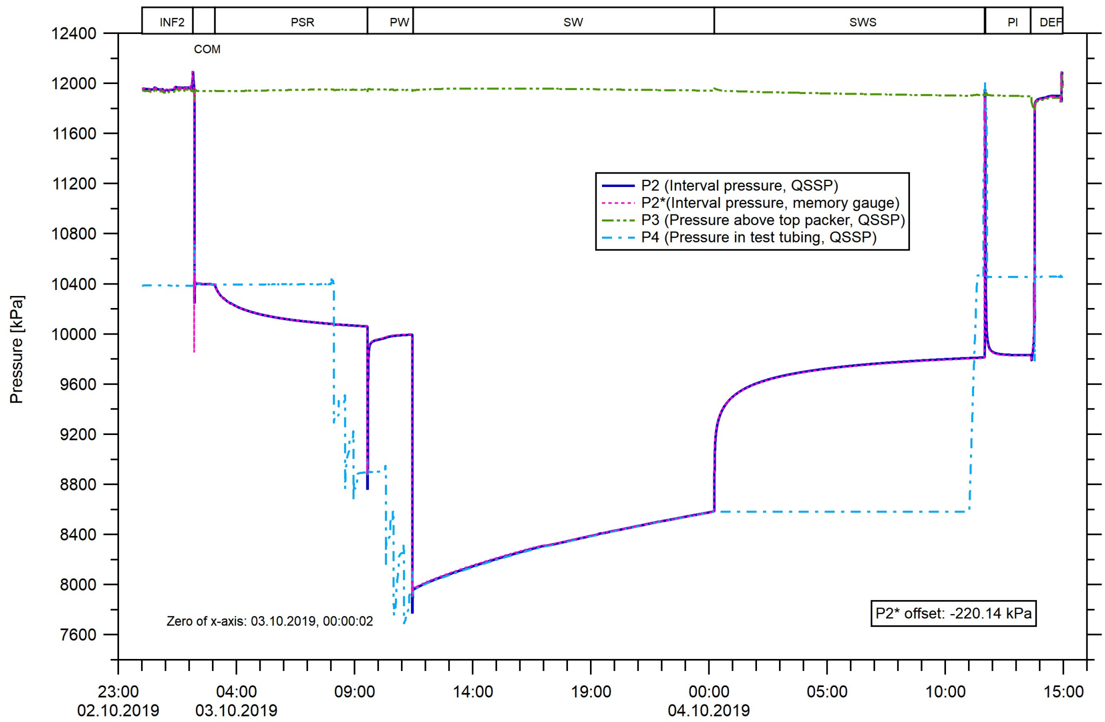

Fig. 4-12: Hydraulic packer test BUL1-1-KEU1: overview plot of pressure vs. time

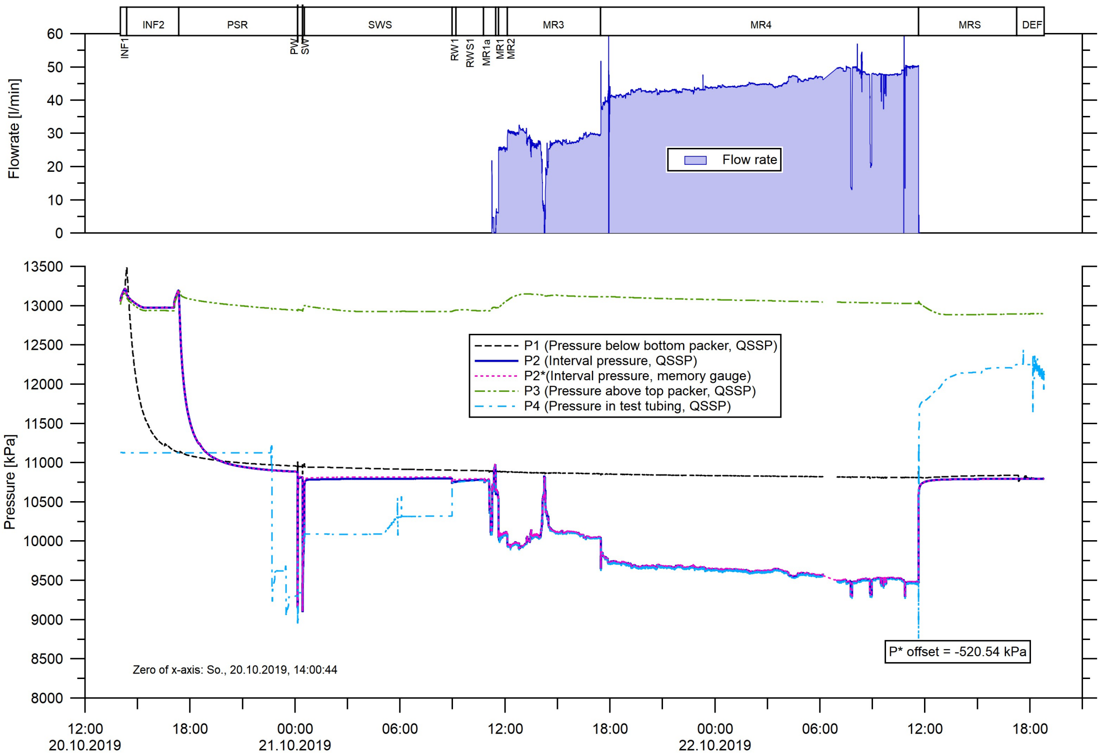

Fig. 4-13: Hydraulic packer test BUL1-1-MUK1: overview plot of pressure vs. time

4.5 Details of selected tests

Two of the hydraulic packer tests are presented below in more detail: BUL1-1-BDO1 and BUL1-1-MUK1. The selected examples reflect the wide range of hydraulic conditions in the borehole. They show the applied analysis strategy and the influence of different effects on, e.g. packer pressure changes due to surface temperature changes, interval temperature changes during testing and borehole pressure history. The results of the two test analyses are provided in the summary chapter together with the results of all other tests performed.

4.5.1 Hydraulic packer test BUL1-1-BDO1

The hydraulic packer test BUL1-1-BDO1 represents an example of testing in formations with low transmissivity.

4.5.1.1 Interval characterisation

The hydraulic test BUL1-1-BDO1 was performed in a double packer configuration. The interval is located in the Dogger Group and the test zone covers the so called 'Herrenwis Unit', a coralligenous limestone with drusy cavities. The test interval was selected because it is located in the upper confining geological unit of the Opalinus Clay. The test objectives were to obtain reliable estimates of T (and K) for the formation, and the freshwater hydraulic head. Details of the interval and test duration are provided in Tab. 4-19.

Tab. 4-19: Hydraulic test BUL1-1-BDO1: information on the test interval

Test	**Depth**		**Length**	**Packer confi-guration**	**Hydraulic testing**		
	from [m bgl]	to [m bgl]	[m]		Start date	End date	Duration [h]
BUL1-1-BDO1	814.0	846.7	32.7	DP[1)]	12.06.2019	14.06.2019	50.7

1) DP: Double packer

4.5.1.2 Test execution

Fig. 4-14 provides the system installation record. The equipment components are those described above. The surface equipment included the packer pressure control unit, which should automatically stabilise the packer pressures over time. Because the packer inflation line on the winch was exposed to fluctuating surface temperature, the packer pressure decreased by about 500 kPa during the initial PSR phase due to concomitant temperature effects in the packer inflation line, which was filled with packer fluid (water with anti-freezing agent). Therefore, a heating blanket was installed on the flat-pack to keep it at a constant temperature of 22 °C and the packers were re-inflated to about 5'000 kPa before the start of the PW test phase. The packer pressures remained stable during the following PW phase; they were, however, unstable during the subsequent test sequence.

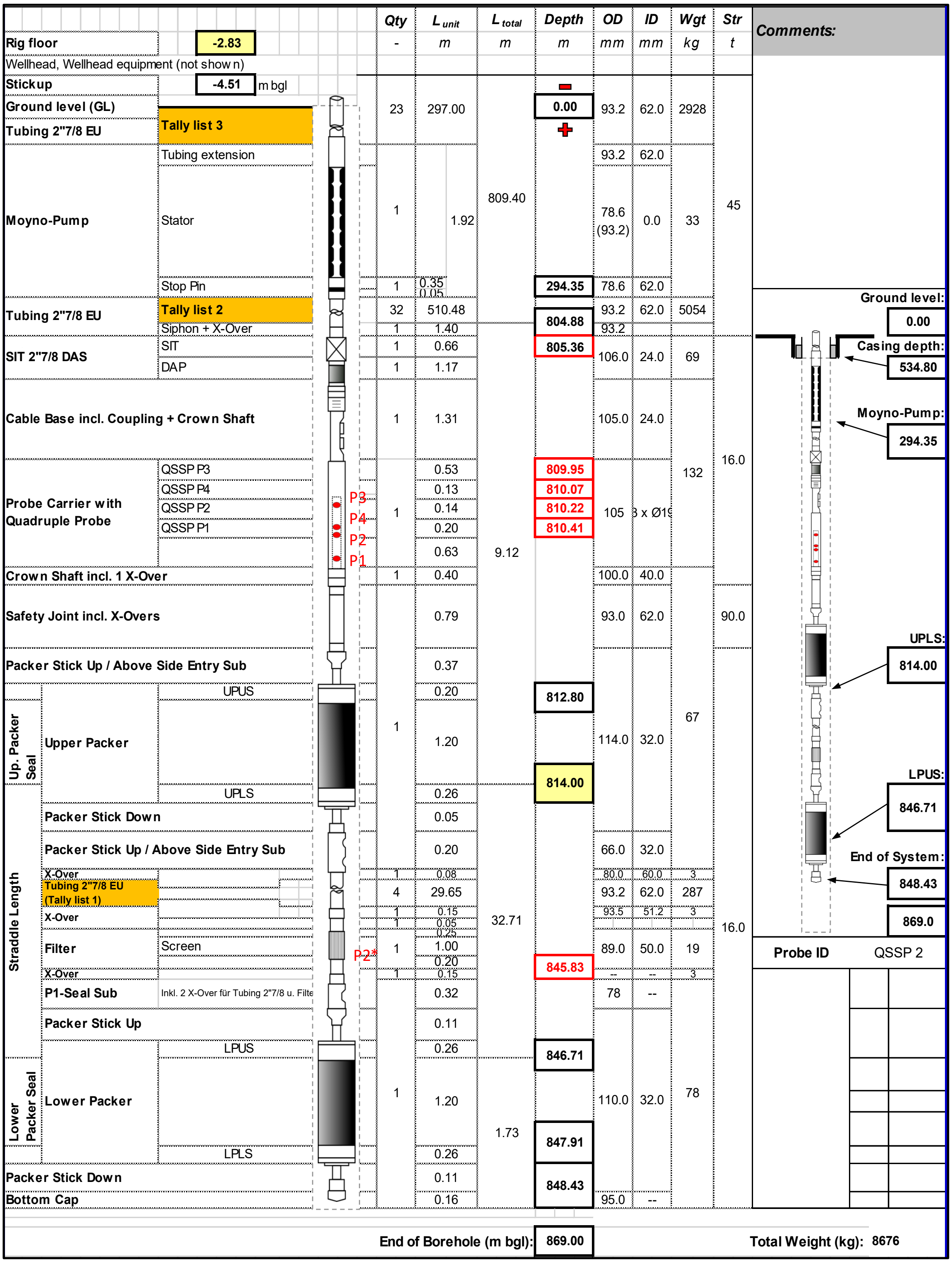

Fig. 4-14: Hydraulic test BUL1-1-BDO1: downhole equipment installation record with system layout as used in the field tests

The HDDP was lowered to the test interval position with regular checks of the QSSP pressure readings during system installation. The test was started by inflating the bottom packer (test phase INF part 1) followed by the top packer (INF part 2). The SIT was opened when the top packer began to isolate the interval volume. By this time the interval pressure started to increase (COM) caused by a further expansion of the packers. After 1 h, the SIT was closed and the 5.5 h long PSR phase initiated. Next, a pulse withdrawal test was conducted (PW) over a period of approximately 5.4 h followed by a slug withdrawal test with a flow phase (SW) of about 9.4 hand a subsequent shut-in phase (SWS) of 23.6 h. Prior to the slug test, a slim tubing with an inner diameter of 6 mm was lowered in the 2⅞" test tubing to a depth of 214 m below the top of the test string. The packer at the bottom of the slim tubing was inflated to a pressure of 25 bar using pressurised nitrogen. A pulse injection test (PI) was performed to complete the test sequence and lasted 3.5 h. The subsequent deflation (DEF) of the packers was carried out with the SIT closed. Fig. 4-10 shows an overview of the recorded pressure measurements.

4.5.1.3 Analysis

Borehole pressure history

A mean density of the drilling fluid of 1'099 kg/m^3 was calculated from the P3 pressure using the measured pressure at tool depth and the measured water (drilling fluid) table in the annulus. The borehole pressure history for interval BUL1-1-BDO1 is summarised in Tab. 4-20 and shown graphically in Fig. B-1.

Tab. 4-20: Hydraulic test BUL1-1-BDO1: borehole pressure history

Description	**Start date and time**	**Duration** [h]	**Pressure**[1)] [kPa]	
			Start	**End**
Drilling[2)]	08.06.2019 07:58	67.7	8'777.0	8'777.0
Preparation[3)]	11.06.2019 03:39	35.7	8'777.0	8'777.0
Start BUL1-1-BDO1	12.06.2019 15:22	-	8'776.9	-

1) Interval pressure at P2 sensor level (811.22 m bgl)
2) Drilling through interval midpoint
3) Includes POOH wireline coring system string, preparation and installation of hydraulic testing equipment

Flow model evaluation

The evaluation of the flow model used in the analysis is based on the analytical methods of PSR, SW and SWS.

For the analysis of PSR, a log-log diagnostic graph including the pressure derivatives was used. It shows a transition phase between the start phase dominated by the wellbore storage and slightly choppy late time data. The slug phase (SW) was analysed with a deconvoluted pressure curve (Peres et al. 1989) using a log-log diagnostic graph (Bourdet et al. 1989). The following shut-in phase (SWS) was also analysed using a log-log diagnostic graph, including the pressure derivatives, by correcting the time according to Agarwal (1980). Fig. B-2 provides the diagnostic graphs. No test sequence allowed the identification of an infinite acting radial flow region (IARF).

The existence of an IARF at later times can neither be confirmed nor excluded (there are no indications of an alternative flow model).

Due to the impact of the borehole pressure history on the pressure measured in the PW, the analysis focused on the later slug phase and the following shut-in phase, SW-SWS. The first and last pulse data were only referred to in order to confirm the analysis results later on.

Residual analysis as confirmation of the flow model

A residual analysis was conducted to check the suitability of a homogeneous and a radial composite 2-zone flow model based on parameter-optimised simulations using both flow models (Fig. B-3). Both residual distributions follow a normal distribution indicating the suitability for usage of the flow model (Fig. B-4). Due to strong correlations between inner and outer zone parameters in the composite model and the higher sensitivity of the formation parameters in the homogeneous model to pressure (sensitivity analysis plot, see Fig. B-5), a homogeneous flow model was preferred for the analysis of SW-SWS.

SW-SWS analysis

During the SW test phase, a total production volume of approximately 1.07 litres was calculated based on the pressure change measured in the test tubing. The best parameter values resulting from an optimisation (best fit) of a radial homogeneous flow model of the SW-SWS sequence correspond to the results of a perturbation analysis. The analysis was conducted to confirm the optimisation result as a global minimum of the objective function of the optimisation procedure (weighted sum of squared errors – SSE value).

Perturbation analysis of SW-SWS and determination of the reference case

The perturbation analysis was performed with 577 parameter optimisations covering the appropriate formation parameter range (K, S_s, P_f). A Latin hypercube sampling algorithm was used to completely cover the parameter space with a limited number of parameter sets (577 runs). A total of 480 runs of the resulting parameter set were clustered in a small sub-region of the parameter space indicating a global minimum of the objective function (see histogram in Fig. B-6). The Cartesian plot of the pressure curve using the resulting best parameter set of the formation parameters is shown in Fig. B-3. Scatter plots of the perturbation results are presented in Fig. B-7 and B-8 together with the corresponding SSE values. The values of the resulting best estimates as well as the resulting uncertainty ranges for the formation parameters are provided in Tab. 4-21. The results are referred to as reference case.

Tab. 4-21: Hydraulic test BUL1-1-BDO1: perturbation results applied for the reference case

Reference case	**K** [m/s]			**Ss** [1/m]			**Pf** [kPa]		
Perturbation result	$2.0 \cdot 10^{-12}$			$1.2 \cdot 10^{-6}$			7'068		
Uncertainty ranges	$8 \cdot 10^{-13}$	-	$4 \cdot 10^{-12}$	$7 \cdot 10^{-7}$	-	$5 \cdot 10^{-6}$	6'900	-	7'240

Uncertainty analysis

The influence of the observed temperature changes was investigated qualitatively. The resulting interval fluid volume change due to observed temperature changes was considered in the numerical simulation using linear thermal expansion. The thermal expansion coefficient used was equal to the thermal expansion coefficient of water, taking into account the mean interval temperature. A pressure change in the interval caused by changes in the interval fluid volume was considered in the numerical calculation based on the compressibility of the interval volume (measured for a closed volume at the start of PW and PI and reflecting the tubing radius for an open interval during SW). All numerical simulations presented consider the interval temperature changes in this manner, except for one simulation carried out to provide a qualitative statement on the influence of temperature changes. Fig. B-9 shows the difference between simulations considering temperature-induced pressure changes (best fit) in the interval and simulations that did not take temperature-induced pressure changes into account. The resulting pressure curves differ by 52.8 kPa after SW-SWS. The influence on SW and SWS is different reflecting the different test zone compressibilities.

The influence of the borehole pressure history as well as the significant packer pressure changes during testing on the resulting formation parameter estimation were investigated quantitatively. Two parameter optimisations were performed taking into account a 10% change in the mud density prior to the test. Tab. 4-22 presents the results.

Tab. 4-22: Hydraulic test BUL1-1-BDO1: results of pre-test borehole pressure variations

Optimisation case	**Mud density** [kg/m³]	**K** [m/s]	**ΔK/Kref** [%]	**Ss** [1/m]	**ΔSs/Ss ref** [%]	**Pf** [kPa]	**ΔPf/Pf ref** [%]
Reference	1'099	$2.0 \cdot 10^{-12}$	0	$1.2 \cdot 10^{-6}$	0	7'068	0
+10% change	1'210	$1.6 \cdot 10^{-12}$	-20	$1.5 \cdot 10^{-6}$	+33	6'835	-3
-10% change	990	$2.4 \cdot 10^{-12}$	+20	$0.9 \cdot 10^{-6}$	-33	7'281	+3

The results provided reflect the correlation between the parameters on the one hand, and the resulting uncertainty of the results according to pressure conditions not exactly known prior to the hydraulic test on the other hand.

The influence of packer pressure changes during the test were investigated with three parameter optimisations done for simulations considering a possible interval volume change due to packer pressure changes. The potential impact was also studied for other intervals and ranged in the same order as the one observed during the re-inflation at PSR (see Section 4.5.1.2). To consider the impact, a linear volume change per packer pressure change of 2, 4 and 10 ml/bar was assumed.

The interval volume change was implemented numerically by interval radius changes. Transmissivity changes due to radius changes were negligible (introduced maximum radius change of 3 µm). The resulting interval volume changes were transformed into pressure changes considering the compressibility of the test interval. Tab. 4-23 presents the results.

Tab. 4-23: Hydraulic test BUL1-1-BDO1: results of packer pressure variations

Optimisation case	**K** [m/s]	**ΔK/K$_{ref}$** [%]	**Ss** [1/m]	**ΔSs/Ss$_{ref}$** [%]	**P$_f$** [kPa]	**ΔP$_f$/P$_{f\,ref}$** [%]
Reference case	$2.0 \cdot 10^{-12}$	0	$1.2 \cdot 10^{-6}$	0	7'068	0
2 ml/bar	$1.9 \cdot 10^{-12}$	-5	$1.3 \cdot 10^{-6}$	+8	7'070	+0.3
4 ml/bar	$1.8 \cdot 10^{-12}$	-10	$1.4 \cdot 10^{-6}$	+17	7'094	+0.4
10 ml/bar	$1.5 \cdot 10^{-12}$	-25	$1.8 \cdot 10^{-6}$	+50	7'137	+1.0

To confirm the results and to estimate the confidence intervals of the parameter determination, two parameter optimisations were carried out for the two test phases that were not investigated in detail, namely PW and PI. The results are listed in Tab. 4-24. Fig. B-10 and B-11show Cartesian representations of both test phases. Due to density differences between interval and formation water, an additional perturbation analysis for the PI was performed and a skin value introduced for PI to consider the different flow behaviour.

Tab. 4-24: Hydraulic test BUL1-1-BDO1: results of single-phase evaluations

Optimisation case	**K** [m/s]	**SS** [1/m]	**Pf** [kPa]	**Skin**[1)] [-]
Reference case (SW-SWS)	$2.0 \cdot 10^{-12}$	$1.2 \cdot 10^{-6}$	7'068	0
PW	$4.9 \cdot 10^{-12}$	$7.2 \cdot 10^{-7}$	7'249	0
PI (parameter optimisation)	$9.0 \cdot 10^{-13}$	$2.0 \cdot 10^{-5}$	7'184	1.42
PI (perturbation)	$4.6 \cdot 10^{-13}$	$2.0 \cdot 10^{-5}$	6'910	1.01

[1)] Used for PI phase only

Overall confirmation simulation

Finally, a parameter optimisation (K, S_s, P_f) of a simulation over all recorded test phases (PSR-PI) was performed. This simulation confirms the previous results and shows the strong influence of the borehole pressure history on PSR and PW, and the different behaviour of the PI. Fig. B-12 provides a Cartesian plot of the simulation results. The resulting formation parameters are provided in Tab. 4-25. Again, due to density differences between interval and formation water, an additional perturbation analysis was performed and a skin value introduced for PI to consider the different flow behaviour.

Tab. 4-25: Hydraulic test BUL1-1-BDO1: results of overall phases performed parameter optimisation

Optimisation case	**K** [m/s]	**S_S** [1/m]	**P_f** [kPa]	**Skin**[1)] [-]
Reference case (SW-SWS)	$2.0 \cdot 10^{-12}$	$1.2 \cdot 10^{-6}$	7'068	0
Parameter optimisation	$8.9 \cdot 10^{-13}$	$6.7 \cdot 10^{-6}$	7'136	0
Perturbation	$9.4 \cdot 10^{-13}$	$6.9 \cdot 10^{-6}$	7'141	0.87

1) Used for PI phase only

4.5.2 Hydraulic packer test BUL1-1-MUK1

The hydraulic packer test BUL1-1-MUK1 is an example for testing in formations with medium to high transmissivity.

4.5.2.1 Interval characterisation

The hydraulic test BUL1-1-MUK1 was performed in a double packer configuration. The interval is located in the Schinznach Formation of the Muschelkalk Group. Details of the test interval and test duration are provided in Tab. 4-26.

The interval was of interest because the Schinznach Formation is a regional deep aquifer in northern Switzerland. The interval was selected because of the drilling fluid losses (dynamic loss of 2 m^3/h to 6 m^3/h occurred at 1'153 m and 0.3 m^3/h to 0.8 m^3/h from 1'156 m to 1'162 m, respectively, making up 5 m^3 in total). In addition, drill core information (cf. Dossier II) was taken into account for the interval selection. The cores in the interval showed small-sized open pores and a prominent sub-vertical fracture. The test objectives were to obtain reliable estimates of T (and K) of the formation, and of the freshwater hydraulic head. In addition, given sufficient productivity of the formation, a groundwater sample was to be collected.

Tab. 4-26: Hydraulic test BUL1-1-MUK1: information on test interval

Test	**Depth**		**Length**	**Packer confi-guration**	**Hydraulic testing**		
	from [m bgl]	to [m bgl]	[m]		Start date	End date	Duration [h]
BUL1-1-MUK1	1'137.70	1'173.73	36.03	DP[1)]	20.10.2019	22.10.2019	52.8

1) DP: Double packer

4.5.2.2 Test execution

Fig. 4-15 provides the system installation record. The equipment components are those described above.

The PC pump stator was integrated in the test tubing for potential groundwater sampling during a production phase. The stop pin of the PC pump was installed at a depth of 296.1 m bgl. The installed stator covered a flow range between 10.0 and 60.0 l/min. For the production phase, the PC pump equipped with the rotor suitable for a temperature range between 30 °C and 50 °C was used.

A heating blanket was installed on the flat-pack to reduce the influence of ambient temperature variations on the packer pressure. The packer pressure variations amounted to a maximum of about 10% of the inflation pressure.

The flow board was used to monitor the water produced during the production phase of BUL1-1-MUK1. The chemistry parameters pH, EC and Eh of the pumped water were measured with the chemistry probes installed in the chemistry cabinet. The O_2 concentration was not measured because it was below the lower bound of the measuring limit.

The test was started by the inflation of the bottom packer (test phase INF part 1) before the top packer (INF part 2) was inflated. The SIT remained closed and PSR started immediately after packer inflation (no COM phase was conducted as there was no significant pressure increase in the interval during inflation). The PSR phase continued for 6.8 h. Then, a pulse withdrawal test was conducted (PW) lasting 16 min.

A slug withdrawal test characterised by a flow phase (SW) of about 6 min was performed, during which a volume of 0.191 m^3 was produced. It was followed by a subsequent shut-in phase (SWS) of 8.4 h.

The sucker rods and PC pump rotor were installed in preparation for the planned pumping test and the associated groundwater sampling. The pump was started but it was hydraulically ineffective and had to be stopped. This caused a short pressure drawdown followed by a pressure build-up. These phases are denoted by the RW and RWS phases, respectively. After proper reconnection of the rods and the rotor, a step drawdown test was carried out with a duration of around 25 h and with medium flow rates of 5.9 l/min for about 10 min (step MR1), 25.3 l/min for about 30 min (step MR2), 27.34 l/min for 5.3 h (step MR3) and finally 45.0 l/min for 18.2 h (step MR4). In total, a volume of 57.1 m^3 was produced from the test interval including the volume from the slug test.

On 22.10.2019 at 06:09, an overpressure event in the chemistry cabinet due to water sampling activities at the water outlet caused leakage and a power outage in the measurement trailer as well as damage to the chemistry cabinet. The chemistry measurements could therefore not be continued. Hence, no chemistry data is available for the last 5.5 h of the step drawdown test (step MR4, cf. Fig. B-13).

Water sampling was started after a pumping period of about 18 h. Sampling was carried out by Hydroisotop on 22.10.2019 between 05:20 and 10:55. Thereafter, the pumping test was continued for 45 min with a constant extraction flow rate of 50.2 l/min, before the interval was shut in. The following recovery phase (MRS) lasted for 5.6 h. The subsequent deflation of the packers (DEF) was carried out with the SIT closed. Fig. 3-13 provides an overview of the recorded pressure measurements indicating the test sequences.

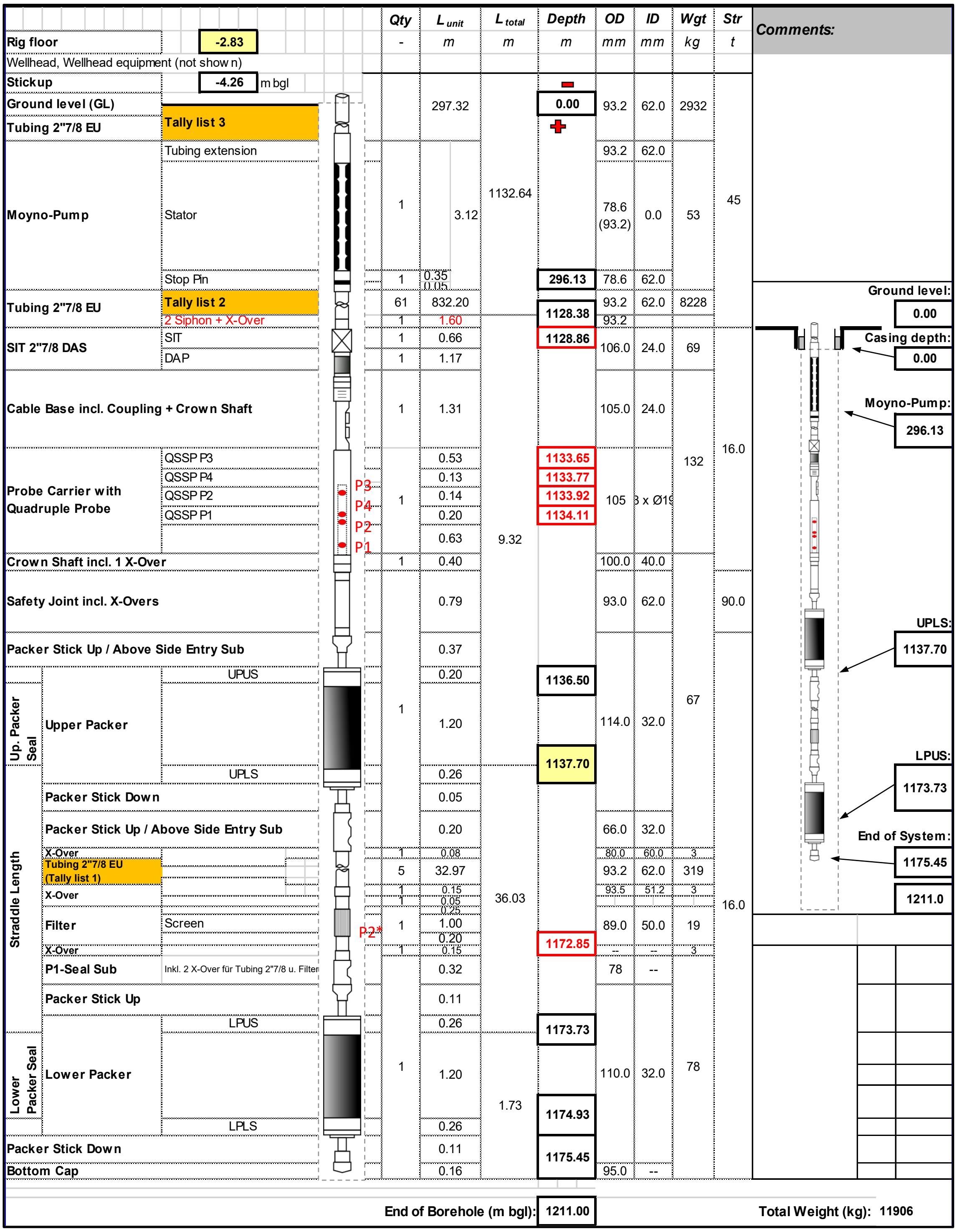

Fig. 4-15: Hydraulic test BUL1-1-MUK1: downhole equipment installation record with system layout as used in the field tests

4.5.2.3 Analysis

Borehole pressure history

A calculation of the mean fluid density yields a density of 1'169.8 kg/m^3 using the P3 pressure values of the QSSP prior to packer inflation, which was considered reliable and was further implemented.

The borehole pressure history for interval BUL1-1-MUK1 is summarised in Tab. 4-27 and illustrated in Fig. B-14.

Tab. 4-27: Hydraulic test BUL1-1-MUK1: borehole pressure history

Description	**Start date and time**	**Duration** [h]	**Pressure**[1)] [kPa]
Drilling[2)]	14.10.2019 06:32	59.4	13'034.9
Geophysical logging, round trip, additional drilling	16.10.2019 17:56	57.2	13'034.9
POOH coring system, stop circulation pump	19.10.2019 03:05	7.9	13'034.9
POOH coring system[3)]	19.10.2019 11:00	0.5	13'034.9
End of POOH of coring system	19.10.2019 11:30		12'369.9
Water table measurement[4)]	19.10.2019 14:50	26.5	12'455.2
Water table measurement[4)]	19.10.2019 19:10		12'567.1
Start RIH test system[5)]	19.10.2019 23:38		12'690.1
Water table measurement[4)]	20.10.2019 02:58		12'994.1
Water table measurement[4)]	20.10.2019 05:00		13'034.9
Testing BUL1-1-MUK1	20.10.2019 14:10	-	13'034.9

1) Interval pressure at P2-sensor level (1'133.92 m bgl)
2) Drilling through interval midpoint
3) POOH of the last three drill pipes finished at 11:30 (information from drilling supervisor and rig manager)
4) Cf. logbook
5) Estimated (extrapolated)

Flow model evaluation

The test phases allowing the evaluation of the flow behaviour are the shut-in phase after the slug test (SWS) and the pressure recovery phase following the step rate pumping test (MRS). The log-log diagnostic plots (Bourdet et al. 1989) for both shut-in phases (SWS, MRS) are displayed using the corrected production time according to Agarwal (1980) in Fig. B-15. The initial pressure recovery phase (PSR) is also displayed as a log-log plot in Fig. B-15.

The derivatives of the shut-in phases of the slug test (SWS) and the step rate pumping test (MRS) both show a continuously descending trend with a gradient close to - ½ (cf. Fig. B-15) at the middle and late stage of the test. This indicates that IARF conditions are unlikely and neither spherical nor radial flow behaviour is effective. The trend of the pressure derivative during the PSR phase (Fig. B-15, top plot) differs from the behaviour observed in the SWS and MRS phases. After a wellbore storage dominated phase at early time, the derivative shows a large transition phase ending in a downward trend, which illustrates the incomplete recovery of the initial pressure recovery phase (PSR).

To account for the flow behaviour resulting from the analytical flow model evaluation, and supported by the drill cores showing fractures in sub-vertical directions, the generalised radial flow model referred to as GRF model (Barker 1988) was used in the numerical analysis.

Residual analysis as confirmation of the flow model

The suitability of the chosen flow model was confirmed by the residual analysis of a Cartesian simulation of the MR-MRS sequence (step rate pumping test and pressure recovery phase). In the parameter optimisation leading to this simulation the flow dimension n (besides the hydraulic conductivity, the specific storage and the formation pressure) was implemented as a fitting parameter ranging between 1 (linear) and 3 (spherical). The residuals of the simulation follow a normal distribution or a cumulative normal distribution function (cf. Fig. B-16) for a flow dimension between 2 (radial) and 3 (spherical flow), which confirms the GRF model being suitable for representing the flow behaviour observed.

MR-MRS analysis

The numerical analysis focused on the MR-MRS sequence and covered the largest part of the test time. The simulation of the preceding test phases PW, SW and SWS exhibited incoherent behaviour compared to the simulation of the MR-MRS sequence. This is caused by the relatively long borehole pressure history biasing especially the PSR and PW phase and the limited duration of the SWS phase (i.e. limited radius of influence in comparison to MR-MRS).

For the determination of the hydraulic conditions in the tested formation (K, S_S, P_f), a generalised flow model with infinite lateral extent, wellbore storage and fractional flow dimension was applied in the numerical analysis. The parameter values of the resulting estimate obtained by an optimisation algorithm for the formation parameters are provided in Tab. 4-28. The simulated pressure and rates used in comparison to the measured data are presented in Fig. B-17.

Tab. 4-28: Hydraulic test BUL1-1-MUK1: reference fit parameter set

Reference case	**K** [m/s]	**S_S** [1/m]	**P_f** [kPa]	**n** [-]
Optimisation result	$4.8 \cdot 10^{-8}$	$2.4 \cdot 10^{-6}$	10'796.9	2.6

Sensitivity analysis

The sensitivity analysis yielded a low sensitivity for the specific storage (S_S) in comparison to the other fitting parameters (P_f, K and n) as shown by the scaled sensitivity (cf. Fig. B-18). The sensitivity of the static pressure (P_f) was high throughout the whole sequence. The sensitivity of the hydraulic conductivity parameter (K) was high during production phases but diminished to a relatively low sensitivity during pressure recovery (MRS). The same applies to the flow dimension; its sensitivity was relatively high during the production phase but decreased rapidly in the pressure recovery phase.

Perturbation analysis

The perturbation analysis was performed with 500 parameter optimisations covering the appropriate formation parameter range (K, S_s, P_f, n). A Latin hypercube sampling algorithm was used to completely cover the parameter space with a limited number of parameter sets (500 runs). Scatter plots of the perturbation results are presented in Fig. B-19 and B-20 in association with the corresponding SSE values. Fig. B-21 provides histograms of the optimised parameter distribution (K, S_S, P_f) calculated for all 500 runs of the perturbation analysis. The results seem to be well defined, however, a local minimum seems to exist for a radial flow dimension (n = 2) because it is possible to recognise a near normal distribution around the radial flow dimension.

The reference parameter values resulting from an optimisation of a radial generalised flow model of the MR-MRS sequence correspond well to the results of the perturbation analysis conducted to confirm the optimisation result as the global minimum of the objective function of the optimisation procedure (weighted sum of squared errors – SSE value). The resulting parameter values as well as their uncertainty ranges are presented in Tab. 4-29.

Tab. 4-29: Hydraulic test BUL1-1-MUK1: perturbation results

	K [m/s]	**S_S** [1/m]	**P_f** [kPa]	**n** [-]
Perturbation result	$4.8 \cdot 10^{-8}$	$2.3 \cdot 10^{-6}$	10'797.0	2.59
Uncertainty ranges	$3.4 \cdot 10^{-8} – 6.4 \cdot 10^{-8}$	$3 \cdot 10^{-7} – 7 \cdot 10^{-6}$	10'792 – 10'800	2.4 – 2.8

Uncertainty analysis

To assess the robustness of the resulting parameter values, the evaluation included, besides the already mentioned residual analysis, sensitivity and perturbation analyses as well as a non-fitting analysis of the flow dimension parameter n performed on the MR-MRS sequence. The parameter sets provided in Fig. B-22 were evaluated by a parameter optimisation in which the flow dimension parameter n was sampled 100 times. Tab. 4-30 provides the parameter values obtained for the lowest SSE.

Tab. 4-30: Hydraulic test BUL1-1-MUK1: non-fitting parameter analysis of flow dimension

	K [m/s]	**S_s** [1/m]	**P_f** [kPa]	**n** [-]
Parameter set of lowest SSE	$4.4 \cdot 10^{-8}$	$2.2 \cdot 10^{-6}$	10'796.9	2.6

Overall confirmation simulation

Finally, a parameter optimisation (K, S_s, P_f, n) of all recorded active test phases (PW – MRS) was performed. A Cartesian plot of the simulation results is provided in Fig. B-23. The resulting formation parameter set is provided in Tab. 4-31.

The visually assessed quality of the match of the simulated data to the measured pressure values is considered good.

Tab. 4-31: Hydraulic test BUL1-1-MUK1: overall simulation parameter set

	K [m/s]	**S_s** [1/m]	**P_f** [kPa]	**n** [-]
Optimisation result	$4.8 \cdot 10^{-8}$	$1.1 \cdot 10^{-6}$	10'787.2	2.6

5 Summary and discussion

5.1 Drilling fluid monitoring

Losses of drilling fluid were only detected by mud logging at a depth of 1'153.0 m and at 1'156.0 to 1'162.0 m in the Schinznach Formation, which were further investigated within the test interval BUL1-1-MUK1.

The mud logging data were the basis for establishing the borehole pressure history needed for the analysis of the hydraulic packer tests.

5.2 Hydraulic packer test data and results

5.2.1 Description of tests

Seven hydraulic packer tests were performed within six test intervals in the borehole BUL1-1 between May and October 2019. All tests were performed in the cored borehole section using an HDDP packer system in single packer or double packer configuration (cf. Tab. 4-18).

Three hydraulic packer tests focused on fractured and karstic limestones of the Malm group ('Felsenkalke'/'Massenkalk'): BUL1-1-MAL1, BUL1-1-MAL2 and BUL1-1-MAL3. Two hydraulic packer tests focused on the Dogger Group ('Herrenwis Unit' to Wedelsandstein Formation): BUL1-1-BDO1 and BUL1-1-BDO2. One hydraulic packer test was performed in the heterogeneous sequence of marls, sandstones anhydrites of the Keuper Group: BUL1-1-KEU1. The final hydraulic packer test investigated the fractured section of the Muschelkalk Group (Schinznach Formation): BUL1-1-MUK1.

No tests could be performed in the Opalinus Clay at the base of the Dogger Group, and in the Lias Group. Instabilities in this section of the borehole prevented any hydraulic testing.

5.2.2 Overview tables and plots

The results of the transmissivity and hydraulic conductivity estimations for all tested intervals are summarised in Tab. 5-1. The estimated freshwater hydraulic heads and static formation pressures are documented in Tab. 5-2. Both tables present the best estimates along with confidence ranges.

The permeabilities for all tested intervals are summarised in Tab. 5-3. They were calculated based on the hydraulic conductivities provided in Chapter 4.5 and Tab. 5-1 and assumed a density of 1'000 kg/m^3 and dynamic viscosity of $1 \cdot 10^{-3}$ Pa s.

The hydraulic parameters T, K, P_{int} and h_s (in terms of m bgl and m asl) are illustrated with respect to the borehole depth and the geological profile in Fig. 5-1 to 5-5. The best estimates are indicated by vertical lines in the corresponding interval position. The confidence ranges are shown as dashed rectangles, delimited vertically by the corresponding interval extent and laterally by the minimum and maximum values.

Tab. 5-1: Summary of hydraulic packer testing in borehole BUL1-1: transmissivity and hydraulic conductivity

Test interval details and hydraulic model							Transmissivity and hydraulic conductivity					
Test name	**Interval depth**				**Interval length**	**Hydraulic model**	**Best estimates**		**Lowest estimates**[1)]		**Highest estimates**[1)]	
	From [m bgl]	**To** [m bgl]	**From** [m asl]	**To** [m asl]	[m]		**T** [m^2/s]	**K** [m/s]	$\mathbf{T_{min}}$ [m^2/s]	$\mathbf{K_{min}}$ [m/s]	$\mathbf{T_{max}}$ [m^2/s]	$\mathbf{K_{max}}$ [m/s]
BUL1-1-MAL1	537.20	545.00	-147.58	-155.38	7.80	2 zones radial composite	$1.5\cdot10^{-11}$	$1.9\cdot10^{-12}$	$3.2\cdot10^{-12}$	$4.1\cdot10^{-13}$	$1.6\cdot10^{-11}$	$2.1\cdot10^{-12}$
BUL1-1-MAL2/3	608.80	641.51	-219.18	-251.89	32.71	2 zones radial composite	$8.5\cdot10^{-7}$	$2.6\cdot10^{-8}$	$5.9\cdot10^{-7}$	$1.8\cdot10^{-8}$	$2.9\cdot10^{-6}$	$9.0\cdot10^{-8}$
BUL1-1-BDO1	814.00	846.71	-424.38	-457.09	32.71	radial homogeneous	$6.5\cdot10^{-11}$	$2.0\cdot10^{-12}$	$2.6\cdot10^{-11}$	$8.0\cdot10^{-13}$	$1.1\cdot10^{-10}$	$3.5\cdot10^{-12}$
BUL1-1-BDO2	848.20	869.00	-458.58	-479.38	20.80	2 zones radial composite	$4.6\cdot10^{-11}$	$2.2\cdot10^{-12}$	$1.7\cdot10^{-11}$	$8.0\cdot10^{-13}$	$2.1\cdot10^{-10}$	$1.0\cdot10^{-11}$
BUL1-1-KEU1	1'052.23	1'074.00	-662.61	-684.38	21.77	radial homogeneous	$2.0\cdot10^{-8}$	$9.3\cdot10^{-10}$	$1.5\cdot10^{-8}$	$7.0\cdot10^{-10}$	$3.3\cdot10^{-8}$	$1.5\cdot10^{-9}$
BUL1-1-MUK1	1'137.70	1'173.73	-748.08	-784.11	36.03	generalised homogeneous	$1.7\cdot10^{-6}$	$4.8\cdot10^{-8}$	$1.2\cdot10^{-6}$	$3.4\cdot10^{-8}$	$2.3\cdot10^{-6}$	$6.4\cdot10^{-8}$

1) The lowest and highest estimates for a given parameter are based on the determined uncertainty intervals.

Tab. 5-2: Summary of hydraulic packer testing in borehole BUL1-1: hydraulic head estimates

The results for hydraulic head and formation pressure refer here to the midpoint of the test interval.

Test interval details and hydraulic model							**Hydraulic head** [m bgl][1)]			**Hydraulic head** [m asl][1)]			**Formation pressure**[1)]		
Test name	**Interval depth**				**Interval length**	**Hydraulic model**	**Best** h_s	**Lowest** h_{min}	**Highest** h_{max}	**Best** h_s	**Lowest** h_{min}	**Highest** h_{max}	**Best** P_{int}	**Lowest** P_{min}	**Highest** P_{max}
	From [m bgl]	**To** [m bgl]	**From** [m asl]	**To** [m asl]	[m]		[m bgl]	[m bgl]	[m bgl]	[m asl]	[m asl]	[m asl]	[kPa]	[kPa]	[kPa]
BUL1-1-MAL1	537.20	545.00	-147.58	-155.38	7.80	2 zones radial composite	40	44	-13	349	346	402	4’912	4’878	5’432
BUL1-1-MAL2/3	608.80	641.51	-219.18	-251.89	32.71	2 zones radial composite	11	17	10	378	373	380	6’022	5’966	6’036
BUL1-1-BDO1	814.00	846.71	-424.38	-457.09	32.71	Radial homogeneous	88	105	70	302	285	320	7’287	7’119	7’459
BUL1-1-BDO2	848.20	869.00	-458.58	-479.38	20.80	2 zones radial composite	-115	-100	-171	505	490	561	9’551	9’405	10’105
BUL1-1-KEU1	1'052.23	1'074.00	-662.61	-684.38	21.77	Radial homogeneous	58	71	34	331	318	355	9’858	9’728	10’091
BUL1-1-MUK1	1'137.70	1'173.73	-748.08	-784.11	36.03	Generalised homogeneous	32	34	29	358	355	360	11’028	11’002	11’052

1) The lowest and highest estimates for a given parameter are based on the determined uncertainty intervals.

Tab. 5-3: Summary of hydraulic packer testing in borehole BUL1-1: permeability

Test interval details						**Permeability estimate**[1)]		
Test name	**Interval depth**				**Interval length**	**Best k**	**Lowest**[2)] k_{min}	**Highest**[2)] k_{max}
	From [m bgl]	**To** [m bgl]	**From** [m asl]	**To** [m asl]	[m]	[m^2]	[m^2]	[m^2]
BUL1-1-MAL1	537.20	545.00	-147.58	-155.38	7.80	$1.9 \cdot 10^{-19}$	$4.2 \cdot 10^{-20}$	$2.1 \cdot 10^{-19}$
BUL1-1-MAL2/3	608.80	641.51	-219.18	-251.89	32.71	$2.7 \cdot 10^{-15}$	$1.8 \cdot 10^{-15}$	$9.2 \cdot 10^{-15}$
BUL1-1-BDO1	814.00	846.71	-424.38	-457.09	32.71	$2.0 \cdot 10^{-19}$	$8.2 \cdot 10^{-20}$	$3.6 \cdot 10^{-19}$
BUL1-1-BDO2	848.20	869.00	-458.58	-479.38	20.80	$2.2 \cdot 10^{-19}$	$8.2 \cdot 10^{-20}$	$1.0 \cdot 10^{-18}$
BUL1-1-KEU1	1'052.23	1074.00	-662.61	-684.38	21.77	$9.5 \cdot 10^{-17}$	$7.1 \cdot 10^{-17}$	$1.5 \cdot 10^{-16}$
BUL1-1-MUK1	1'137.70	1173.73	-748.08	-784.11	36.03	$4.9 \cdot 10^{-15}$	$3.5 \cdot 10^{-15}$	$6.5 \cdot 10^{-15}$

1) The calculation is based on the hydraulic conductivity and standard conditions (density: 1'000 kg/m^3, dynamic viscosity: $1 \cdot 10^{-3}$ Pa s).

2) The lowest and highest estimates for a given parameter are based on the determined uncertainty intervals.

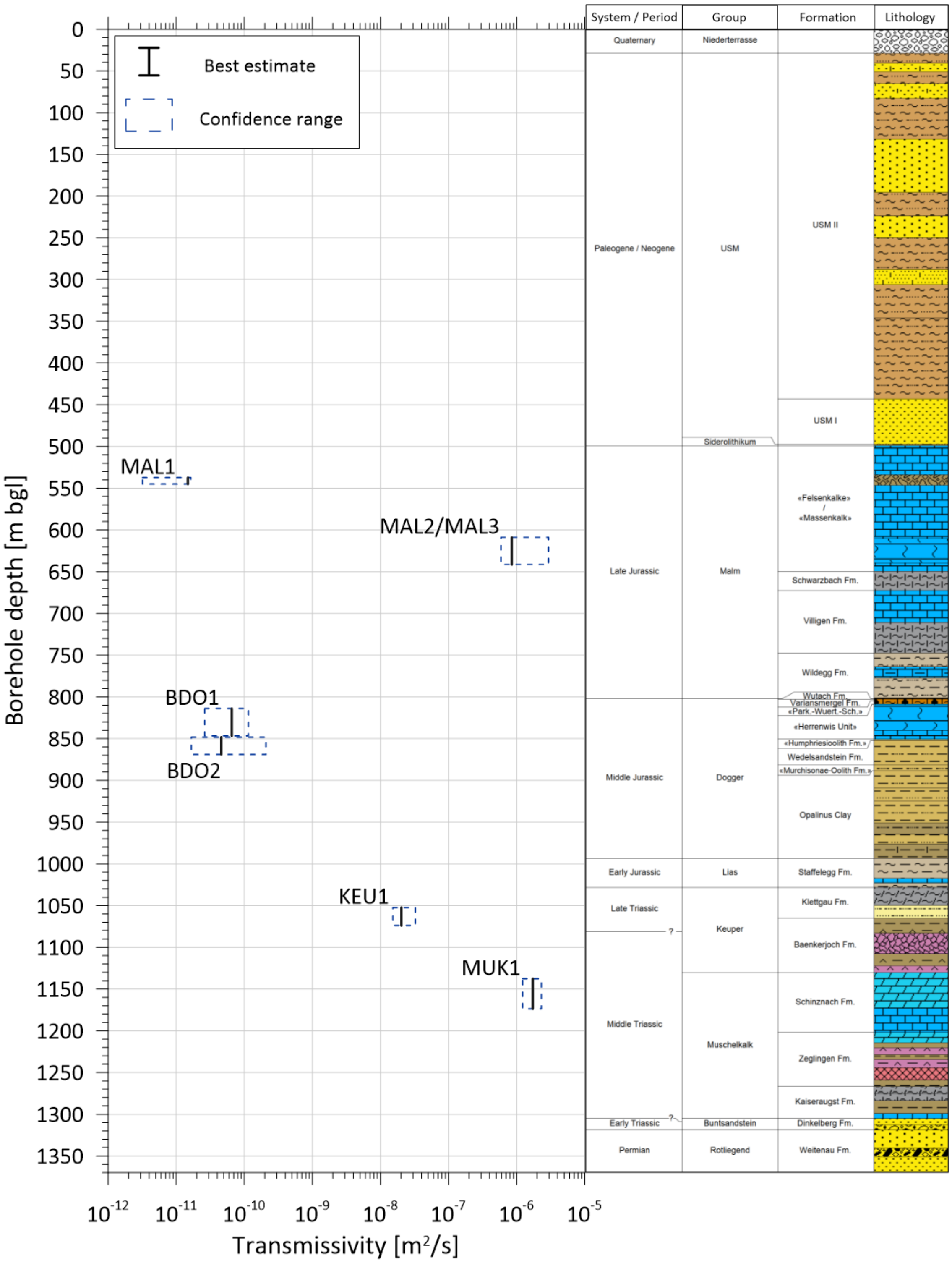

Fig. 5-1: Summary of hydraulic testing in borehole BUL1-1: transmissivity profile

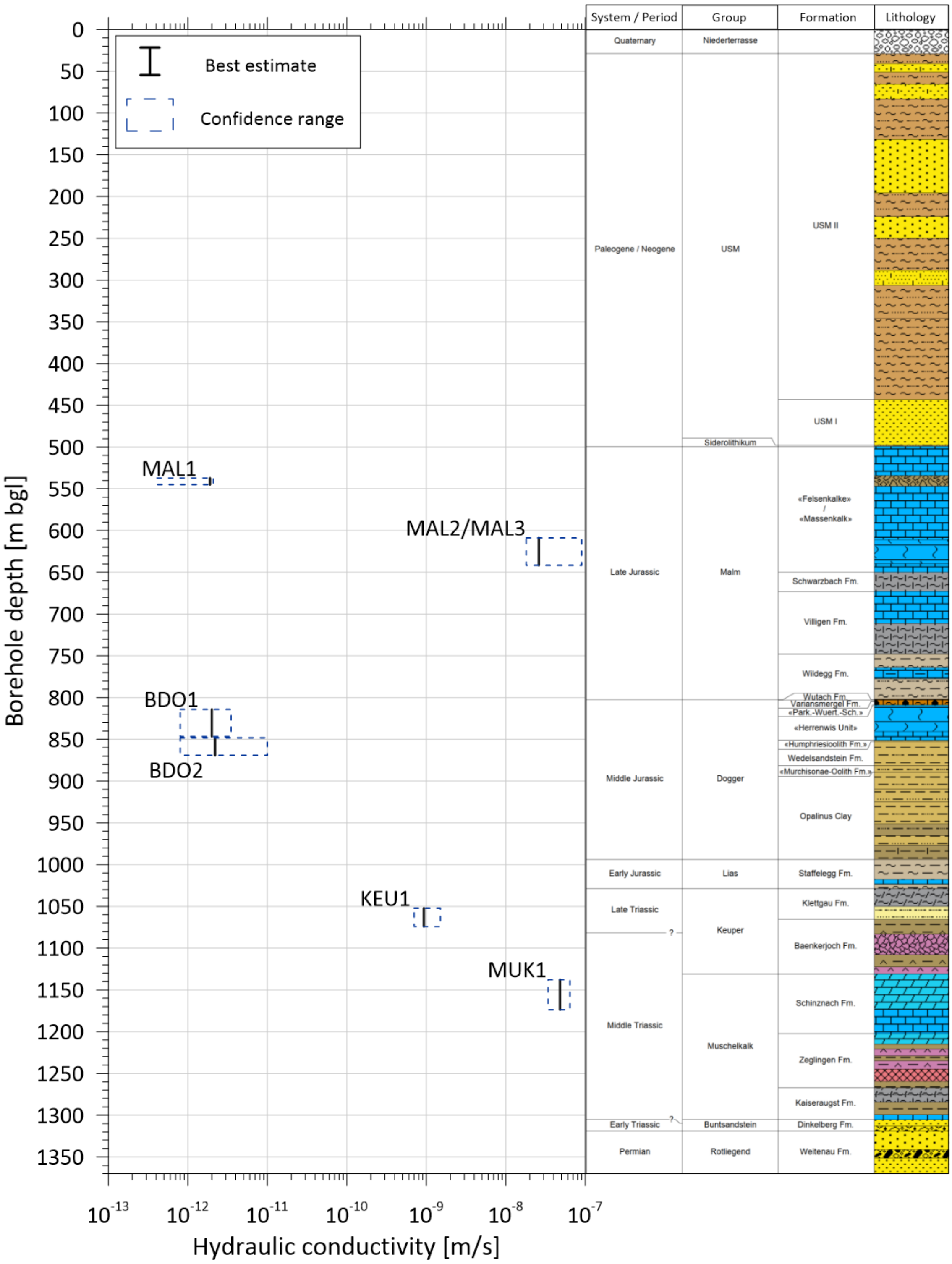

Fig. 5-2: Summary of hydraulic testing in borehole BUL1-1: hydraulic conductivity profile

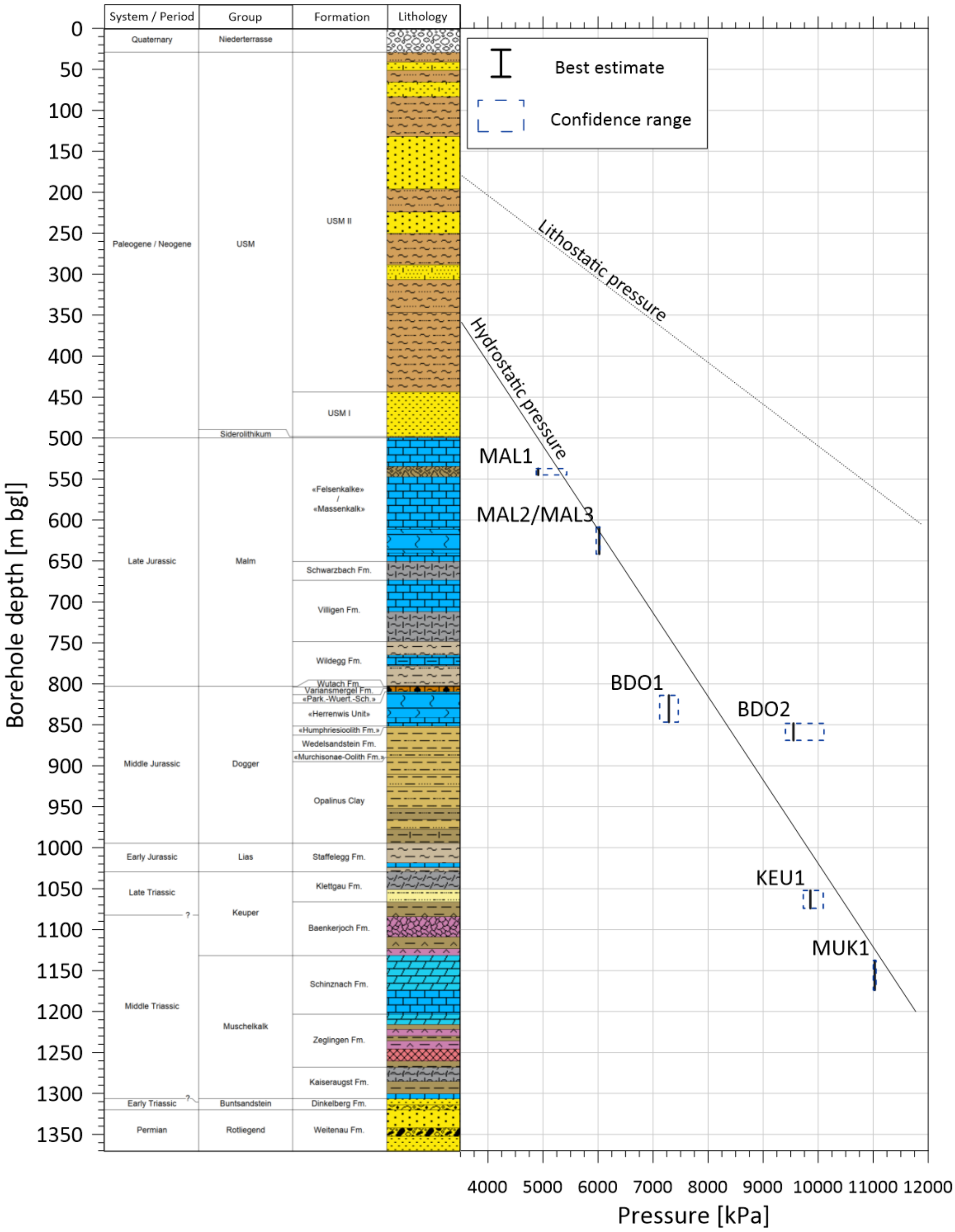

Fig. 5-3: Summary of hydraulic testing in borehole BUL1-1: static formation pressure profile

The results for formation pressure refer here to the midpoint of the test interval (P_{int}).

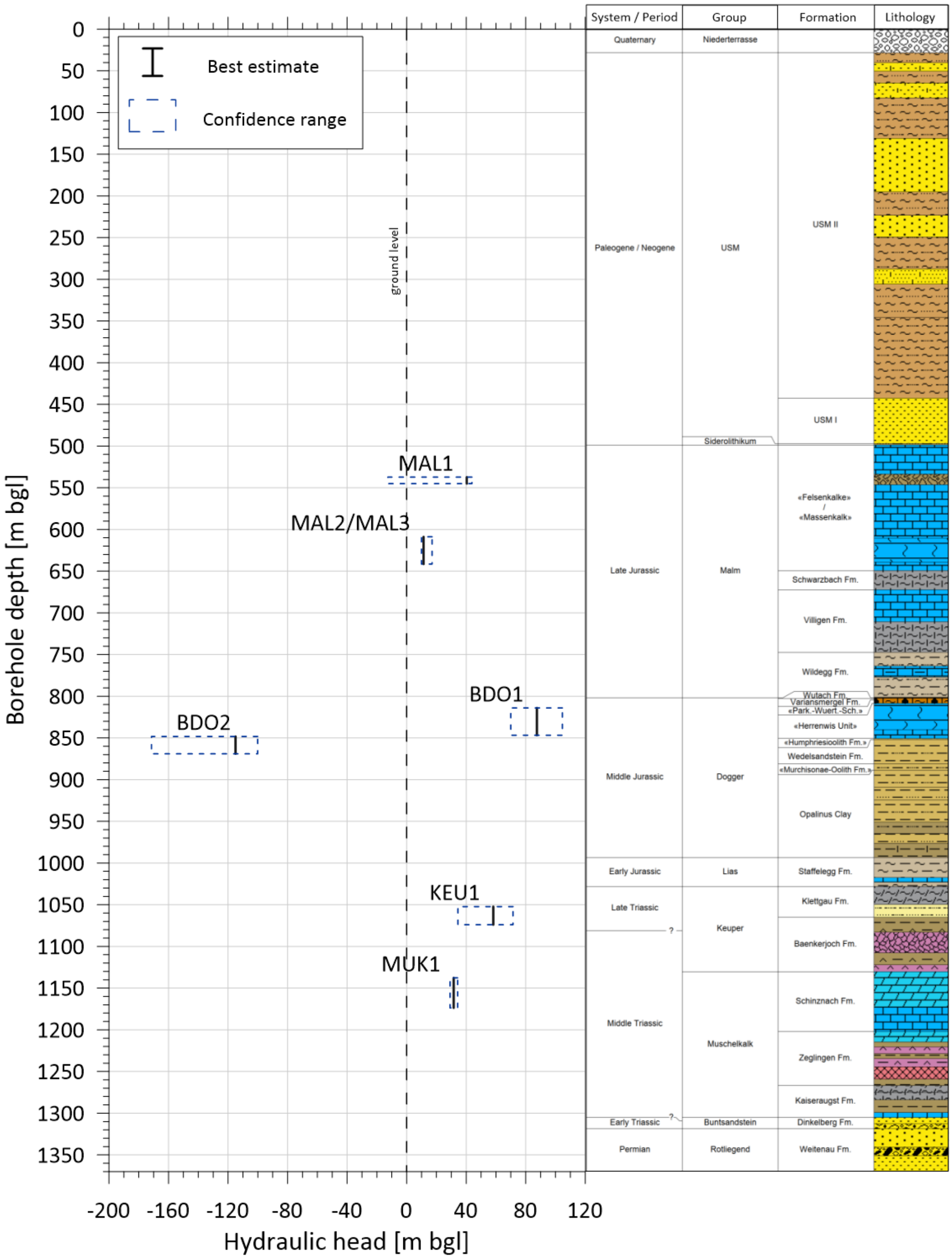

Fig. 5-4: Summary of hydraulic testing in borehole BUL1-1: hydraulic head profile (m bgl)

The results for hydraulic head refer here to the midpoint of the test interval and are freshwater heads.

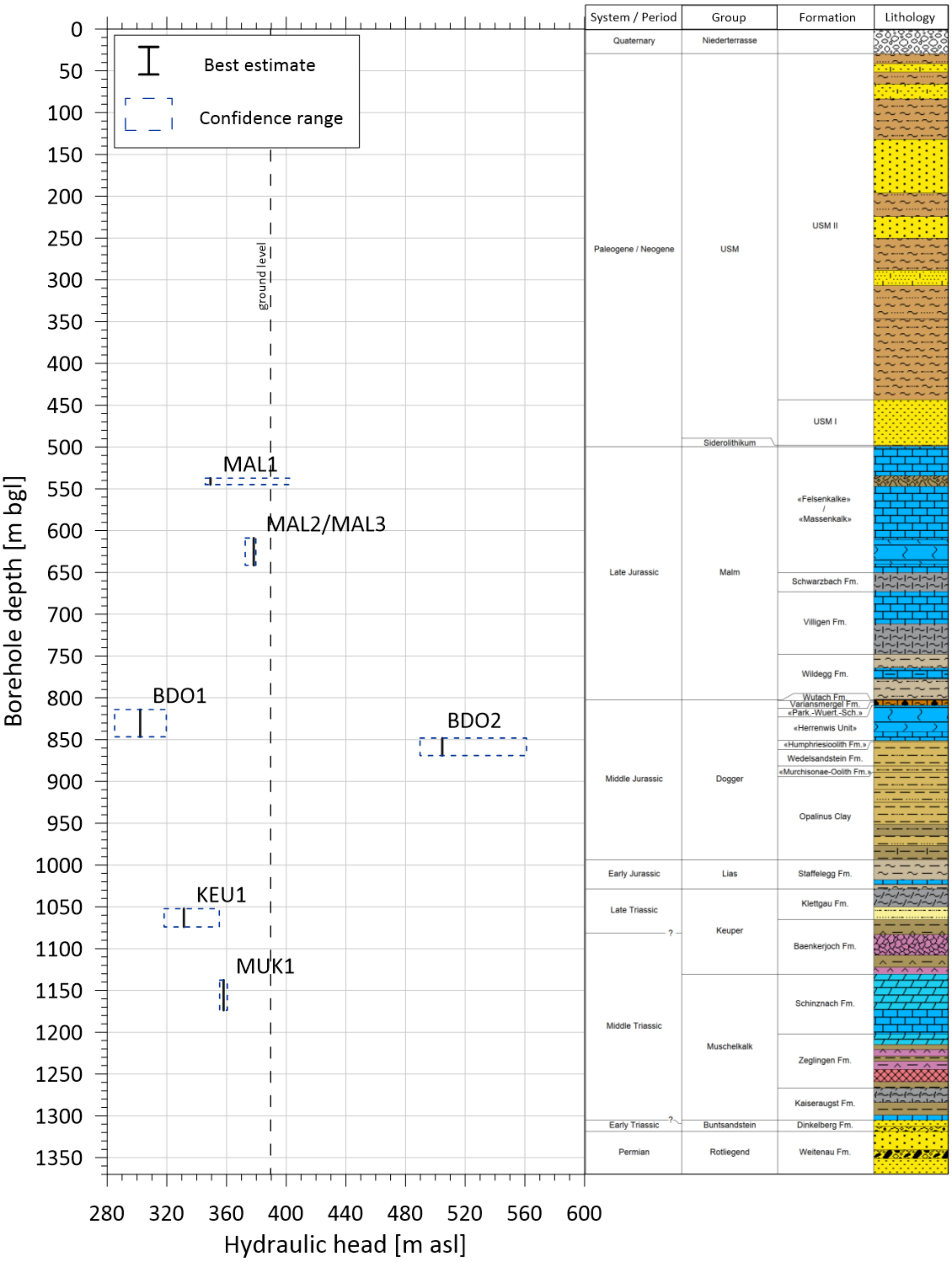

Fig. 5-5: Summary of hydraulic testing in borehole BUL1-1: hydraulic head profile (m asl)

The results for hydraulic head refer here to the midpoint of the test interval and are freshwater heads.

5.2.3 Discussion of data and results

The recorded measurements are of high accuracy and quality. Very few short interruptions in the data acquisition were reported and did not influence the analyses due to their times of occurrence and duration (and were consequently neglected).

When the surface temperature varied strongly, pressure changes (in the range of ± 200 – 500 kPa) in the packer inflation lines occurred. These packer pressure changes affected the pressure in some test intervals, but could be corrected in the detailed analysis.

The best estimates and the uncertainty of all results were quantitatively assessed and are defendable. The results of the analysis for the hydraulic conductivities and transmissivities were found to be reliable. They lie within a reasonable range within the expected range of values for the evaluated formations (e.g. Nagra 2008, Nagra 2014).

Similarly, the ranges for the hydraulic head are within what would be expected and are considered reliable (Luo et al. 2014). This applies in particular to the two recovery phases after the pumping tests were conducted in BUL1-1-MAL3 and BUL1-1-MUK1. However, the hydraulic head estimated for BUL1-1-BDO2 appears to be affected by an overestimation and has to be considered as 'apparent'. Both hydraulic tests, BUL1-1-BDO1 and BUL1-1-BDO2, were conducted within borehole intervals with low transmissivity (Dogger Group). The estimated hydraulic conductivity (best estimate) differs by only 10 %. The best estimates of the hydraulic heads however differ by 200 m, which was assessed to be unrealistic given the short distance between both test intervals. Test BUL1-1-BDO1 shows the lowest hydraulic head, but fits better to the overall picture and to the observed trend in the Benken long-term monitoring data. The reason for the overestimation of the hydraulic head for the test BUL1-1-BDO2 may be the long duration of pressure history. The interval pressure history differs by approximately a factor of 3 (BUL1-1-BDO1 ~ 100 h, BUL1-1-BDO2 ~ 300 h). In addition, temperature effects and mechanical processes in the formation may not have been represented adequately in the numerical analysis tool.

5.3 Summary

Borehole BUL1-1 was the first TBO borehole drilled in the siting region Nördlich Lägern. A total of six test intervals were investigated in borehole BUL1-1 by means of hydraulic packer tests. Due to borehole instabilities the planned tests in the Opalinus Clay and the Lias Group could not be performed. However, it was possible to study the hydraulic barrier properties of the upper confining geological units above the Opalinus Clay. In addition, the regional aquifers Malm and Muschelkalk and the potential Keuper aquifer (Klettgau Formation) could be investigated. The results were assessed as reliable, except for the hydraulic head estimation of BUL1-1-BDO2, which was assessed as 'apparent'.

The pressures and rates measured during all tests are illustrated in Fig. 4-7 to 4-13. Two hydraulic test analyses were selected to present the general analysis procedure as well as single effects taken into account for the analyses of hydraulic tests in formations with low or medium to high transmissivity. Sections 4.5.1 and 4.5.2 provide overviews of parts of the performed analyses for the hydraulic tests BUL1-1-BDO1 and BUL1-1-MUK1, respectively.

Two tests could be conducted in the Malm Group. While the hydraulic conductivity of the first one (BUL1-1-MAL1), which was performed on a calcareous breccia with claystone matrix showing faults and joints, was very low, the hydraulic conductivity of the second one (BUL1-1-MAL2 and MAL3), which was performed on cm-sized open karst cavities, was high and groundwater samples could be taken. In addition, a pumping test and groundwater sampling could be performed in the Schinznach Formation of the Muschelkalk Group. The transmissivity of the tested section of the Keuper Group was too low for pumping and for taking a groundwater sample.

In the Dogger Group the 'Herrenwis Unit' to Wedelsandstein Formation could be investigated by tests BUL1-1-BDO1 and BUL1-1-BDO2. The transmissivities were very low.

All hydraulic tests were supported by an on-site field analysis to optimise the test procedure.

6 References

Agarwal, R.G. (1980): A New Method to Account for Producing Time Effects When Drawdown Type Curves Are Used to Analyze Pressure Buildup and Other Test Data, Society of Petroleum Engineers, SPE Paper 9289, presented at SPE-AIME Meeting, Dallas, Texas, September 21-24.

Barker, J.A. (1988): A generalized radial flow model for hydraulic tests in fractured rock. Water Resources Research, Vol. 24 (10), pp. 1796-1804.

Bourdet, D., Ayoub, J.A. & Pirard, Y.M. (1989): Use of Pressure Derivative in Well-Test Interpretation. Society of Petroleum Engineers, SPE Formation Evaluation, pp. 293-302.

Bredehoeft J.D. & Papadopulos, S.S. (1980): A Method for Determining the Hydraulic Properties of Tight Formations. Water Resources Research, Vol. 16 (1), pp. 233-238.

Cooper, H.H. JR., Bredehoeft, J.D. & Papadopulos, S.S. (1967): Response of a Finite-Diameter Well to an Instantaneous Charge of Water, Water Resources Research, First Quarter 1967, pp. 263-269.

Grauls, D. (1999): Overpressures: Causal mechanisms, conventional and hydromechanical approaches. Oil & Gas Science and Technology – Rev. IFP 54, 667-678.

Isler, A., Pasquier, F. & Huber, M. (1984): Geologische Karte der zentralen Nordschweiz 1:100'000. Herausgegeben von der Nagra und der Schweiz. Geol. Komm.

Jäggi, K. & Vogt, T. (2020): OPA: Sondierbohrung Benken, Langzeitbeobachtung 2019, Dokumentation der Messdaten. Nagra Arbeitsbericht NAB 20-05, Nagra, Wettingen, Switzerland.

Lorenz, G.D. (2020): Borehole BUL1-1 (Bülach): Fluid sampling and analytical hydrochemical data report. Unpubl. Nagra Interner Bericht.

Luo, J., Monningkoff, B. & Becker, J.K. (2014): Hydrogeological model Nördlich Lägern. Nagra Arbeitsber. NAB 13-25.

Marschall, P., Croisé, J., Schlickenrieder, L., Boisson, J.Y., Vogel, P. & Yamamoto, S. (2003): Synthesis of hydrogeological investigations at the Mont Terri site (Phases 1–5). Mont Terri Tech. Rep. TR2001-02.

Nagra (1997): Hydrological Investigations at Wellenberg: Hydraulic Packer Testing in Boreholes SB4a/v and SB4a/s. Methods and Field Results. Nagra Technischer Bericht NTB 95-02.

Nagra (2001): Sondierbohrung Benken – Untersuchungsbericht. Nagra Technischer Bericht NTB 00-01.

Nagra (2008): Vorschlag geologischer Standortgebiet für das SMA- und das HAA-Lager – Geologische Grundlagen. Nagra Technischer Bericht. NTB 08-04.

Nagra (2014): SGT Etappe 2: Vorschlag weiter zu untersuchender geologischer Standortgebiete mit zugehörigen Standortarealen für die Oberflächenanlage. Geologische Grundlagen. Dossier II: Sedimentologische und tektonische Verhältnisse. Nagra Technischer Bericht NTB 14-02.

Nagra (2014): SGT Etappe 2: Vorschlag weiter zu untersuchender geologischer Standortgebiete mit zugehörigen Standortarealen für die Oberflächenanlage. Geologische Grundlagen. Dossier VI, Barriereneigenschaften der Wirt- und Rahmengesteine. Nagra Technischer Bericht. NTB 14-02.

Nagra (2017): Gesuch um Erteilung einer Bewilligung für erdwissenschaftliche Untersuchungen im Standortgebiet Nördlich Lägern (NL) – Sondierbohrungen Bülach. Nagra Sondiergesuch NSG 17-02.

Nagra (2019): Implementation of the Full-scale Emplacement Experiment at Mont Terri: Design, Construction and Preliminary Results. Nagra Technischer Bericht NTB 15-02.

Peres, A.M., Onur, M. & Reynolds, A.C. (1989). A new analysis procedure for determining aquifer properties from slug test data. Water Resources Research, Vol. 25 (7), pp. 1591-1602.

Pietsch, J. & Jordan, P. (2014): Digitales Höhenmodell Basis Quartär der Nordschweiz – Version 2013 (SGT E2) und ausgewählte Auswertungen. Nagra Arbeitsbericht NAB 14-02.

Swiss Federal Office of Energy (SFOE) (2008): Sectoral Plan for Deep Geological Repositories, Conceptual Part. Swiss Federal Office of Energy, Bern, Switzerland.

Appendix A: Abbreviations, nomenclature and definitions

Tab. A-1: Geological formation abbreviations for test names in BUL1-1

Geological formation	**Abbreviation**
Malm	MAL
Brauner Dogger (Dogger parts above OPA in regions NL and ZNO)	BDO
Keuper	KEU
Muschelkalk	MUK

Tab. A-2: Test name definitions for hydraulic packer testing

Abbreviation	**Example**
Drill site abbreviation – formation abbreviation[1)] + number of test	BUL1-1-MUK1: First test interval in Muschelkalk aquifer in borehole BUL1-1

[1)] Based on the preliminary lithostratigraphic information

Tab. A-3: Test event abbreviations for hydraulic packer testing

Test phase	**Abbr.**
Compliance phase	COM
Packer deflation phase	DEF
Packer inflation phase	INF
Multi-rate pumping test with stepwise constant flowrates	MR
Pressure recovery after multi-rate pumping test (shut-in)	MRS
Pulse injection test	PI
Initial pressure recovery 'static pressure recovery' (SIT closed)	PSR
Pulse withdrawal test	PW
Pumping test with constant flowrate ('rate withdrawal test')	RW
Pressure recovery after pumping test with constant flowrate (shut-in)	RWS
Slug withdrawal test (flow phase)	SW
Slug withdrawal test – pressure recovery with closed SIT (shut-in)	SWS

Tab. A-4: Parameter definitions

Tab. A-4: Parameter definitions

Abbreviation/ symbol	**Description**	**Unit**
h_s	Static hydraulic head (freshwater head) $$h_s = z_{ref} - z_{int} + \left[\frac{P_s + \rho_{int}\, g\, (z_{int} - z_2) - P_{atm} - P_{offset}}{\rho_w\, g}\right]$$	m asl
k	Intrinsic permeability	m^2
K	Hydraulic conductivity	$m\ s^{-1}$
K_s	Hydraulic conductivity of skin zone	$m\ s^{-1}$
n	Fractural flow dimension, e.g. Barker (1988)	-
P	Pressure (at QSSP-P2 level, if not otherwise specified)	Pa, kPa
P1	Pressure below bottom packer/ P1-interval (downhole probe)	Pa, kPa
P2	Pressure in test interval (downhole probe)	Pa, kPa
P2*	Pressure in test interval (memory gauge)	Pa, kPa
P3	Pressure in annulus (above top packer, downhole probe)	Pa, kPa
P4	Pressure in test tubing above SIT (downhole probe)	Pa, kPa
P_{atm}	Atmospheric pressure	Pa, kPa
P_f	Static formation pressure (fitting parameter, at QSSP-P2 level)	Pa, kPa
P_{int}	Static formation pressure at midpoint of test interval	Pa, kPa
P_{offset}	Offset of a pressure probe at atmospheric pressure	Pa, kPa
q	Flow rate	$m^3\ s^{-1}$
Q, Q_{tot}	Cumulative flow volume	m^3
ρ_{int}	Density of interval fluid	$kg\ m^{-3}$
ρ_w	Density of formation water (fluid)	$kg\ m^{-3}$
S	Storage	-
s	Skin factor	-
S_s	Specific storage	m^{-1}
S_{ss}	Specific storage of skin zone	m^{-1}
T	Transmissivity	$m^2\ s^{-1}$
t, dt	Time, elapsed time	s
T_{int}, T_2	Temperature in test interval, temperature triple probe (Sensor 2)	°C
z_2	Depth of pressure sensor of test interval P2	m bgl
z_{int}	Depth interval midpoint	m bgl
z_{ref}	Reference point elevation	m asl

Appendix B: Analysis plots of the hydraulic packer tests BUL1-1-BDO1 and BUL1-1-MUK1

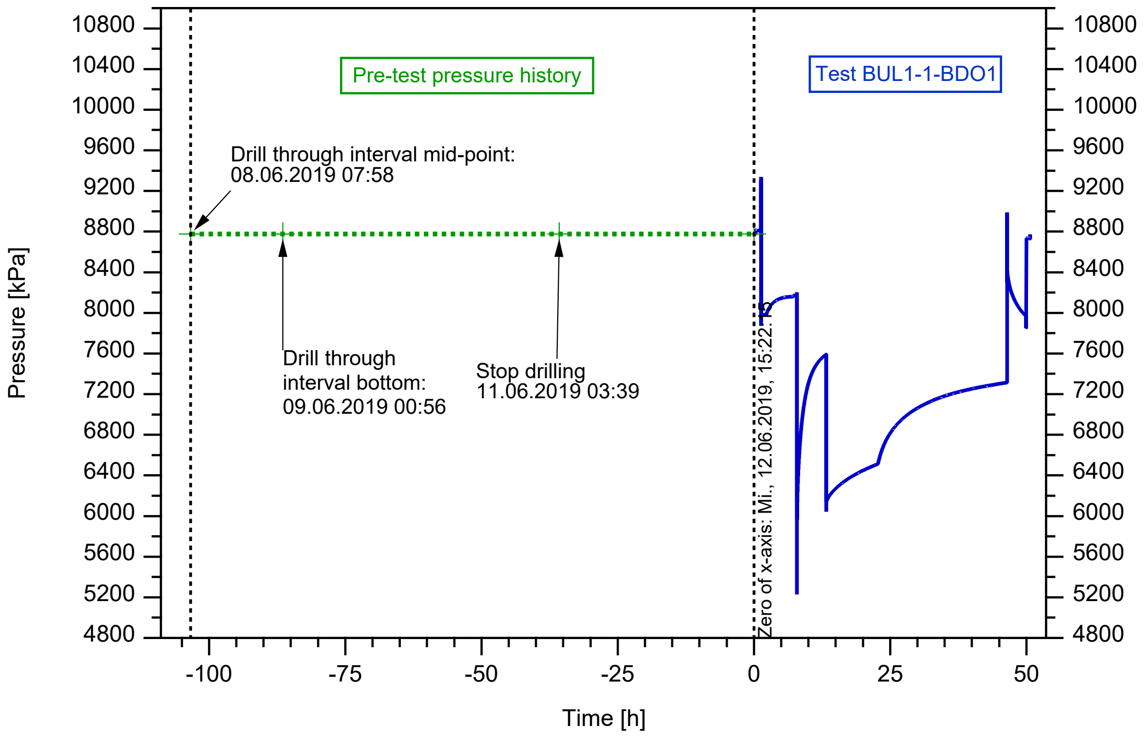

Fig. B-1: Hydraulic test BUL1-1-BDO1, borehole history

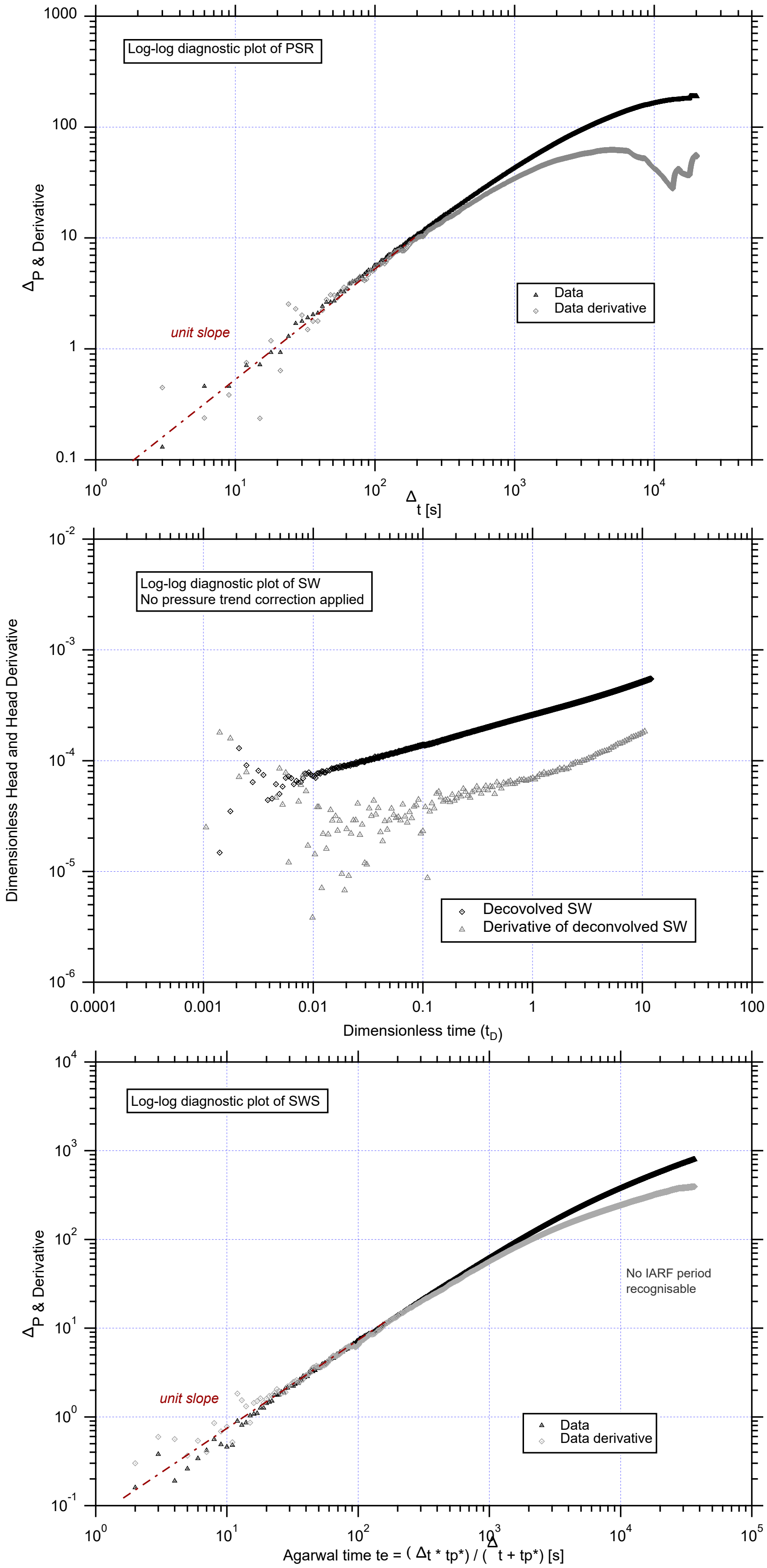

Fig. B-2: Hydraulic test BUL1-1-BDO1, log-log diagnostic plots of PSR phase (top), SW-deconvolved (middle) and SWS phase (bottom)

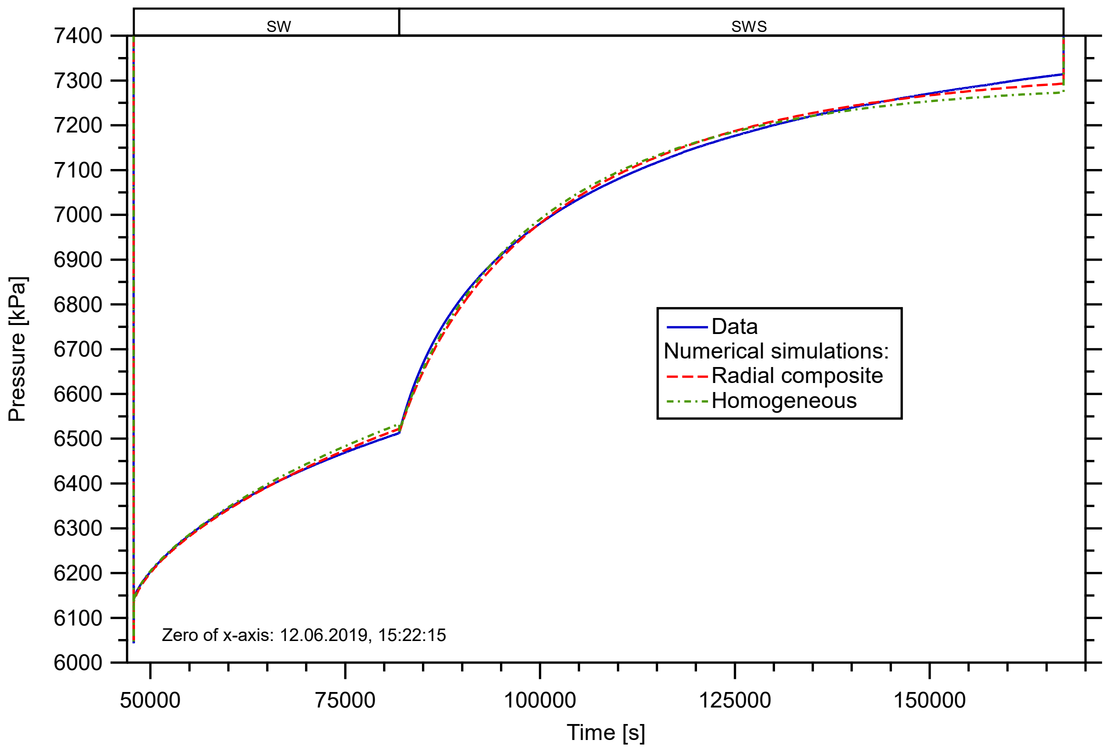

Fig. B-3: Hydraulic test BUL1-1-BDO1, SW-SWS sequence: Cartesian pressure plot and numerical fits based on the best fit of 577 perturbations using a homogeneous model (green) and a composite model (red)

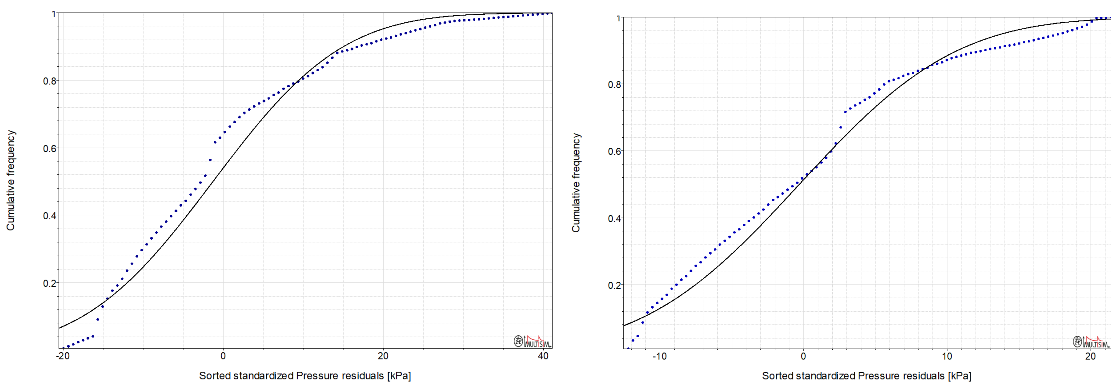

Fig. B-4: Hydraulic test BUL1-1-BDO1, SW-SWS sequence: cumulative distribution function plots based on a homogeneous model (left) and a composite model (right)

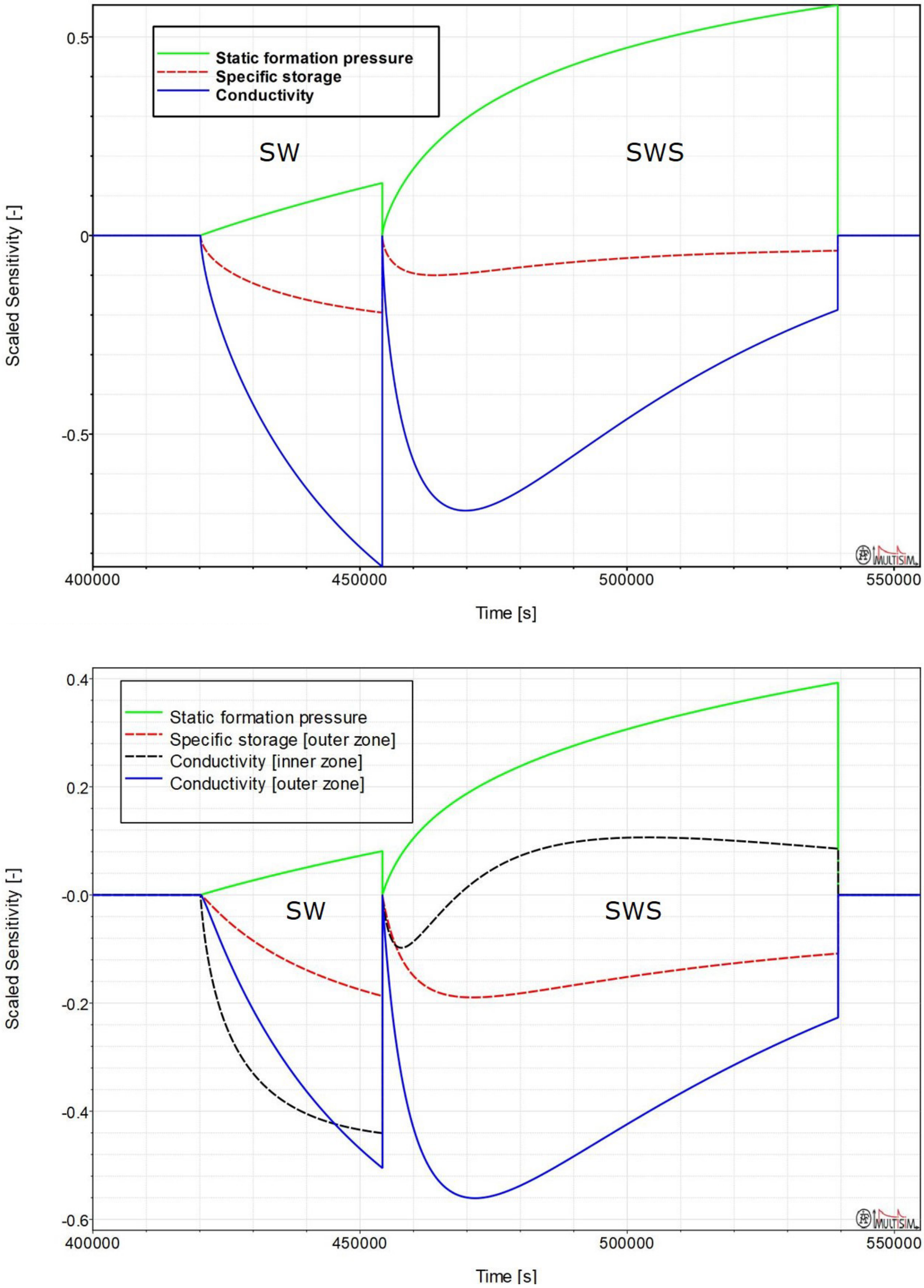

Fig. B-5: Hydraulic test BUL1-1-BDO1, SW-SWS sequence: varied parameter scaled sensitivities for the radial-homogeneous model (top) and the radial-composite (skin) model (bottom)

Time denotes seconds since start of borehole pressure history.

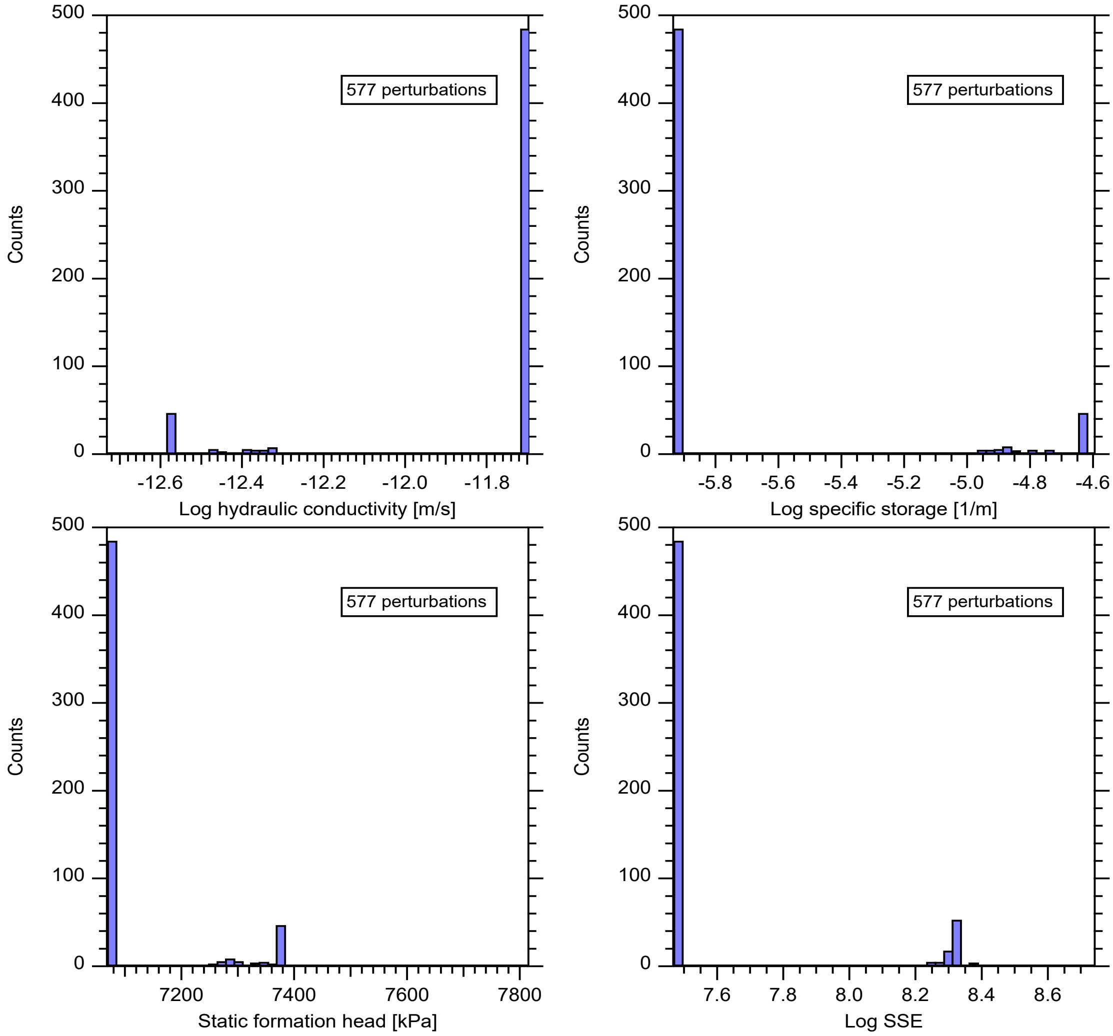

Fig. B-6: Hydraulic test BUL1-1-BDO1, SW-SWS sequence: histograms of optimized parameters (K, S_S and P_f) and SSE values from the perturbation analysis using a homogeneous model

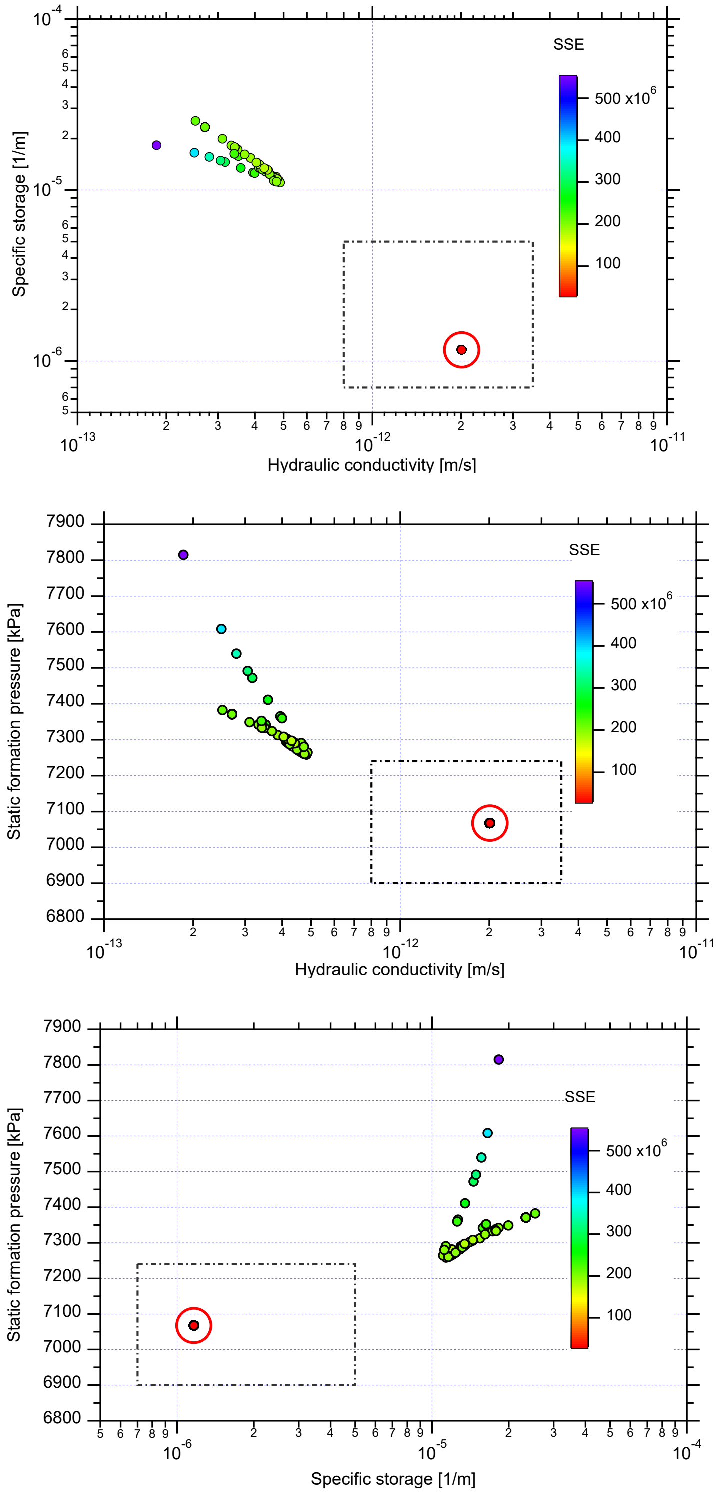

Fig. B-7: Hydraulic test BUL1-1-BDO1, SW-SWS sequence, radial homogeneous flow model: scatter plots and associated SSE values of the optimised parameters K, S_S and P_f from perturbation analysis

The dashed rectangles visualise the uncertainty ranges derived from the perturbation analysis and the circled red points indicate the lowest SSE value.

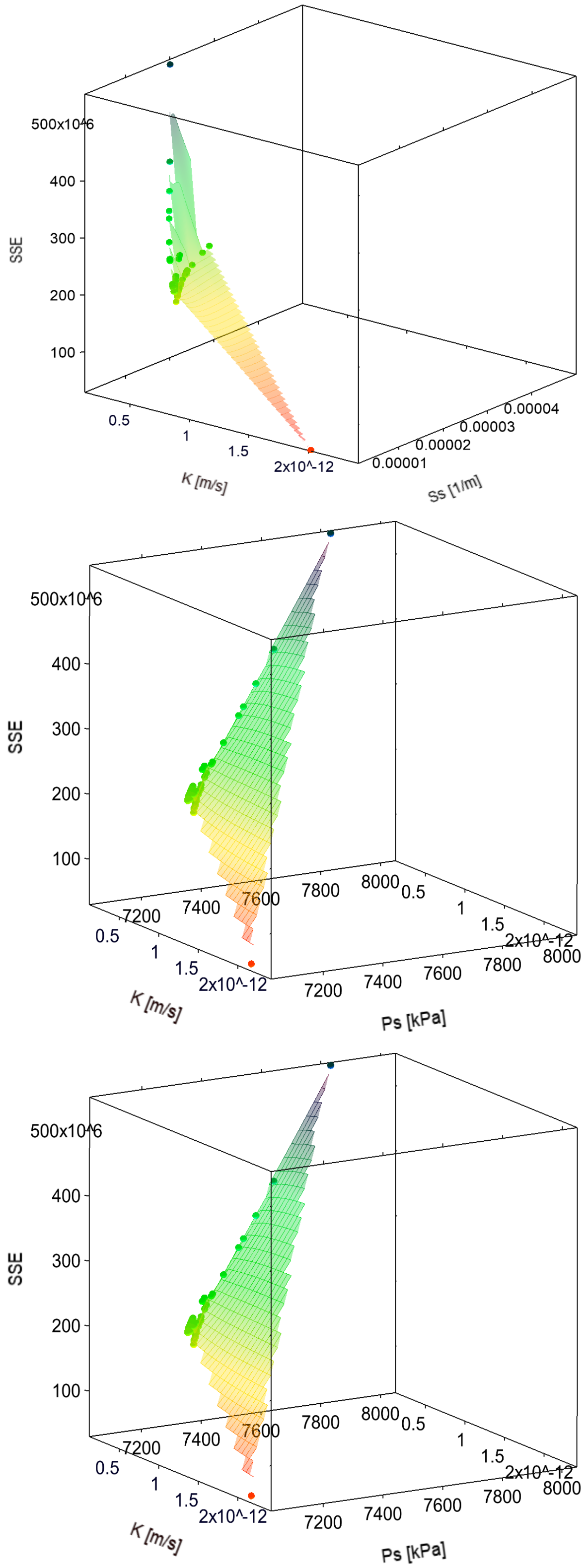

Fig. B-8: Hydraulic test BUL1-1-BDO1, SW-SWS sequence, radial homogeneous flow model: 3D plots and associated SSE values of the optimised parameters K, S_S and P_f from perturbation analysis

The red points indicate on the lowest SSE value.

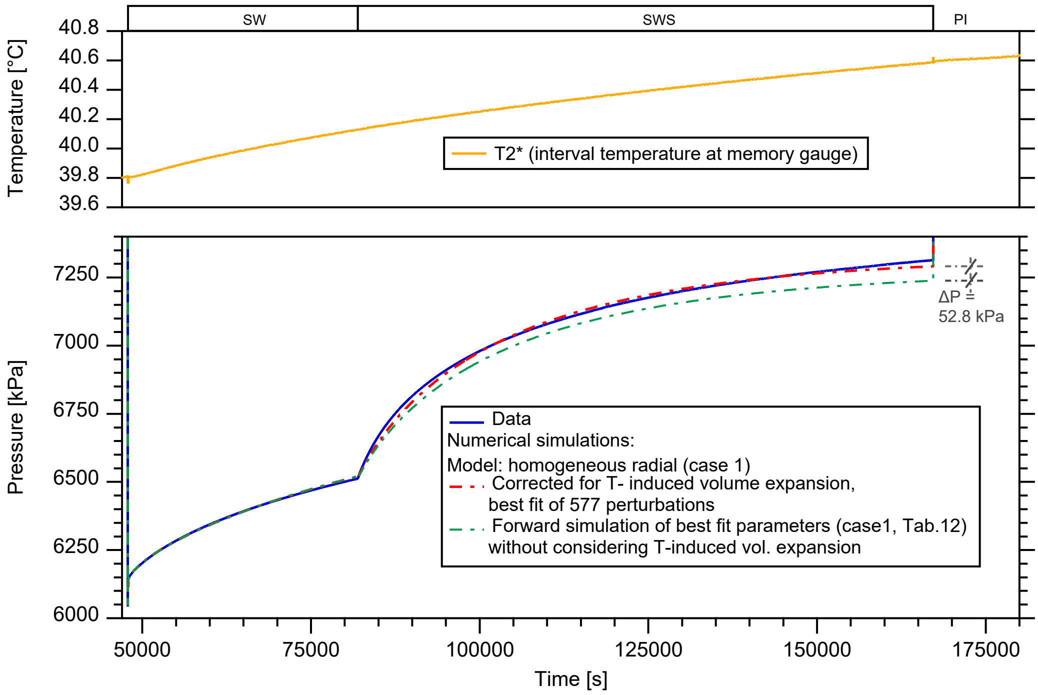

Fig. B-9: Hydraulic test BUL1-1-BDO1, SW-SWS sequence: Cartesian pressure plot and best fit based on 577 perturbations and forward simulation without temperature-induced volume change using the best-fit parameters

The temperature used for the volume change of the fluid is shown in the top part of the graph.

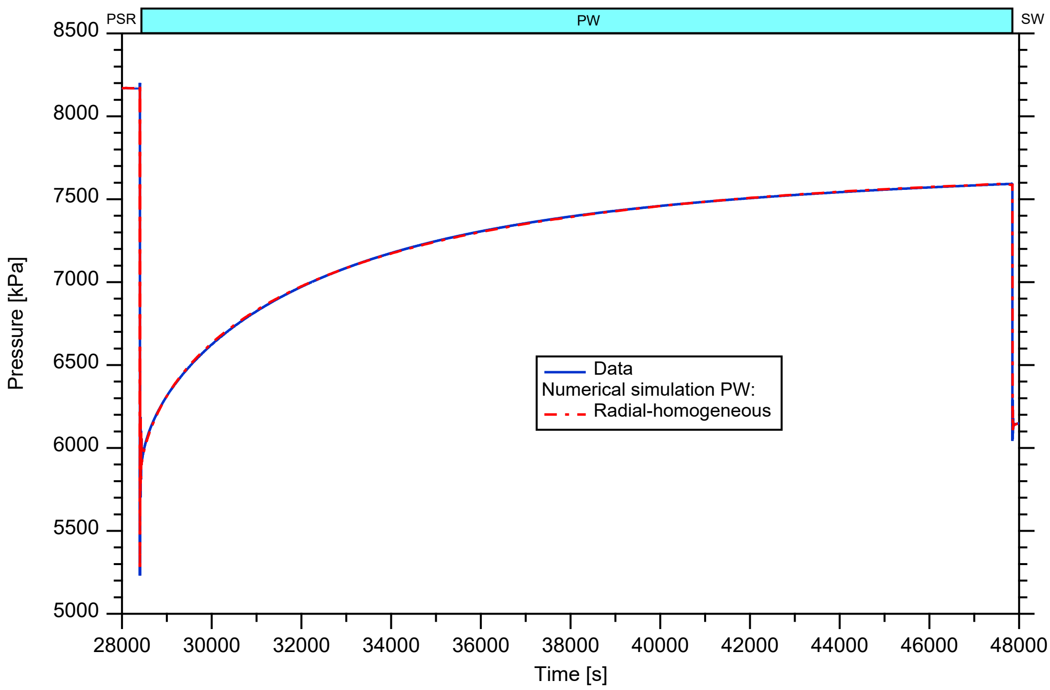

Fig. B-10: Hydraulic test BUL1-1-BDO1, PW test phase: Cartesian pressure plot of the PW test phase and numerical fit based on a homogeneous model

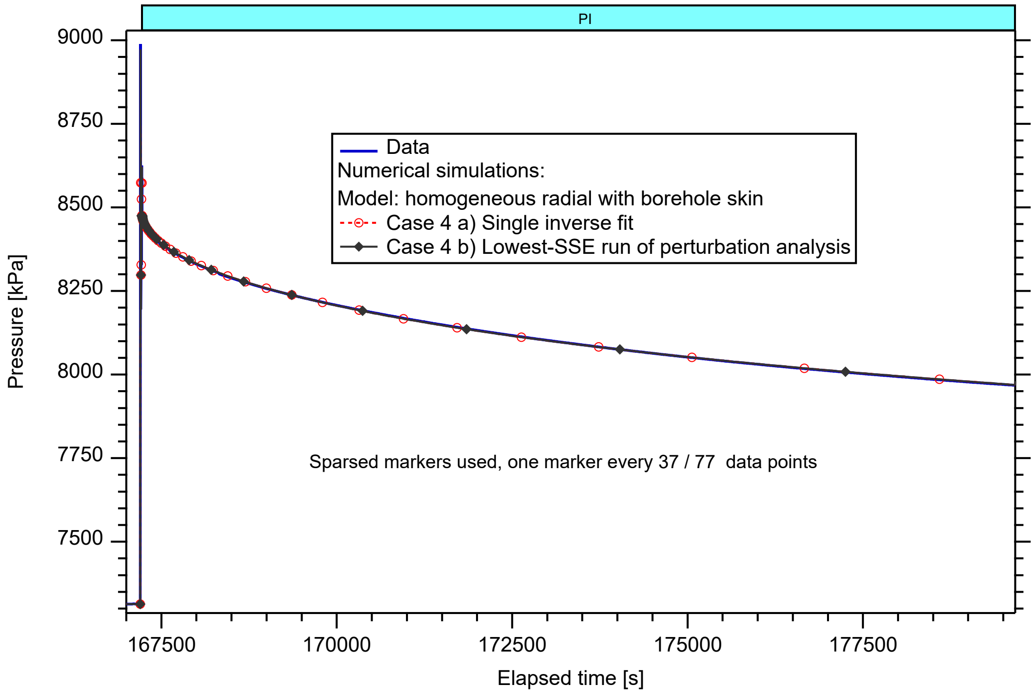

Fig. B-11: Hydraulic test BUL1-1-BDO1, PI test phase: Cartesian pressure plot of the PI test phase and numerical fits based on a homogeneous model

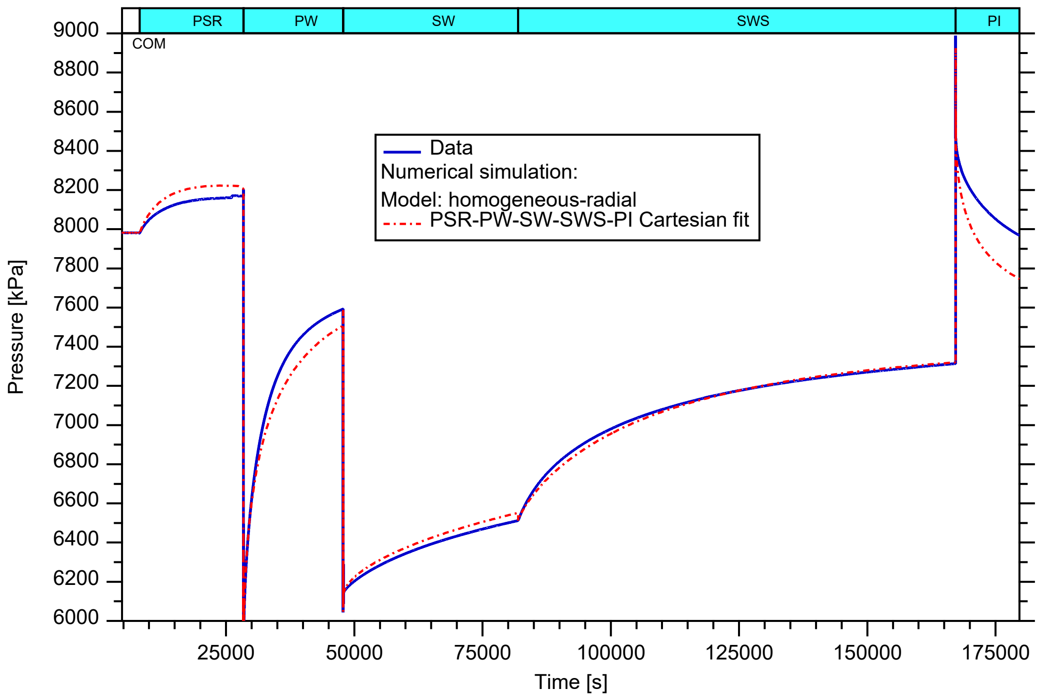

Fig. B-12: Hydraulic test BUL1-1-BDO1, PI test phase, PSR to PI entire sequence fit: Cartesian pressure plot of the entire sequence and the numerical fit based on a homogeneous model

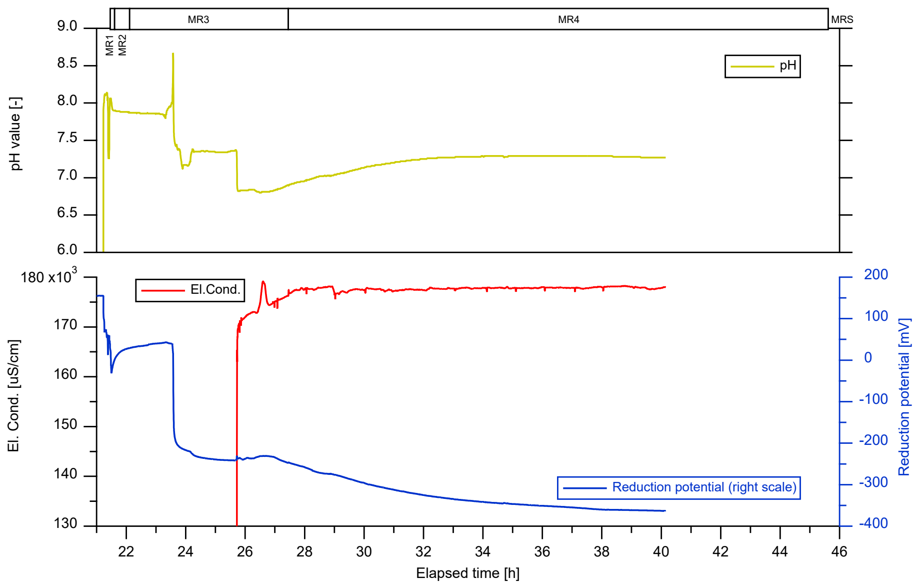

Fig. B-13: Hydraulic test BUL1-1-MUK1, chemical parameters measured during the step rate test

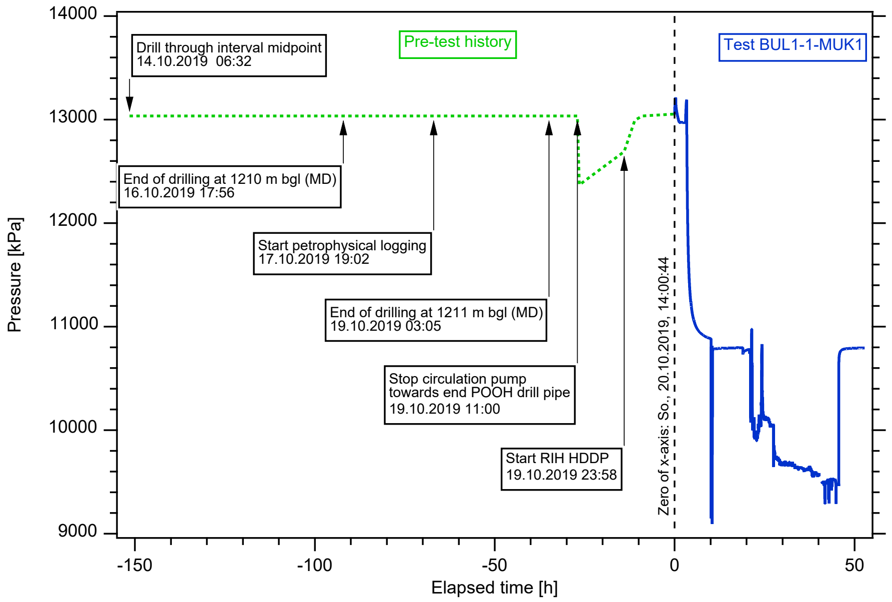

Fig. B-14: Hydraulic test BUL1-1-MUK1, borehole pressure history and measured interval test data

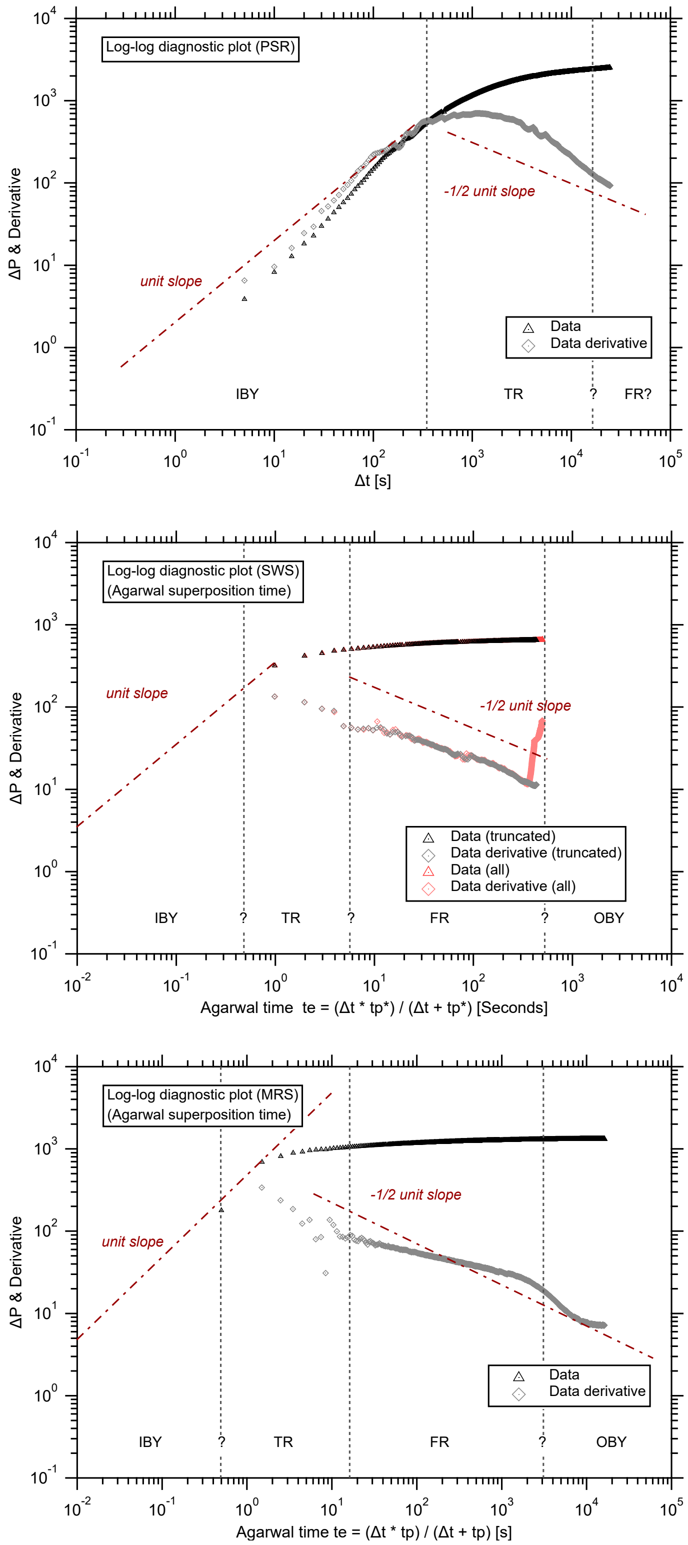

Fig. B-15: Hydraulic test BUL1-1e-MUK1, diagnostic plots of PSR phase (no superposition plot, top), slug shut-in phase (SWS, log-log plot using Agarwal time, middle) and the recovery phase after the step rate test (MRS, Agarwal time, bottom)

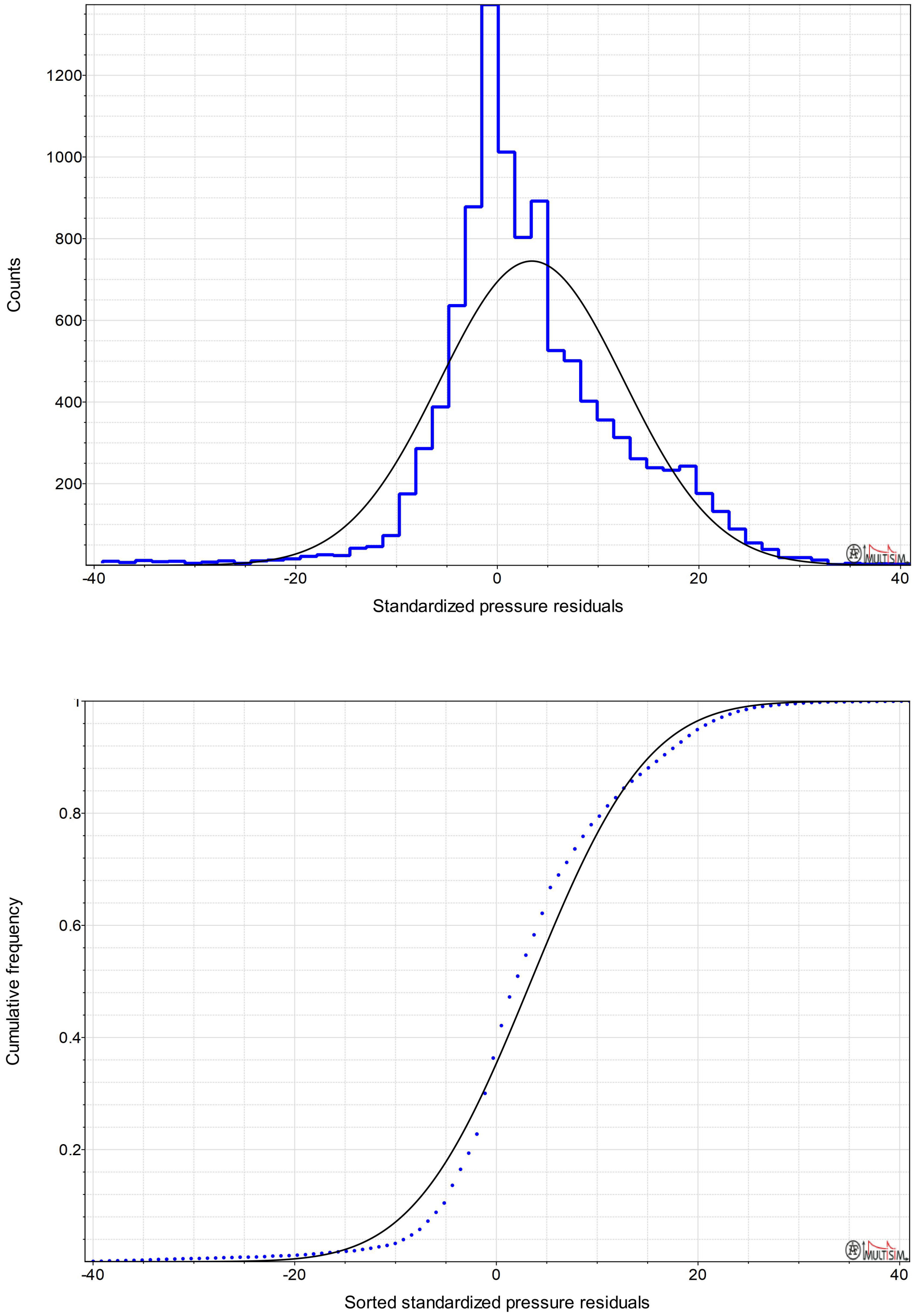

Fig. B-16: Hydraulic test BUL1-1-MUK1, MR-MRS sequence, GRF model, reference fit: normalised (top) and cumulative distribution function plot (bottom)

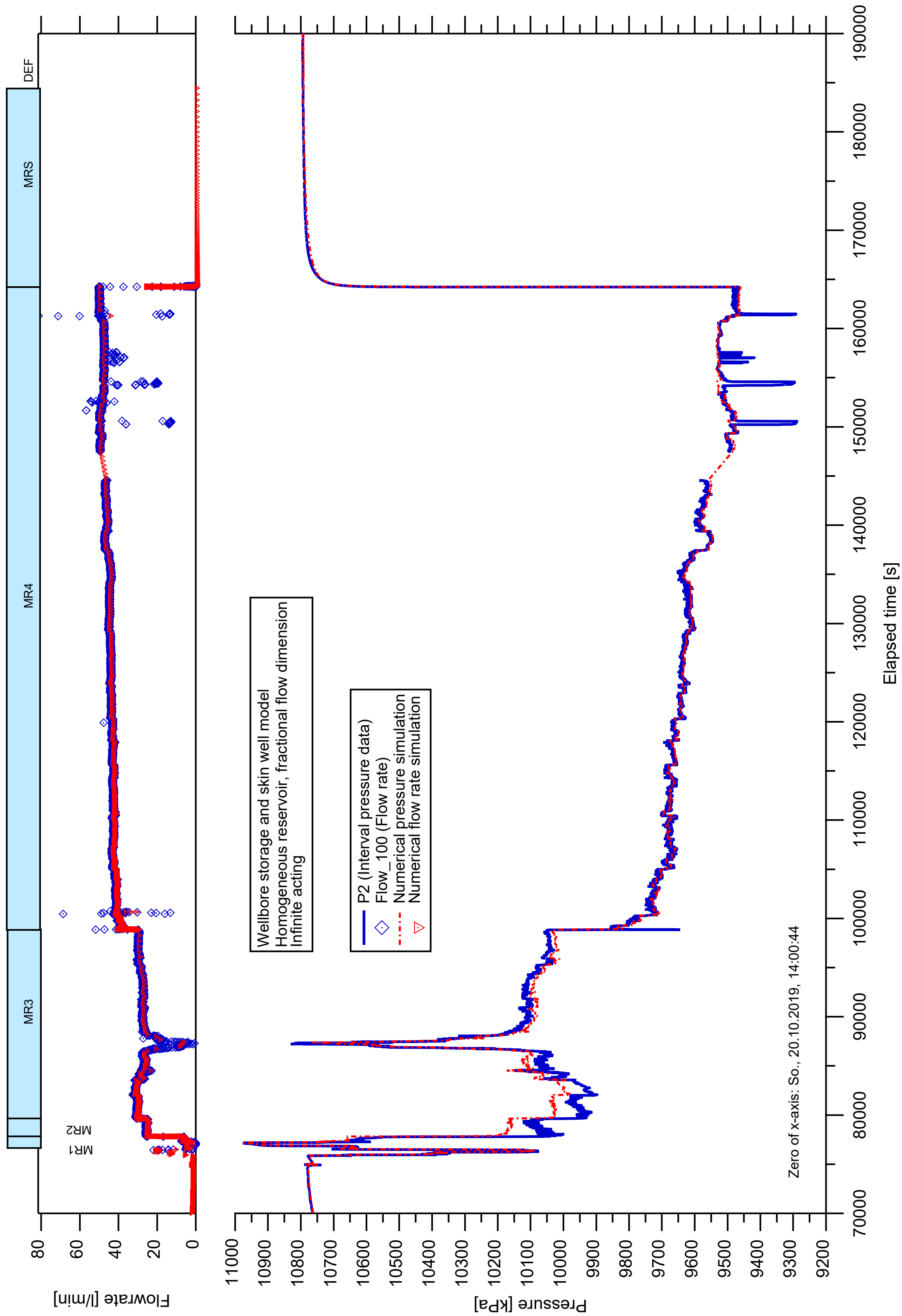

Fig. B-17: Hydraulic test BUL1-1-MUK1, MR-MRS sequence, best fit: Cartesian pressure and flow data and numerical Cartesian fit on the pressure data of the MR1-MR2-MR3-MR4-MRS sequence using the GRF model

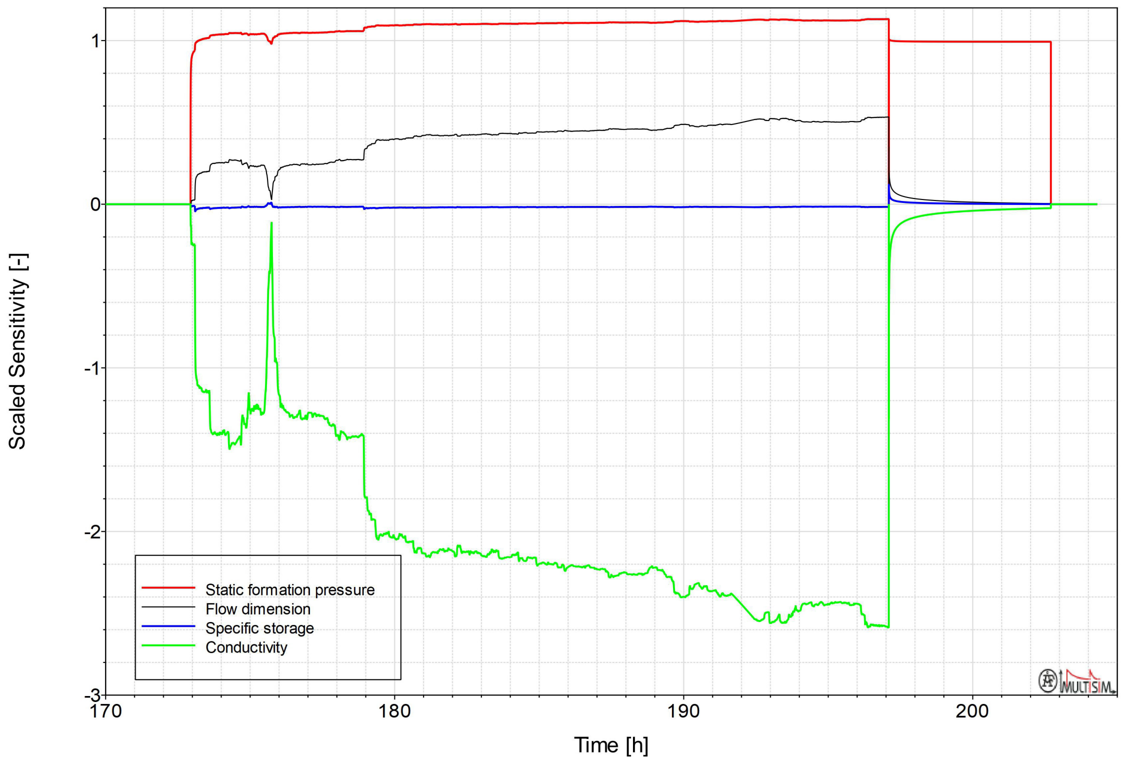

Fig. B-18: Hydraulic test BUL1-1-MUK1, MR-MRS sequence, GRF model, reference fit: scaled sensitivities of the fitting parameters

Time denotes hours since start of borehole pressure history.

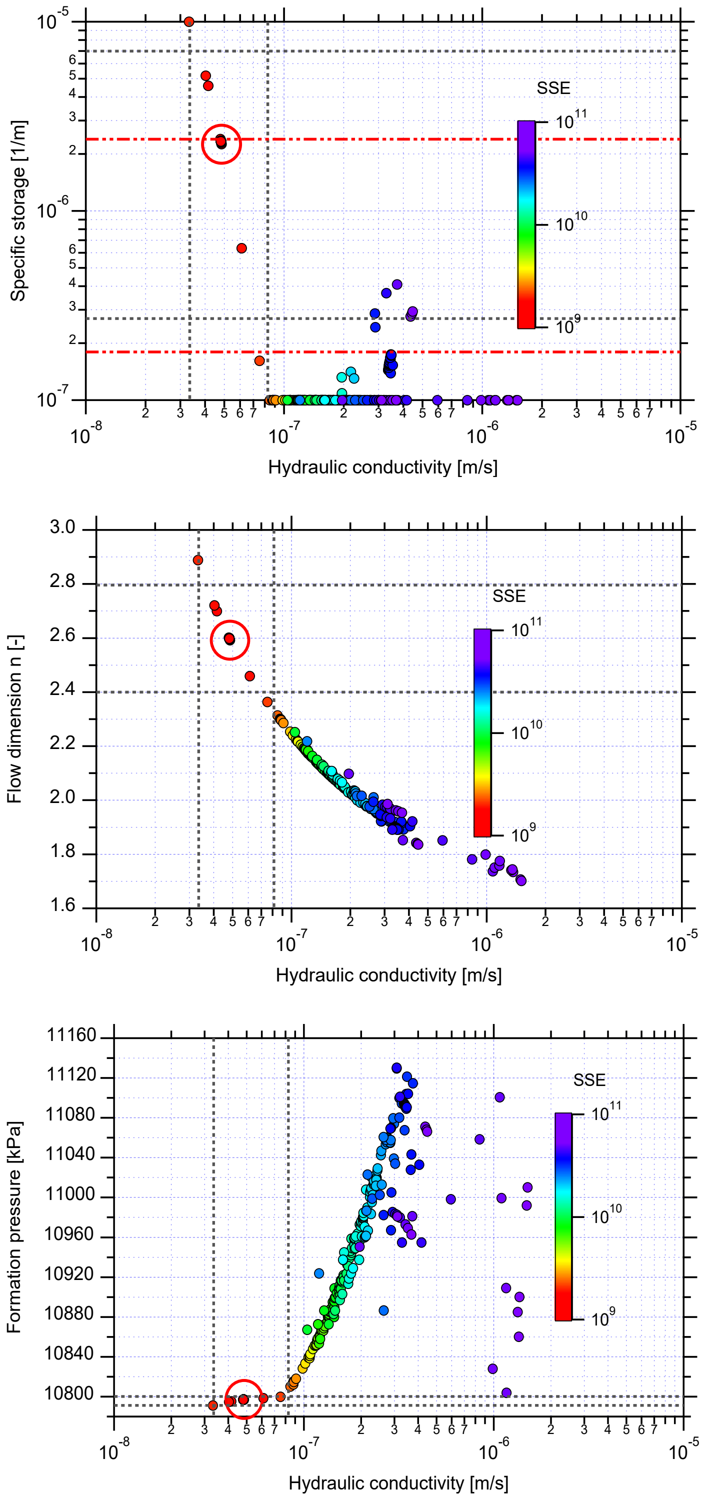

Fig. B-19: Hydraulic test BUL1-1-MUK1, MR-MRS sequence, GRF model, perturbation analysis: scatter plots and associated SSE values of the optimised parameters from perturbation analysis showing K versus S_S (top), K versus n (middle) and K versus P_f (bottom)

The red circle in each figure indicates the minimum SSE value; dark grey lines indicate estimated uncertainty ranges; red lines indicate plausibility range of S_S.

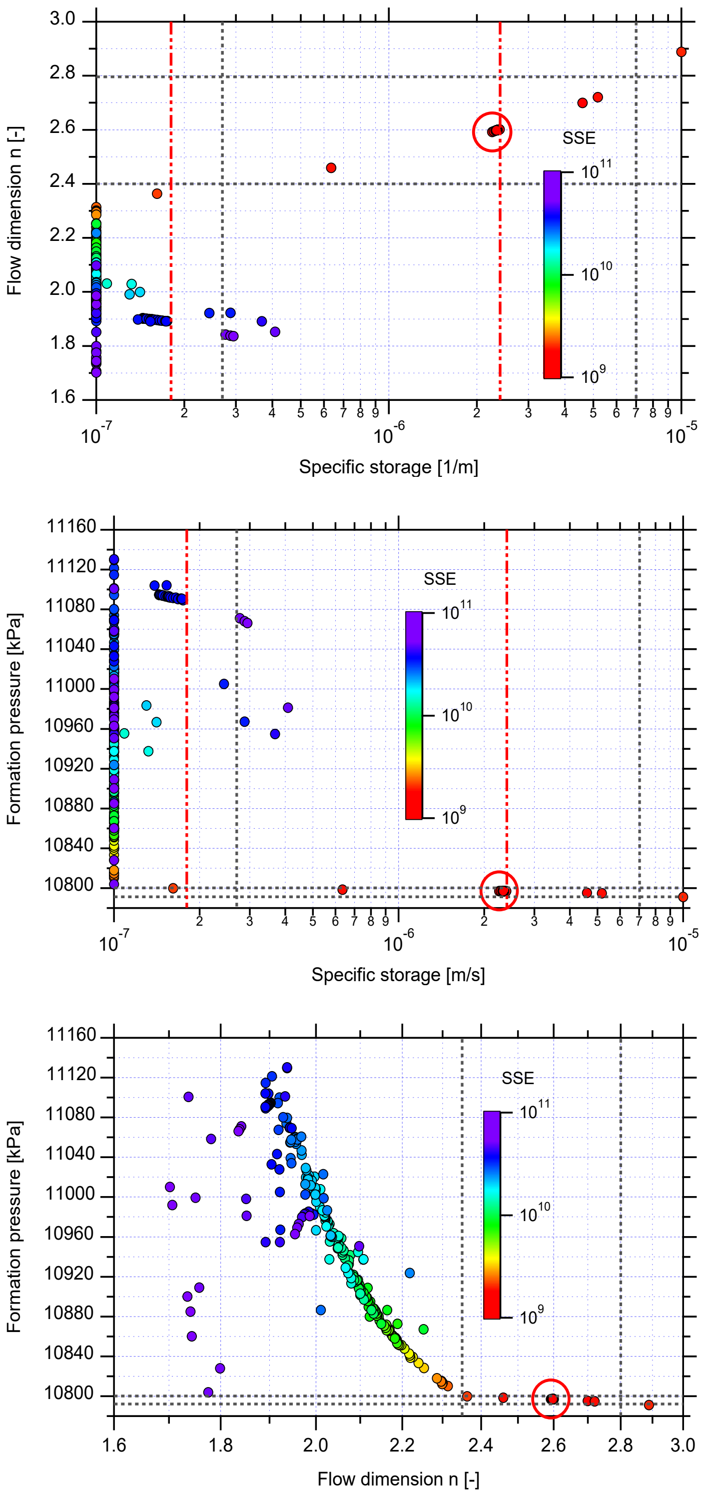

Fig. B-20: Hydraulic test BUL1-1-MUK1, MR-MRS sequence, GRF model, perturbation analysis: scatter plots and associated SSE values of the optimised parameters from perturbation analysis showing S_S versus P_f and n (top and middle) and n versus P_f (bottom)

The red circle in each figure indicates the minimum SSE value; dark grey lines indicate estimated uncertainty ranges; red lines indicate plausibility range of S_S.

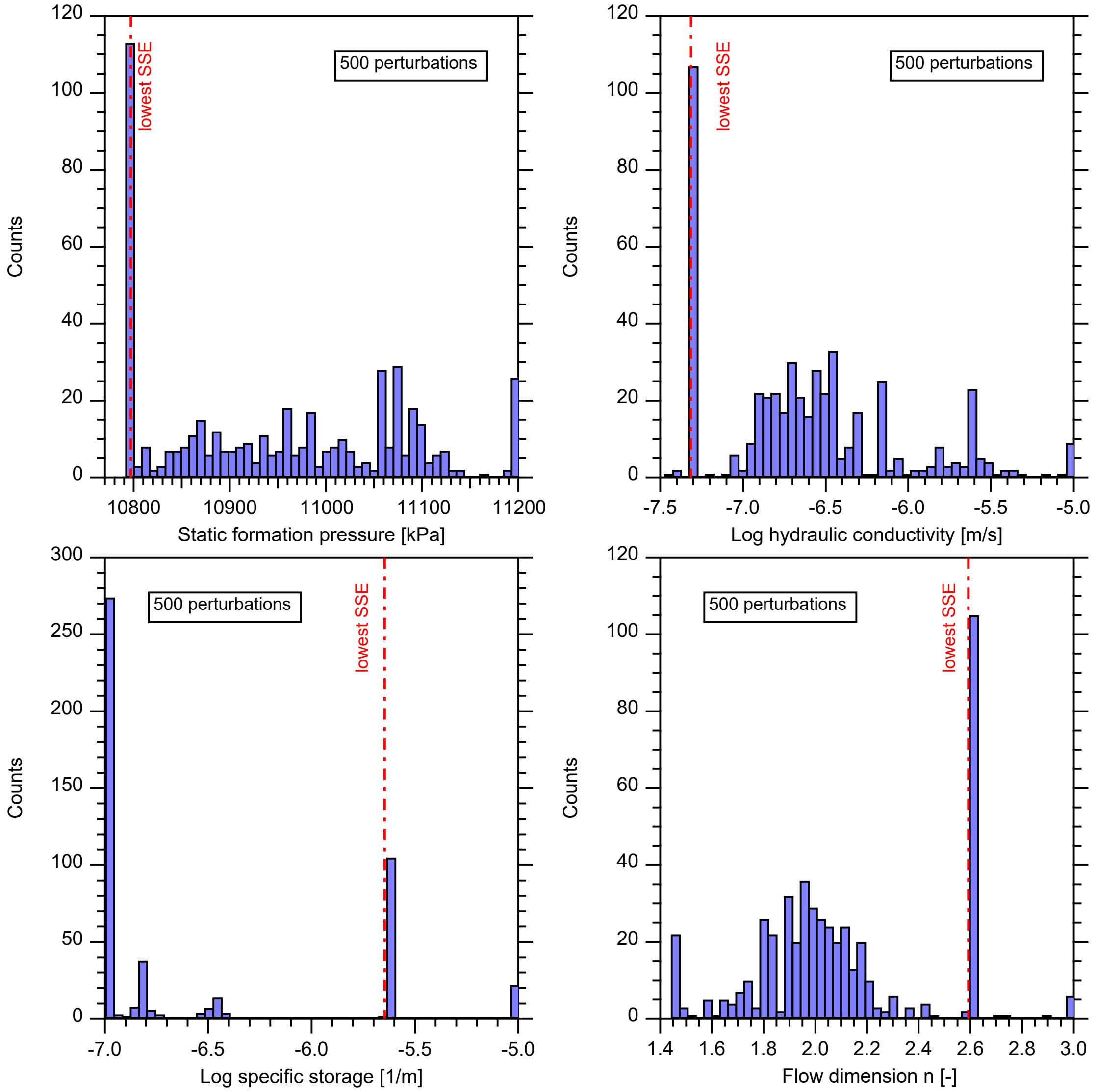

Fig. B-21: Hydraulic test BUL1-1-MUK1, MR-MRS sequence, GRF model, perturbation analysis: histograms of optimized parameters K, S_S, P_f

Lowest SSE result is marked with a red dashed line.

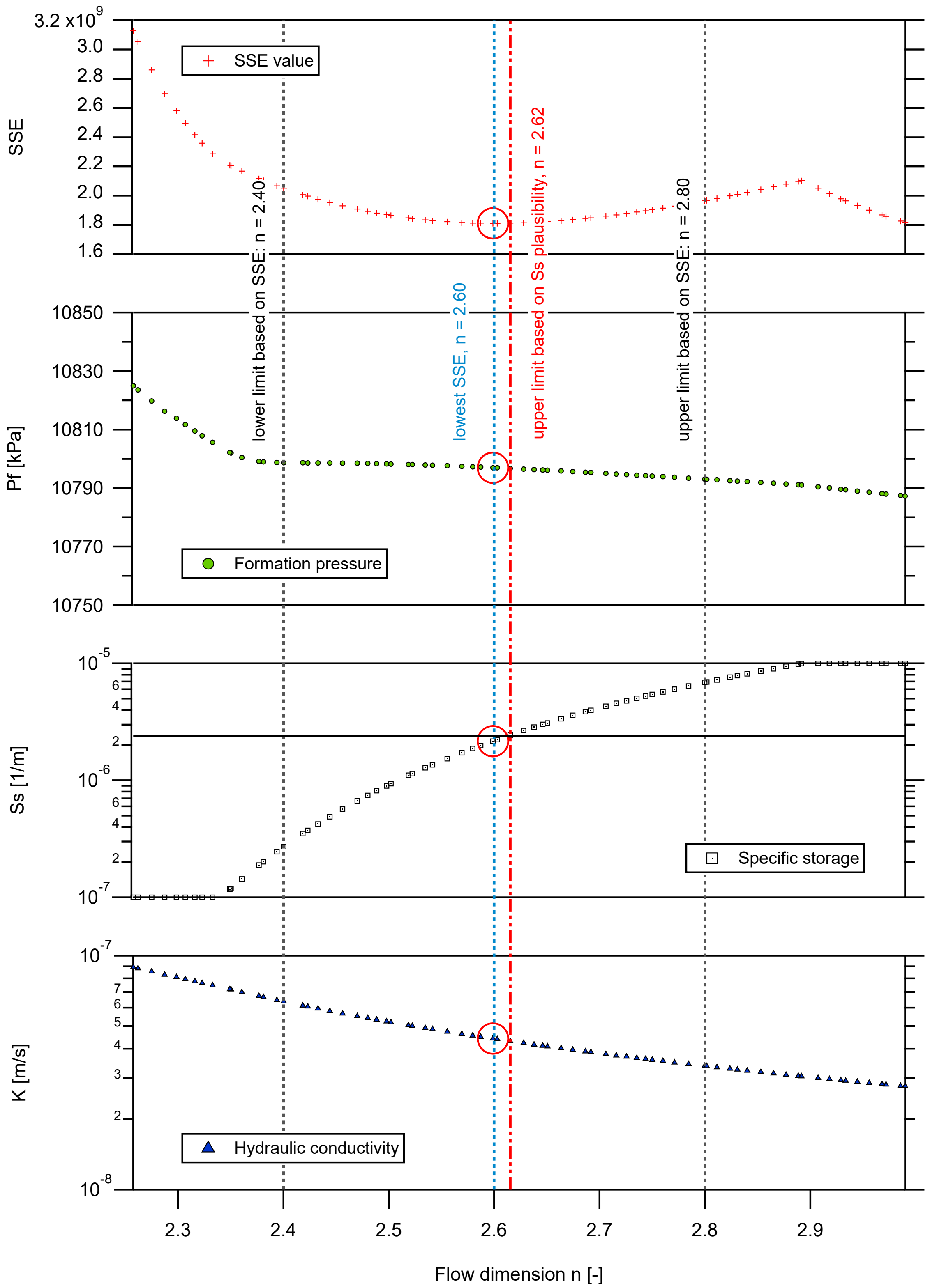

Fig. B-22: Hydraulic test BUL1-1-MUK1, MR-MRS sequence, GRF model: parameter ranges of the parameters K, S_S and P_f together with respective SSE values against the flow dimension n using the sampling technics

Red line: lowest SSE; grey lines: upper and lower range of the flow dimension parameter.

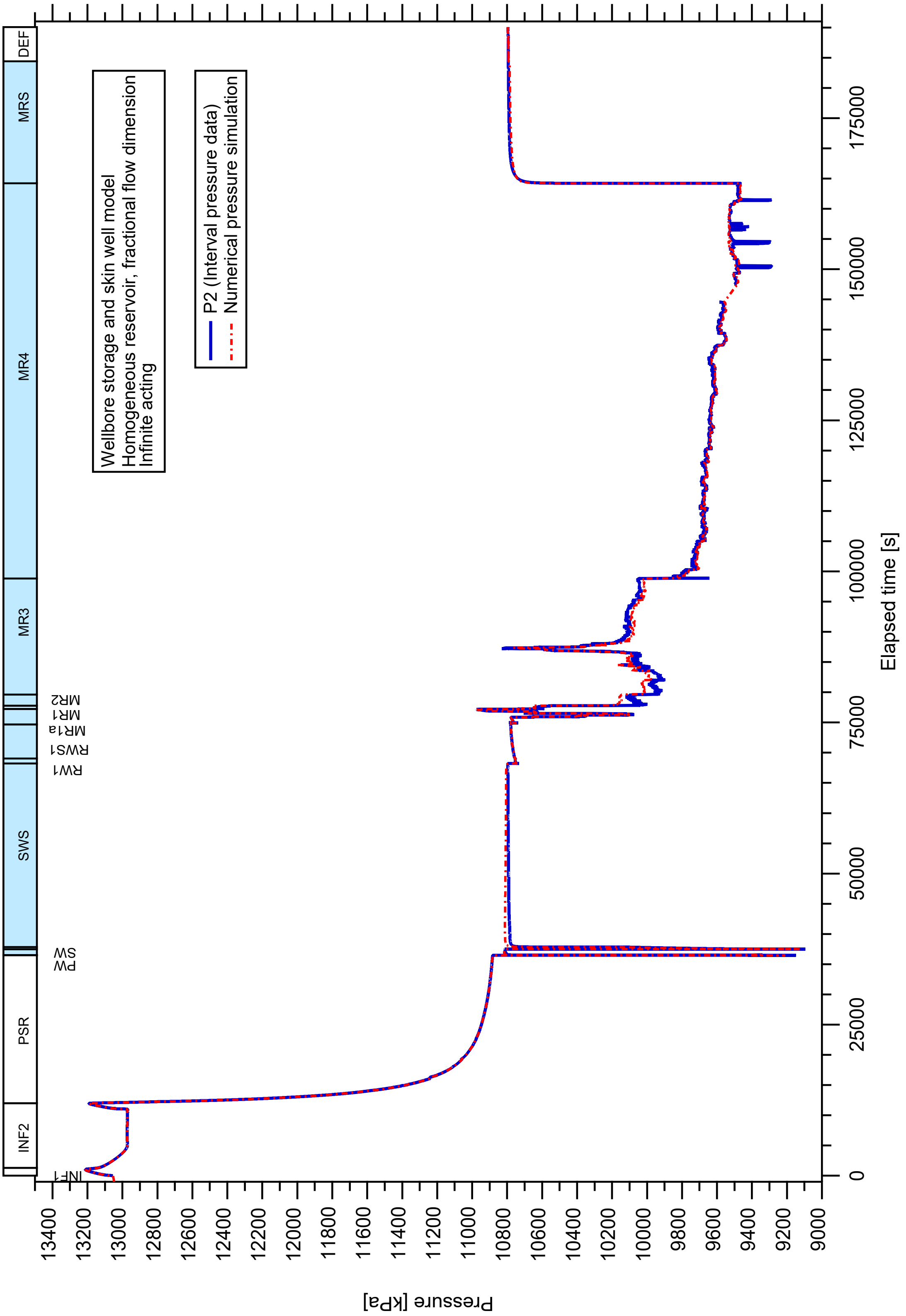

Fig. B-23: Hydraulic test BUL1-1-MUK1, PW-MRS entire sequence fit: pressure data and numerical pressure fit of the entire test sequence in a Cartesian plot using the GRF mode